# Journal of the Anatomical Society of India

Print ISSN: 0003-2778

## GENERAL INFORMATION

**About the Journal**

Journal of the Anatomical Society of India (ISSN: Print 0003-2778) is peer-reviewed journal. The journal is owned and run by Anatomical Society of India. The journal publishes research articles related to all aspects of Anatomy and allied medical/surgical sciences. Pre-Publication Peer Review and Post-Publication Peer Review Online Manuscript Submission System Selection of articles on the basis of MRS system Eminent academicians across the globe as the Editorial board members Electronic Table of Contents alerts Available in both online and print form. The journal is published quarterly in the months of January, April, July and October.

**Scope of the Journal**

The aim of the *Journal of the Anatomical Society of India* is to enhance and upgrade the research work in the field of anatomy and allied clinical subjects. It provides an integrative forum for anatomists across the globe to exchange their knowledge and views. It also helps to promote communication among fellow academicians and researchers worldwide. The Journal is devoted to publish recent original research work and recent advances in the field of Anatomical Sciences and allied clinical subjects. It provides an opportunity to academicians to disseminate their knowledge that is directly relevant to all domains of health sciences.

The Editorial Board comprises of academicians across the globe.

JASI is indexed in Scopus, available in Science Direct.

**Abstracting and Indexing Information**

The journal is registered with the following abstracting partners:

Baidu Scholar, CNKI (China National Knowledge Infrastructure), EBSCO Publishing's Electronic Databases, Ex Libris – Primo Central, Google Scholar, Hinari, Infotrieve, Netherlands ISSN center, ProQuest, TdNet, Wanfang Data

The journal is indexed with, or included in, the following:

SCOPUS, Science Citation Index Expanded, IndMed, MedInd, Scimago Journal Ranking, Emerging Sources Citation Index.

Impact Factor® as reported in the 2019 Journal Citation Reports® (Clarivate Analytics, 2020): 0.227

**Information for Authors**

Article processing and publication charges will be communicated by the editorial office. All manuscripts must be submitted online at www.journalonweb.com/jasi.

**Subscription Information**

| A subscription to JASI comprises 4 issues. Prices include postage. Annual Subscription Rate for non-members- | | |
|---|---|---|
| **Rates of Membership (with effect from 1.1.2019)** | | |
| | **India** | **International** |
| Ordinary membership | INR 1500 | US $ 100 |
| Couple membership | INR 2250 | |
| Life membership | INR 8000 | US $ 900 |
| **Subscription Rates (till 31st August)** | | |
| Individual | INR 4500 | US $ 600 |
| Library/Institutional<br>Trade discount of 10% for agencies only | INR 10000 | US $ 900 |
| **Subscription Rates (after 31st August)** | | |
| Individual | INR 5000 | |
| Library/Institutional | INR 10500 | |
| *The Journal of Anatomical Society of India* (ISSN: 0003-2778) is published quarterly **Subscriptions** are accepted on a prepaid basis only and are entered on a calendar year basis. Issues are sent by standard mail Priority rates are available upon request. | | |

**Information to Members/Subscribers**

All members and existing subscribers of the Anatomical Society of India are requested to send their membership/existing subscription fee for the current year to the Treasurer of the Society on the following address: Prof (Dr.) Punit Manik, Treasurer, ASI, Department of Anatomy, KGMU, Lucknow - 226003. Email: punitamanik@yahoo.co.in. All payments should be made through an account payee bank draft drawn in favor of the **Treasurer, Anatomical Society of India,** payable at **Lucknow** only, preferably for **Allahabad Bank, Medical College Branch, Lucknow.** Outstation cheques/drafts must include INR 70 extra as bank collection charges.

All complaints regarding non-receipt of journal issues should be addressed to the Editor-in-Chief, JASI at editorjasi@gmail.com. The new subscribers may, please contact wkhlrpmedknow_subscriptions@wolterskluwer.com.

Requests of any general information like travel concession forms, venue of next annual conference, etc. should be addressed to the General Secretary of the Anatomical Society of India.

For mode of payment and other details, please visit www.medknow.com/subscribe.asp

Claims for missing issues will be serviced at no charge if received within 60 days of the cover date for domestic subscribers, and 3 months for subscribers outside India. Duplicate copies cannot be sent to replace issues not delivered because of failure to notify publisher of change of address. The journal is published and distributed by Wolters Kluwer India Pvt. Ltd. Copies are sent to subscribers directly from the publisher's address. It is illegal to acquire copies from any other source. If a copy is received for personal use as a member of the association/ society, one cannot resale or give-away the copy for commercial or library use.

The copies of the journal to the subscribers are sent by ordinary post. The editorial board, association or publisher will not be responsible for non receipt of copies. If any subscriber wishes to receive the copies by registered post or courier, kindly contact the publisher's office. If a copy returns due to incomplete, incorrect or changed address of a subscriber on two consecutive occasions, the names of such subscribers will be deleted from the mailing list of the journal. Providing complete, correct and up-to-date address is the responsibility of the subscriber.

*Nonmembers*: Please send change of address information to subscriptions@medknow.com.

**Advertising Policies**

The journal accepts display and classified advertising. Frequency discounts and special positions are available. Inquiries about advertising should be sent to Wolters Kluwer India Pvt. Ltd, advertise@medknow. com.

The journal reserves the right to reject any advertisement considered unsuitable according to the set policies of the journal.

The appearance of advertising or product information in the various sections in the journal does not constitute an endorsement or approval by the journal and/or its publisher of the quality or value of the said product or of claims made for it by its manufacturer.



**Addresses**

*Editorial Office*

Dr. Vishram Singh, Editor-in-Chief, JASI
OC-5/103, 1st floor, Orange County Society,
Ahinsa Khand-I, Indirapuram, Ghaziabad,
Delhi, NCR- 201014.
Email: editorjasi@gmail.com

*Published by*

Wolters Kluwer India Pvt. Ltd
A-202, 2nd Floor, The Qube,
C.T.S. No.1498A/2 Village Marol, Andheri (East),
Mumbai - 400 059, India.
Phone: 91-22-66491818
Website: www.medknow.com

*Printed at*

Dhote Offset Tech. P. Ltd
Goregaon (E), Mumbai, India

# Journal of the Anatomical Society of India

Print ISSN: 0003-2778

## EDITORIAL BOARD

# Journal of the Anatomical Society of India

Print ISSN: 0003-2778

## EXECUTIVE COMMITTEE

# Journal of the Anatomical Society of India

Volume 69 | Issue 3 | July-September 2020

## CONTENTS

# Journal of the Anatomical Society of India on Web

## http://www.journalonweb.com/jasi

The Journal of the Anatomical Society of India now accepts articles electronically. It is easy, convenient and fast. Check following steps:

### 1 Registration

- Register from http://www.journalonweb.com/jasi as a new author (Signup as author)
- Two-step self-explanatory process

### 2 New article submission

- Read instructions on the journal website or download the same from manuscript management site
- Prepare your files (Article file, First page file and Images, Copyright form & Other forms, if any)
- Login as an author
- Click on 'Submit new article' under 'Submissions'
- Follow the steps (guidelines provided while submitting the article)
- On successful submission you will receive an acknowledgement quoting the manuscript ID

### 3 Tracking the progress

- Login as an author
- The report on the main page gives status of the articles and its due date to move to next phase
- More details can be obtained by clicking on the ManuscriptID
- Comments sent by the editor and reviewer will be available from these pages

### 4 Submitting a revised article

- Login as an author
- On the main page click on 'Articles for Revision'
- Click on the link "Click here to revise your article" against the required manuscript ID
- Follow the steps (guidelines provided while revising the article)
- Include the reviewers' comments along with the point to point clarifications at the beginning of the revised article file.
- Do not include authors' name in the article file.
- Upload the revised article file against New Article File - Browse, choose your file and then click "Upload" OR Click "Finish"
- On completion of revision process you will be able to check the latest file uploaded from Article Cycle (In Review Articles-> Click on manuscript id -> Latest file will have a number with 'R', for example XXXX_100_15R3.docx)

### Facilities

- Submission of new articles with images
- Submission of revised articles
- Checking of proofs
- Track the progress of article until published

### Advantages

- Any-time, any-where access
- Faster review
- Cost saving on postage
- No need for hard-copy submission
- Ability to track the progress
- Ease of contacting the journal

### Requirements for usage

- Computer and internet connection
- Web-browser (Latest versions - IE, Chrome, Safari, FireFox, Opera)
- Cookies and javascript to be enabled in web-browser

### Online submission checklist

- First Page File (rtf/doc/docx file) with title page, covering letter, acknowledgement, etc.
- Article File (rtf/doc/docx file) - text of the article, beginning from Title, Abstract till References (including tables). File size limit 4 MB. Do not include images in this file.
- Images (jpg/jpeg/png/gif/tif/tiff): Submit good quality colour images. Each image should be less than 10 MB) in size
- Upload copyright form in .doc / .docx / .pdf / .jpg / .png / .gif format, duly signed by all authors, during the time mentioned in the instructions.

### Help

- Check Frequently Asked Questions (FAQs) on the site
- In case of any difficulty contact the editor

# Acceptance of Donor Bodies and Their Embalming During COVID-19 Period: A Challenge to Anatomists

The journey of a medical student begins with learning anatomy by cadaveric dissection. It not only helps to acquire knowledge about the anatomy of a human body but also helps in developing surgical skills and other clinical skills required as a physician.[1] With the adoption of the Curriculum-Based Medical Education, there has been a change in the teaching methodologies in medical education.[2] Many medical colleges are now using modern teaching aids such as E-learning, simulation, role play, case study, and virtual dissectors, but nothing can replace the traditional method of teaching by cadaveric dissection.

In the present scenario of COVID-19, when the Ministry of Health and Family Welfare, the Government of India, and the Board of Governors of Medical Council of India have issued guidelines to all the medical institutions to suspend classes for courses such as M. B. B. S., B. Sc., nursing, and other paramedical and allied health sciences,[3] teaching is now being carried out by taking online lectures and practical demonstrations using video software such as Zoom, Google Classroom, Teams, and YouTube. Even in pre-COVID times, there has been a reduction in number of body donations in most parts of the world; hence, many institutions are adopting alternative models, especially for the teaching of gross anatomy. Hence, conducting anatomy dissection classes online has become very challenging for both teachers and students.

The COVID-19 pandemic has taken a toll on body donations for research in many parts of our country. Medical colleges/hospitals are not accepting donated bodies which have dealt a severe blow to the effort of raising awareness on body donations for scientific research.

Numerous guidelines have been produced by organizations and governments during the present novel coronavirus pandemic, which will be of great use to anatomists who facilitate donor programs.

The COVID-19 virus is mainly transmitted through large respiratory droplets by inhalation or contact with mucosal surfaces, but other modes of transmission have been suggested (airborne, fecal-oral,[4] and contact with contaminated surfaces).[5] There is no evidence so far that the virus is transmitted through contact with the skin of a deceased person, but as the virus is known to persist on surfaces for hours or days, depending on the nature of the surface,[6] this mode of transition cannot be ruled out. The risk of transmission likely increases with direct contact with bodily fluids, and certainly increases with invasive handling of the cadaver, as in autopsy procedures, if it produces droplets or aerosols.[7]

No evidence has been found so far of individuals who have become infected from exposure to the bodies of persons who have died from 2 COVID-19 (WHO 2020b). In general, the potential risk of transmission related to the handling of bodies of deceased persons with suspected or confirmed COVID-19 is considered low[7] (ECDC 2020a). While there is no evidence yet that the COVID-19 virus is specifically inactivated in a preserved body donor, the commonly used preservatives, formaldehyde and ethanol, appear to be efficient against the virus.[8]

In general, the safety precautions applied in the basic handling of any human cadaver should cover the risk of a COVID-19 infection. As in any given case, any cadaver should be treated as potentially infectious. In the absence of a test for COVID-19, this also applies to the risk of a COVID-19 infection. All the staff who are responsible for the collection, transportation and preparation of bodies which are infected or suspected of being infected with COVID-19, must be trained specifically for their tasks. They should be well trained in donning and doffing of personal protective equipment (PPE). They should also be trained to use Infection Prevention and Control practices while handling the bodies. The staff should be trained in performing the last rites in a dignified way. The staff must be trained in, and apply, standard precautions for hand hygiene. The staff handling the bodies should take care of proper disinfection of instruments, washing them with detergent, and sterilizing in autoclave. All the instruments should be sterilised chemically with 70% alcohol, diguanide or 2% glutaraldehyde or 1 % hypochlorite. The area of the body receiving unit and of the embalming room and adjacent environment should also be disinfected using chemicals such as 70%–90% ethanol, hypochlorite based products (0.1%), and hydrogen peroxide (0.5%). Any tubes, drains, and catheters on the dead body must be removed with caution; any puncture holes or wounds on the dead body should be disinfected with 1% hypochlorite and dressed with impermeable material; oral and nasal orifices should be plugged. Extreme cautions should be undertaken while using sharp objects, IV catheters, etc., All medical waste should be handled by the following biomedical waste management rules. All surfaces of the isolation area should be wiped with 1% sodium hypochlorite solution giving a contact time of 30 min and then allowed to dry.

Embalming of bodies infected by the novel coronavirus is not recommended by the WHO,[9] but this is in the context of advice for funeral homes. In the case of anatomy departments, embalming cannot be avoided, especially for cosmetic embalming and for transportation of bodies. The

reason provided by the WHO[9] and the New South Wales Health authority for not recommending embalming is in order to minimize manipulation of the body and thus the possible generation of aerosol. The Department of Health of South Africa (2020) asserts that embalming of a body infected with the novel coronavirus does not pose a risk. However, forced inflation of the lungs, which may occur during fixation, may generate aerosol[10] (RCP, 2020b). Thus, any aerosol-generating procedures and splashes of contaminated fluids should be avoided during embalming. The use of PPE, as described above, applies during all embalming procedures.

Body donation is voluntary, and there is no compulsion. In this period of COVID-19 pandemic, we can deny acceptance of a donated body even if the body is COVID-19 negative, considering the risk of community transmission via the staff who are handling the body in hospital or the relatives accompanying the body, as there are chances of them being asymptomatic COVID-19 carriers.

Due to lack of clear cut guidelines regarding the acceptance or non-acceptance of a non COVID body, we may accept the donated body, provided the deceased is COVID negative, doesn't come from a containment zone, has no suspected history and is fulfilling other criteria for body donation.

Keeping in view of the risks associated with handling of dead bodies and the necessity of cadaveric dissection on donated bodies, every medical teaching institution should formulate the best practice guidelines for handling body donation and embalming procedures during the novel coronavirus pandemic.

**Vishram Singh, Rohini Pakhiddey[1]**

*Department of Anatomy, Adjunct Visiting Faculty, Kasturba Medical College, Mangalore, Manipal Academy of Higher Eduction, Manipal, Karnataka, [1]ESIC Dental College and Hospital, New Delhi, India*

***Address for correspondence:*** *Prof. Vishram Singh, Adjunct Visiting Faculty, Department of Anatomy, KMC Manglore, Manipal Academy of Higher Education, Karnataka, India. Email: drvishramsingh@gmail.com*

## References

1. Khan AN, Baig S, Zain S. Importance of cadaveric dissection in learning gross anatomy. Pak J Med Dent 2014;4:31-5.
2. Aruna V. Teaching learning methods in medical education-merits and demerits. Int J Res Rev 2019;6:215-21.
3. Government of India. Covid-19: Guidelines on Dead Body Management. 1st ed.. New Delhi, India: Government of India, Ministry of Health and Family Welfare, Directorate General of Health Services (EMR Division); 2020.
4. Hindson, J. COVID-19: Faecal – Oral transmission? Nat Rev Gastroenterol Hepatol 2020;17:259.
5. World Health Organization (WHO). Infection Prevention and Control of Epidemic-and Pandemic Prone Acute Respiratory Infections in Health Care. Geneva: World Health Organization; 2014.
6. Kampf G, Todt D, Pfaender S, Steinmann E. Persistence of coronaviruses on inanimate surfaces and their inactivation with biocidal agents. J Hosp Infect 2020;104:246-51.
7. Finegan O, Fonseca S, Guyomarc'h P, Morcillo Mendez MD, Rodriguez Gonzalez J, Tidball-Binz M, *et al*. International Committee of the Red Cross (ICRC): General Guidance for the management of the dead related to COVID-19. Forensic Sci Int 2020;2:129-37.
8. Shidham VB, Frisch NK, Layfield LJ. Severe acute respiratory syndrome coronavirus 2 (the cause of COVID 19) in different types of clinical specimens and implications for cytopathology specimen: An editorial review with recommendations. Cytojournal 2020;17:7.
9. World Health Organization (WHO). Infection Prevention and Control for the Safe Management of a Dead Body in the Context of COVID-19. -1. Interim Guidance. World Health Organization; 24 March, 2020.
10. Royal College of Pathologists. Briefing on COVID-19: Autopsy Practice Relating to Possible Cases of COVID-19 (2019-nCov, Novel Coronavirus from China 2019/2020); 2020a.



**Article Info**

**Received:** 05 September 2020
**Accepted:** 07 September 2020
**Available online:** ***

**Access this article online**

Quick Response Code:

**Website:** www.jasi.org.in

**DOI:** 10.4103/JASI.JASI_173_20

**How to cite this article:** Singh V, Pakhiddey R. Acceptance of donor bodies and their embalming during COVID-19 period: A challenge to anatomists. J Anat Soc India 2020;XX:XX-XX.

Original Article

# Morphometric Variations of Nasal Parameters in Gujarati Population: An Anatomical Study

**M. M. Rohith, Jyotirmoy Roy, Abraham Johnson**

*Laboratory of Forensic Odontology, Institute of Forensic Science, Gujarat Forensic Sciences University, Gujarat, India*

## Abstract

**Introduction:** Nasal morphology is an important factor in forensic investigations and facial reconstructive procedures. Found to be strongly related to ethnicity and environmental factors, and known to be sexually dimorphic, the study of nasal parameters is useful in forensic facial reconstruction. The aim of the study is to evaluate the nasal morphological characteristics of the Gujarati population as an indicator for personal identification and to assess the prevalent nasal morphology of the study population determined. **Material and Methods:** The study involved randomly selected 180 healthy subjects (90 males and 90 females) between three age groups. Nasal width and nasal height were measured using a digital vernier caliper, and nasal index was calculated along with other parameters. The data were statistically analyzed. **Results:** The mean nasal width for male and female was 38.23 mm and 34.94 mm while the mean nasal height was 47.59 mm and 44.35 mm, respectively. The mean nasal index for male subjects (81.08) was also higher than for female subjects (77.30). The morphological classification showed the mesorrhine nose type as the most prevalent among both the males (58.88%) and females (66.66%). **Discussion and Conclusion:** The population under the study exhibits mesorrhine type of the nose and shows sexual dimorphism in the values of nasal measurements. Thus, the current study is valuable not only in forensic facial reconstruction but also as an added method for determining the gender and ethnicity of an unidentified individual.

**Keywords:** *Anthropometry, forensic identification, morphology, nasal height, nasal index, nasal width, sexual dimorphism, variation*

## Introduction

The qualitative and quantitative assessment of the human body has a long history dating back as far as the middle kingdom where local artisans used square grid patterns to produce standard proportions of human figures establishing different formula for males and females.[1] Nasal anthropometry involves the systematic measurement and analysis of the human nose which aims to provide baseline data for the study of different human populations.

Nose is a pyramidal structure located in the midline of the mid-face and attached to the facial skeleton made up of bones, cartilages, muscles, and soft tissue.[2] During racial evolution, nose shows a high degree of variation.[3] Both genetic and environmental factors influence the shape of the nose.[4] Due to the natural selection, in cold and dry climates, the nose tends to be narrower, while in warmer and moist environment, it is broader in humans.[4] Hence, the anthropometric parameters changes with ethnicity, race, and gender. These baseline data are of great importance in nasal reconstructive surgeries, forensic science, facial reconstruction, and anthropology.

Any alteration in the shape of the nose leads to a gross change in the facial appearance of an individual. Hence, population-specific data regarding the nasal morphology are of utmost importance for the plastic surgeons in reconstructive studies and forensic investigators in facial identification and reconstructions. In any nasal reconstructive procedure, there should be a thorough analysis of the nasal morphology of population of a particular geographic area. Hence, plastic surgeons and forensic investigators both can benefit from a regional database regarding nasal anthropometry.

Nasal index is measured as the ratio of maximum breadth of nose with the maximum length of nose multiplied by 100, which helps characterize nasal morphology

**How to cite this article:** Rohith MM, Roy J, Johnson A. Morphometric variations of nasal parameters in Gujarati population: An anatomical study. J Anat Soc India 2020;69:XX.



**Article Info**

**Received:** 07 October 2019
**Accepted:** 28 July 2020
**Available online:** ***

***Address for correspondence:***
*Dr. Abraham Johnson, Institute of Forensic Science, Gujarat Forensic Sciences University, Sector 9, Near DFS Head Quarter, Gandhinagar 382 007, Gujarat, India.*
*E-mail: drabrahamjohnson4000@yahoo.com*

**Access this article online**

**Website:** www.jasi.org.in
**DOI:** 10.4103/JASI.JASI_139_19
**Quick Response Code:**

into five types.[5] Thus, it is clearly understood that the study and comparison of nasal index form the basis of racial, ethnic, and gender determination among different populations.

It is noted that Berom, Igbos, Yorubas, and Ijaws ethnic tribes from African region fall under the platyrrhine nose type, whereas Western Uttar Pradesh region and South Indian males have mesorrhine type of nose and females have leptorrhine type of nose.[6-9] At present, there are very little data about the nasal morphology of Gujarati population. Therefore, the present study aims toward measuring and analyzing the nasal parameters of Gujarati population, thereby obtaining the mean nasal index and assessing the sexual dimorphism related to nasal morphology. The study also tries to establish the distribution of basic nose types, shape of the nose, nasal tip angle, and nostril model in Gujarati population to provide the baseline anthropometrical data for nasal reconstructive surgeries, forensic science, and anthropological studies.

## Material and Methods

The study group consisted of 180 subjects, comprising 90 males and 90 females, in the age range of 20 years and above who were randomly chosen. They were further divided into three age groups, i.e., 20–40 years, 41–60 years, and 61 years onward [Table 1]**.** All the subjects were volunteers and were made aware of the study. Written consent was also obtained from each and every individual. The subjects were included in the study after recording demographic data, brief history of the present illness, and medical/surgical history. Apparently healthy individuals with average-to-good built and no visible facial deformity were included, while those with hereditary facial asymmetries, history of esthetic treatment or orthognathic surgery, history of maxillofacial trauma, and history or clinical characteristics of any type of systemic disorders such as bone diseases, nutritional diseases, and endocrinal diseases were excluded. Total six parameters of the nasal structure were included in this study and they are as follows.

1. Nasal breadth
2. Nasal height
3. Nasal index
4. Nose tip angle
5. Nostril model
6. Nose shape from lateral aspect.

The nasal breadth was measured from the alare (al) of the one side to the alare (al) of the other side by using a vernier caliper. The nasal height was measured from the nasion (n) (a fixed point between the eyes) to the subnasale (nasolabial junction) [Figure 1]. The nose tip angle is an internal angle formed between the line drawn from nasion (n) to pronasale (prn) and the line connecting pronasle (prn) and the subnasale (sn) [Figure 2]. The angle was measured by placing a protractor on the lateral aspect of the nose. The horizontal reference line of the protractor was made parallel to that of the prn–sn line, and the angle formed by the n–prn line in relation to the prn–sn line was recorded [Figure 2]. The nasal index was calculated from the nasal breadth and the nasal height as the formula for nasal index is given below:

$$\text{Nasal index} = \frac{\text{Nasal breadth}}{\text{Nasal height}} \times 100$$

Based on the nasal index, the general nose shape was determined to be one of the following types.[5]

1. Hyperleptorrhine (≤54.9) – Very long and narrow nose
2. Leptorrhine (55–69.9) – Long and narrow nose

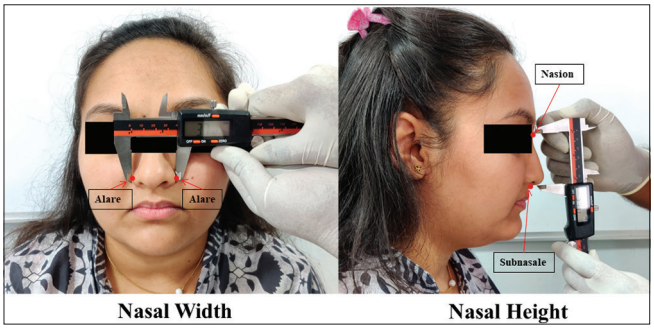


**Figure 1: Measurement of nasal width and nasal height**

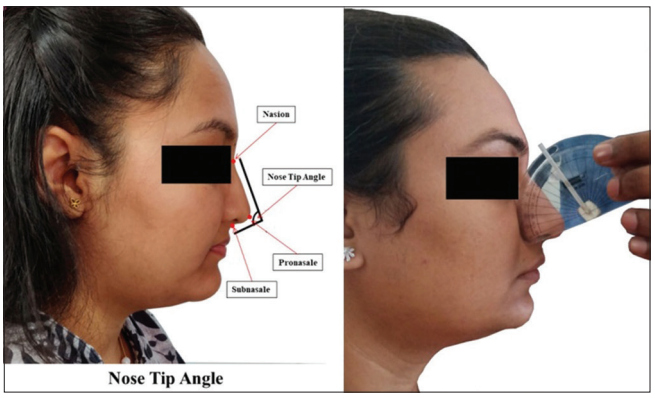


**Figure 2: Measurement of nasal tip angle**

**Table 1: Age group and number of participants**

| | Number of subjects | | | Mean age (years) | | |
|---|---|---|---|---|---|---|
| | Male | Female | Total | Male | Female | Total |
| Group 1 - 21-30 years | 30 | 30 | 60 | 23.6 | 22.07 | 22.79 |
| Group 2 - 31-40 years | 30 | 30 | 60 | 35.78 | 34.42 | 35.21 |
| Group 3 - 41 years and above | 30 | 30 | 60 | 57.20 | 51.36 | 55.37 |

3. Mesorrhine (70–84.9) – Moderate nose of moderate size
4. Platyrrhine (85–99.9) – Broad nose
5. Hyperplatyrrhine (≥100) – Very broad nose [Figure 3].

The nose shape from the lateral aspect and the nostril model were determined by comparing the parameters with the chart provided by a study done by Uzun and Ozdemir[10] [Figure 4].

### Statistical analysis

The data recorded were compiled using MS Excel Spreadsheet (version-2010) and subjected to statistical analysis using Statistical Package of the Social Sciences Version 20. (SPSS 20.0, IBM, Armonk, NY, United States of America). The existence of significant differences between the means of all the parameters for the gender was analyzed using independent Student's *t*-test. One-way ANOVA was also performed to determine any significant changes in the parameter values due to age progression. A $P < 0.05$ was considered to be statistically significant.

## Results

### Nasal index

The nasal index showed statistically significant difference between males and females in all the age groups. The nasal index was found to be higher for males than females in all the age groups [Table 2]. Based on the nasal index, the general shape of the nose was also determined. Mesorrhine type of nasal shape was found to be prevalent for both males and females [Table 3].

### Nasal width and nasal height

Nasal width and height were found to be significantly different among males and females. Both of the metric parameters were found to be higher for males and lower for females. One-way ANOVA was performed for these parameters which revealed that these parameters were significantly different among the three age groups. The data suggest that these metric parameters increase with age. The results are described in Table 4.

### Nasal shape from lateral aspect and nostril model

The nasal shape from the lateral aspect and nostril model was determined by a chart provided by Uzun and Ozdemir.[10] In case of the nasal shape from lateral aspect, "Type III" was found to be prevalent for males, and "Type I" was common for females [Table 5]. "Type II" nostril model was found to be prevalent for both male and female [Table 6].

### Nasal tip angle

The minimum value for this parameter was found to be 45° and the maximum value was 89°. Based on these data, the

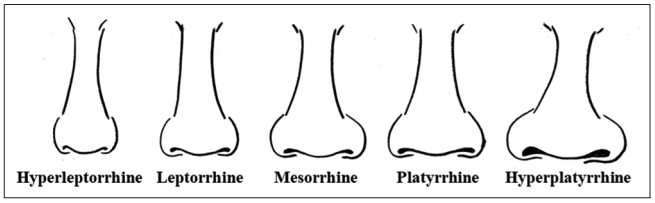


**Figure 3: Variations in the nasal morphology based on nasal index**

**Table 2: Nasal index**

| Nasal index | Male | | | | Female | | | |
|---|---|---|---|---|---|---|---|---|
| | Group 1 | Group 2 | Group 3 | Total | Group 1 | Group 2 | Group 3 | Total |
| M | 81.89 | 81.19 | 80.17 | 81.08 | 76.56 | 78.11 | 77.25 | 77.30 |
| SD | 9.40 | 6.98 | 8.62 | 8.61 | 8.45 | 8.41 | 8.76 | 9.02 |

M: Mean value, SD: Standard deviation

**Table 3: Prevalence of general nose shape based on nasal index**

| | Type I, *n* (%) | Type II, *n* (%) | Type III, *n* (%) | Type IV, *n* (%) | Type V, *n* (%) |
|---|---|---|---|---|---|
| Male | 0 (0) | 8 (8.88) | 53 (58.88) | 27 (30) | 2 (2.22) |
| Female | 0 (0) | 12 (13.33) | 60 (66.66) | 16 (17.77) | 2 (2.22) |

Type I: Hyperleptorrhine, Type II: Leptorrhine, Type III: Mesorrhine, Type IV: Platyrrhine, Type V: Hyperplatyrrhine

**Table 4: Mean value and standard deviation of different metric nasal parameters among male and females of different age groups**

| Sex | Nasal parameters | Different age groups, mean±SD | | |
|---|---|---|---|---|
| | | 20-30 years (mm) | 31-40 years (mm) | 41 years and above (mm) |
| Male | Nasal width | 37.51±2.306 | 38.44±2.17 | 38.75±3.10 |
| | Nasal height | 46.17±4.335 | 47.54±3.02 | 49.06±2.87 |
| Female | Nasal width | 33.64±2.54 | 35.17 ±1.95 | 36.01±3.30 |
| | Nasal height | 43.64±3.24 | 44.15±3.32 | 45.28±4.58 |

SD: Standard deviation

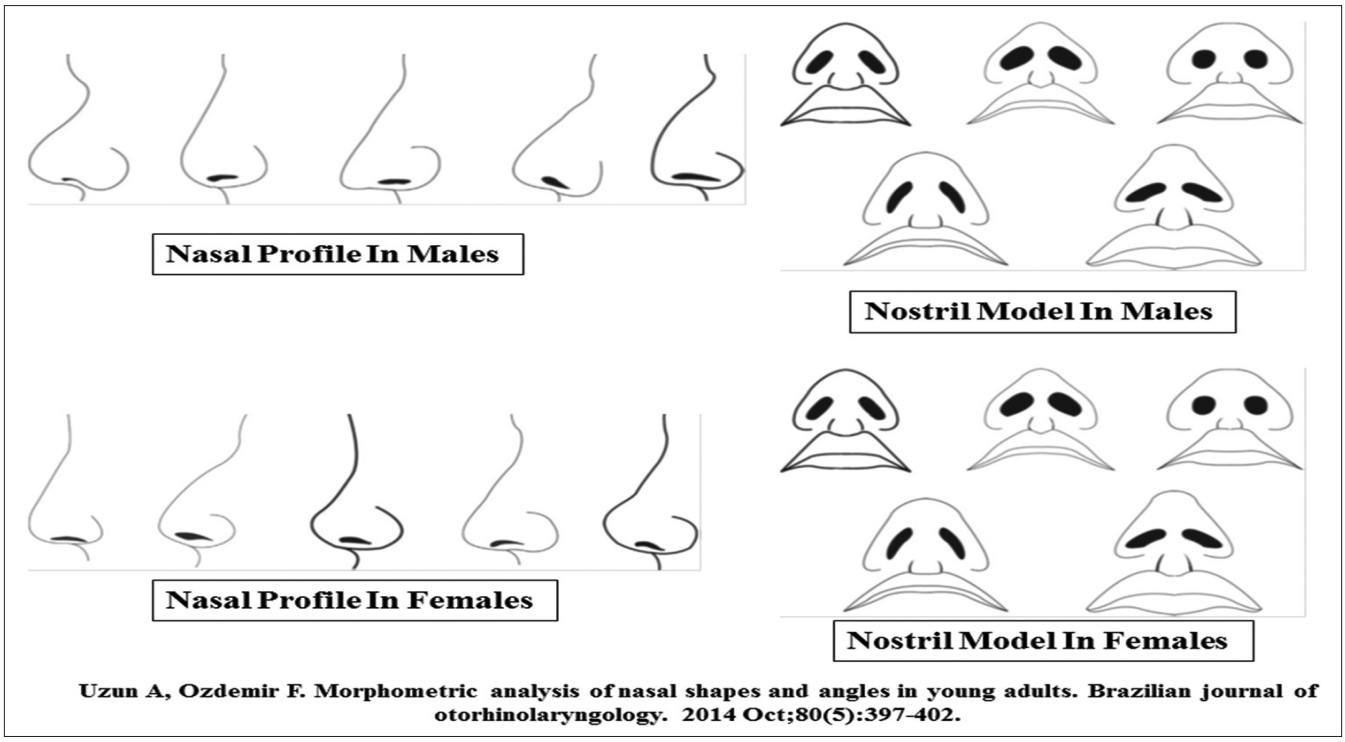


**Figure 4: Reference anatomical scale for nasal parameters**

**Table 5: Prevalence of nasal shape from lateral aspect**

| | Type I, *n* (%) | Type II, *n* (%) | Type III, *n* (%) | Type IV, *n* (%) | Type V, *n* (%) |
|---|---|---|---|---|---|
| Male | 6 (6.66) | 13 (14.44) | 35 (38.88) | 29 (32.22) | 7 (7.77) |
| Female | 45 (50) | 9 (10) | 3 (3.33) | 22 (24.44) | 11 (12.22) |

**Table 6: Prevalence of nostril model**

| | Type I, *n* (%) | Type II, *n* (%) | Type III, *n* (%) | Type IV, *n* (%) | Type V, *n* (%) |
|---|---|---|---|---|---|
| Male | 5 (5.55) | 55 (61.11) | 14 (15.55) | 13 (14.44) | 3 (3.33) |
| Female | 3 (3.33) | 58 (64.44) | 17 (18.88) | 8 (8.88) | 4 (4.44) |

nasal tip angle was categorized into five types, and they are as follows:

- Type I – 41°–50°
- Type II – 51°–60°
- Type III – 61°–70°
- Type IV – 71°–80°
- Type V – 81°-90°.

"Type IV" (71°–80°) was found to be most prevalent in both males and females [Table 7 and Figure 5].

The data derived from all the parameters can be used to establish the difference in the nasal index among various racial groups. This may help in identification and may be used as an add-on parameter for forensic identification [Table 8].

## Discussion

Nose being the most prominent structure of the face is of great significance in both medical science and forensic science. Because of the variations in the nasal parameters, many studies have been carried out on different population to establish the racial and ethnic differences. Previous studies have shown that there is a marked variation of nasal parameters without any specific pattern until 20 years of age. After the age of 20 years, the morphometric changes in the nose occur in a stable manner.[11,12]

The study conducted on Yoruba tribe of Africa by Oladipo *et al.* suggests that males have mean nasal index of 90 and females have 88.1.[7] Another study conducted by Esomonu *et al.* shows male and female mean nasal index to be 94.65 and 90.33, respectively.[13] Patil *et al.* conducted a study on the South Indian population and suggested that the mean nasal index of males was 84.91 and of females was 67.75.[8] However, the current study on Gujarati populations shows mean nasal index of males to be 81.08 ± 8.61 and mean nasal index of females to be 77.30 ± 9.02.

This study also shows a significant difference in the value of nasal index among males and females, where the Gujarati

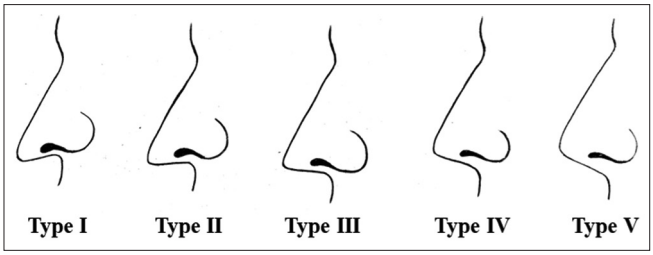


**Figure 5: Variations in nasal tip angle among Gujarati population**

**Table 7: Prevalence of nasal tip angle**

| | Male, *n* (%) | Female, *n* (%) |
|---|---|---|
| Type I - 40°-50° | 1 (1.11) | 2 (2.22) |
| Type II - 51°-60° | 7 (7.77) | 5 (5.55) |
| Type III - 61°-70° | 33 (36.66) | 28 (31.11) |
| Type IV - 71°-80° | 39 (43.33) | 39 (43.33) |
| Type V - 81°-90° | 10 (11.11) | 16 (17.77) |

**Table 8: Comparison of other studies with the present study**

| Race/population | Nasal index | Author(s), Year |
|---|---|---|
| Nigerian Igbos | 85.7 | Akpa *et al*., 2003 |
| Ijaws | 96.37 | Oladipo *et al*., 2007 |
| Yorubas | 89.2 | Oladipo *et al*., 2007 |
| Igbos | 94.1 | Oladipo *et al*., 2007 |
| Bheel-Meena males(Rajasthan) | 83 | Gangrade *et al*., 2012 |
| Bheel-Meena females(Rajasthan) | 79.73 | Gangrade *et al*., 2012 |
| Brahmin Males (Punjab) | 70.02 | Kaushal *et al*., 2013 |
| Brahmin Females (Punjab) | 69.89 | Kaushal *et al*., 2013 |
| Majhabi-Sikh Males (Punjab) | 76.51 | Kaushal *et al*., 2013 |
| Majhabi-Sikh Females (Punjab) | 68.95 | Kaushal *et al*., 2013 |
| Muslim Males (Punjab) | 67.04 | Kaushal *et al*., 2013 |
| Muslim Females (Punjab) | 69.38 | Kaushal *et al*., 2013 |
| Males(Bekwarra ethnic group) | 94.65 | Esomonu *et al*., 2013 |
| Females(Nigeria-Cross River State) | 90.33 | Esomonu *et al*., 2013 |
| Hindu males (Gwalior region) | 80.59 | Sharma *et al*., 2014 |
| Hindu females (Gwalior region) | 77.29 | Sharma *et al*., 2014 |
| South Indian males | 84.91 | Patil *et al*., 2014 |
| South Indian females | 67.75 | Patil *et al*., 2014 |
| Berom males | 93.66 | Ekwere *et al*., 2015 |
| Berom females | 92.52 | Ekwere *et al*., 2015 |
| Males (Western Uttar Pradesh) | 75.86 | Ray *et al*., 2016 |
| Females (Western Uttar Pradesh) | 72.08 | Ray *et al*., 2016 |
| Gujarati males | 81.08±8.61 | Present study |
| Gujarati females | 77.30±9.02 | Present study |

males were found to be having higher value of nasal index than females. This is in accordance with a previous study conducted by Sharma *et al*.[5] Another study conducted on the Bheel-Meena tribe by Gangrade and Babel also is in correspondence with this study.[14] The study conducted by Kaushal *et al*., on various ethnic groups belonging to Punjab, has also concluded significant sexual dimorphism in the value of nasal index and suggested that males are having higher value for nasal index than females in most of the ethnic groups.[15]

The present study found the nasal breadth and nasal height of Gujarati males to be higher than that of the females in all the age groups ($P < 0.05$). This difference of nasal width between males and females was earlier described by Akpa *et al*. (2003) in their study on Igbo tribe.[16] Esomonu *et al*. also stated this variation in their study on the Bekwarra ethnic group.[13] A study conducted by Patil *et al*. on South Indian population also corroborates with the result of the current study.[8]

The present study also concludes that the general shape of nose based on the nasal index was mesorrhine for both males and females. It was also noted that the nasal width and nasal height increase with age. Sforza *et al*. demonstrated similar findings in their skeletal maturity study where they correlated the increase in nasal linear measurements with microscopic changes of the muscle and cartilage of the mid face region.[17] Numerous studies have also concluded that the elasticity and resilience of the skin due to aging attribute to the increase in the linear dimensions of nose.[18-20]

From the above data, we can understand that in the Gujarati population, the mean nasal index, nasal height, and nasal width values are having significant sexual dimorphism. Hence, we can use nasal index as a useful parameter for the identification of gender in Gujarati population. Nasal anthropometric and morphologic study of the various ethnic groups of India will help to establish a baseline database of all the nasal parameters as the parameters changes with geographic and environmental conditions. These data will be of great importance in corrective surgeries of the nasal and paranasal structures, forensic facial identification, forensic facial reconstruction, and future anthropological studies.

## Conclusion

Nose is the most prominent feature of the face, and it shows significant variation among different races. Thus, it is a reliable parameter for the determination of racial orientation of an individual. The significant differences in the metric and morphologic parameters may also be useful for the medical fraternity for reconstructive or corrective surgery of the nose. Determination of gender is an important aspect of forensic identification which ultimately helps in the establishment of identity of an individual. This study shows significant differences in the mean values of the

nasal index, nasal height, and nasal width, which may help in forensic facial identification and gender determination. Thus, it can be stated that the nasal metric and nonmetric parameters are of great importance in medical science, forensic science, and anthropological studies. With further research involving a large sample size, the parameters will be validated. Subsequent studies with sample from various parts of the country will establish the importance of nasal parameters in medical, as well as forensic science.

### Declaration of patient consent

The authors certify that they have obtained all appropriate patient consent forms. In the form, the patients have given their consent for their images and other clinical information to be reported in the journal. The patients understand that their names and initials will not be published and due efforts will be made to conceal their identity, but anonymity cannot be guaranteed.

### Financial support and sponsorship

Nil.

### Conflicts of interest

There are no conflicts of interest.

## References

1. Slice DE, editor. Modern Morphometrics in Physical Anthropology. Springer Science & Business Media; 2006. p. 1.
2. Standring S, editor. Gray's Anatomy: The Anatomical Basis of Clinical Practice. Elsevier Health Sciences; 2015. p. 556.
3. Grant M. The passing of the great race. The Palingenesis Project (Wermod and Wermod Publishing Group); 2012. p. 24.
4. Hall RL, Hall DA. Geographic variation of native people along the Pacific Coast. Hum Biol 1995;67:407-26.
5. Sharma SK, Massarat J, Raj LS, Sudhir S, Akhilesh T, Vipendra B. Anthropometric Comparison of nasal parameters between male and female of Gwalior region. J Dent Med Sci 2014;1:57-62.
6. Ekwere EO, Yohanna UM, Lawal IS. A study of the nasal index of Berom students in Plateau State Polytechnic, Jos. Ann Bioanthropol 2015;3:70-2.
7. Oladipo GS, Olabiyi AO, Oremosu AA, Noronha CC. Nasal indices among major ethnic groups in Southern Nigeria. Sci Res Essays 2007;2:20.
8. Patil GV, Kumar S, Apoorva D, Thejeswari D, Sharif J, Sheshgiriand C, Sushanth NK. Study on nasal index in south Indian population. Int J Curr Res 2014;6:8163-4.
9. Ray SK, Saha K, Kumar A, Banjare S. Anthropometric study of nasal index among the population of Western Uttar Pradesh region. Int J Sci Study 2016;4:65-70.
10. Uzun A, Ozdemir F. Morphometric analysis of nasal shapes and angles in young adults. Braz J Otorhinolaryngol 2014;80:397-402.
11. Hegazy AA. Anthropometric study of nasal index of Egyptians. Int J Anat Res 2014;2:761-7.
12. Zankl A, Eberle L, Molinari L, Schinzel A. Growth charts for nose length, nasal protrusion, and Philtrum length from birth to 97 years. Am J Med Genet 2002;111:388-91.
13. Esomonu UG, Ude RA, Lukpata PU, Nandi EM. Anthropometric study of the nasal index of Bekwara ethnic group of cross river state, Nigeria. Int Res J Appl Basic Sci 2013;5:1262-5.
14. Gangrade PR, Babel H. Anthropometric study of the nasal index of the Bheel-Meena tribe of Southern Rajasthan. Int J Cur Res Rev 2012;4:88-91.
15. Kaushal S, Patnaik VV, Kaur P. Somatometric analysis of nasal morphology in the endogamous groups of Punjab. Hum Biol Rev 2013;2:1-11.
16. Akpa AO, Ugwu C, Maliki AO, Maliki SO. Morphometric study of the nasal parameters in Nigerian Igbos. J Exp Clin Anatomy 2003;2:24-5.
17. Sforza C, Grandi G, De Menezes M, Tartaglia GM, Ferrario VF. Age- and sex-related changes in the normal human external nose. Forensic Sci Int 2011;204:205.e1-9.
18. Ito I, Imada M, Ikeda M, Sueno K, Arikuni T, Kida A. A morphological study of age changes in adult human auricular cartilage with special emphasis on elastic fibers. Laryngoscope 2001;111:881-6.
19. Farkas LG, Eiben OG, Sivkov S, Tompson B, Katic MJ, Forrest CR. Anthropometric measurements of the facial framework in adulthood: Age-related changes in eight age categories in 600 healthy white North Americans of European ancestry from 16 to 90 years of age. J Craniofac Surg 2004;15:288-98.
20. Coleman SR, Grover R. The anatomy of the aging face: Volume loss and changes in 3-dimensional topography. Aesthet Surg J 2006;26:S4-9.

Original Article

# Morphometry of Sphenoid Air Sinus and its Ostium for Surgical Relevance: A Cadaveric Study

**Senthil Kumar B, Panneer Selvi G**

*Department of Anatomy, Vinayaka Mission's Kirupananda Variyar Medical College and Hospital, Vinayaka Mission's Research Foundation (Deemed to be University), Salem, Tamil Nadu, India*

## Abstract

**Introduction:** The sphenoid air sinuses and their ostia are highly variable structures. The ostia are located on either side of the midline. The exact location of the sphenoid ostium is very much essential in endoscopic sinus surgeries as well as for the transsphenoidal hypophyseal approach. The present study was done to determine the anatomical location of the sphenoid sinus ostium in relation to the surrounding landmarks. It is a descriptive study. **Material and Methods:** The study was carried out in the Department of Anatomy, VMKV Medical College and Hospital, Salem, on forty sagittal head and neck sections of adult formalin-fixed cadavers. The length and width of the sinus were measured. The shape and type of the sphenoid sinus ostia were also noted. The distance of the sinus ostium from various landmarks was measured using Vernier calipers. The morphometric parameters were compared by Student's *t*-test on both sides. **Results:** Most of the specimens showed sellar variety than presellar variety on both right and left sides. The shape of the sphenoid sinus ostia was predominantly round shape, followed by oval and slit shape. The length and width of the sinus on the right side were less when compared to the left side. The distance between the sphenoidal ostia and several landmarks showed no significant difference except the distance from ostium to superior concha. **Discussion and Conclusion:** During the endoscopic approach of the sphenoid sinus ostium, it is not always easy to locate the ostium. The present morphometric study will serve as a guideline for the endoscopic surgical approach of the sphenoid sinus ostium using the various anatomical landmarks.

**Keywords:** *Concha, sphenoid ostium, transsphenoidal hypophyseal approach*

## Introduction

The advancement in endoscopic sinus surgery (ESS) had facilitated a clear cut idea about anatomy and pathophysiology of paranasal air sinuses for surgeons. The surgeon aims to aerate the sinuses and restore the mucociliary clearance so that the paranasal air sinuses are retained back to normal function.[1] ESS helps the surgeons for the diagnosis and treatment of sinusitis.[2] The anatomy of sinuses can be visualized clearly by high-resolution computed tomography (CT) which also helps to diagnose the mucosal disease.[3] The normal anatomy along with any variations of sinus structure, its pathologic appearances in disease condition, has to be well understood by the surgeons and radiologists to provide appropriate patient care.[4] Anatomic variation of the sphenoid sinus is not so common, but if it is present, then it may complicate the surgery, and henceforth, the knowledge of these variations should be known precisely to surgeons. Accurate evaluation of the variations is possible with preoperative CT scans of the sinuses.[5] A comprehensive knowledge of the variable regional anatomy of the sphenoid sinus will reduce the surgical complications that occur during the transsphenoidal approach and functional ESS.[6-9] The anatomic variations of the sphenoid sinus predispose to recurrent or chronic sinusitis.[10]

The body of the sphenoid bone is pneumatized to form the sphenoid air sinus. The pneumatization of bones of the skull base is most common. The sphenoid sinus and adjacent bony structures may show various degrees of pneumatization. Sometimes, a pneumatization can be so extensive that it reaches the anterior clinoid process (ACP), foramen rotundum, vidian canal, pterygoid process (PP), or maxilloethmoid recess. The ACP and PR are the frequent sites of pneumatization in the skull base. The clinical significance of the pneumatization requires clarification.[5]

**How to cite this article:** Kumar SB, Selvi PG. Morphometry of sphenoid air sinus and its ostium for surgical relevance: A cadaveric study. J Anat Soc India 2020;69:XX-XX.



**Article Info**

**Received:** 22 August 2019
**Accepted:** 04 August 2020
**Available online:** XXXX

***Address for correspondence:***
*Dr. Senthil Kumar B, Department of Anatomy, Vinayaka Mission's Kirupananda Variyar Medical College and Hospital, Vinayaka Mission's Research Foundation (Deemed to be University), Salem - 636 308, Tamil Nadu, India.*
*E-mail: skdrchinu88@ gmail. com*

**Access this article online**

**Website:** www.jasi.org.in
**DOI:** 10.4103/JASI.JASI_110_19
**Quick Response Code:**

The sphenoid sinus communicates with the nasal cavity through sphenoid ostia, which are located on each side of the midline. The sphenoid air sinus opens into the sphenoethmoidal recess. Sphenoid sinuses and their ostia are highly variable structures. The sinus is related to various structures such as optic nerve in its superolateral wall, carotid artery in the lateral wall, trigeminal nerve in the inferolateral wall, and the vidian nerve in the floor of the sinus.[11] The above structures are separated from the sinus only by a thin bony wall/septum of around 0.5 mm thickness, and even sometimes, the bony wall is replaced by bony dehiscence.[12] The pituitary gland lies on the roof of the sphenoidal air sinus which is separated only by a thin bony wall. The sphenoidal air sinus is related to the cavernous sinus and internal carotid artery laterally which may be accidently injured during the transsphenoidal approach of the pituitary gland. The extent of pneumatization of sphenoid air sinus is highly variable.[13] The exact location of the sphenoid ostium is very much essential in ESSs as well as the transsphenoidal hypophyseal approach. During the endoscopic approach of the sphenoid sinus ostium, it is not always easy to locate the ostium; only few studies were carried out in India on this perspective. The accessibility of the sphenoid sinus is most difficult as it is known for the most variable cavity of the human body.[14] The present study will serve as a guideline for identifying the location of sinus ostium during the endoscopic surgical approach using the various anatomical landmarks.

## Material and Methods

The present descriptive study was carried out in the Department of Anatomy, VMKV Medical College and Hospital, Salem, on forty sagittal head and neck sections of adult formalin-fixed cadavers after obtaining ethical clearance from the institution reference number (VMKVMC/IEC/18/51). The length of the sinus was measured from the lower margin of the sphenoid ostium to the midpoint of the posterior wall of the sphenoid sinus, whereas the width was measured from the midpoint of the roof to the midpoint of the floor of the sphenoid sinus. The shape and type of sphenoid sinus ostia were noted [Figures 1 and 2]. The distance of the ostium from the major anatomical landmarks was measured using Vernier calipers. The various surgical relevant anatomical landmarks used include midpoint of choana, nasion, anterior end of the superior concha, and midpoint of basisphenoid [Figure 1]. The extent of pneumatization toward the sella was also noted.

## Results

Majority of specimens showed sellar variety (23, 57.5%) than presellar variety (17, 42.5%) on both right and left sides. The shape of the sphenoid sinus ostia was predominantly round shape (16, 40%), followed by oval

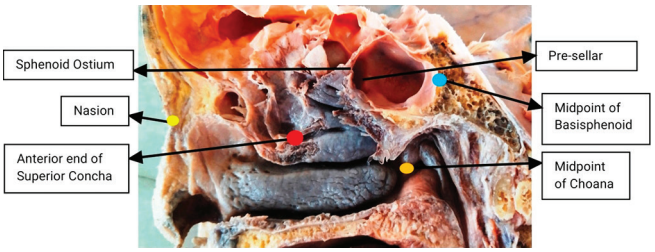


**Figure 1: Anatomical landmarks for measurements and types of sphenoid air sinus**

(12, 30%) and slit shape (12, 30%). The morphometry of sphenoidal air sinus was measured and compared between the right and left sides by independent *t*-test [Table 1]. The length of the sinus on the right side was less when compared to the left side. The width of the sinus showed a significant difference among the sides and was found to be more on the left side when compared to the right side. When analyzed, the morphometric data of the sphenoid air sinus were found to be statistically significant ($P < 0.01$) [Table 1].

The distance of the ostium from the various anatomical landmarks was measured and compared between the sides, and the distance from the ostium to superior concha was found to be significant, whereas other measurements were insignificant when compared [Table 2]. The various surgical relevant anatomical landmarks used include choana, nasion, anterior end of the superior concha, and basisphenoid.

## Discussion

### Type of sphenoid sinus pneumatization

The sphenoid pneumatization can be classified as three main types.[15] Type 1 is the conchal type or the fetal type which shows a small sinus separated from the sella turcica by a very thin layer of trabecular bone. Type 2 is the presellar type or juvenile type and is pneumatized up to the level of sella turcica. Type 3 is the sellar type or adult type and is pneumatized below the sella or further posteriorly.[10] In a study done by Sareen *et al.*, the sellar type was found to be more frequent. It appears in 75%–86% of cases, followed by the presellar type which is found to be present in 10%–25%, followed by conchal type seen in only 2% of cases.[16] In a study done by Tan and Ong,[17] the sellar type was found in 55% of sinuses, followed by conchal (28%) and presellar type (17%). In another study, the sellar pneumatization was most common. Sellar pneumatization is an ideal anatomical configuration for transsphenoidal hypophysectomy because the bulge of the sella turcica floor is easily visualized in the operative field.[18,19] In the present study, the sellar variety was found in 23 (57.5%), whereas the presellar variety was found in 17 (42.5%) on both right and left sides together, whereas conchal type was not seen in any of the specimens as found by other authors Tan and Ong and Sareen *et al*.[17,18]

**Table 1: Morphometry of sphenoidal air sinus**

| Side | Length (cm) | Width (cm) |
|---|---|---|
| Right | 1.95±0.23 | 1.01±0.09 |
| Left | 2.84±0.13 | 1.68±0.11 |
| *P*.Value | 0.01** | 0.01** |

Values are expressed as mean±SEM, *n*=40 with 20 right side and 20 left side, #Nonsignificant, *Significant, **$P$<0.01. Statistical analysis – Independent *t*-test. SEM: Standard error of mean[10]

**Table 2: Measurement of sphenoidal ostium from various anatomical landmarks**

| Side | Mean±SD | | | |
|---|---|---|---|---|
| | SO-C (cm) | SO-N (cm) | SO-SC (cm) | SO-BS (cm) |
| Right | 3.30±0.10 | 4.94±0.27 | 1.80±0.15 | 3.94±0.28 |
| Left | 3.46±0.22 | 5.00±0.31 | 2.43±0.17 | 4.07±0.21 |
| *P*.Value | 0.72# | 0.81# | 0.01** | 0.75# |

SO: Sphenoid ostium, C: Choana, N: Nasion, SC: Anterior end of superior concha, BS: Basisphenoid. Values are expressed as mean±SEM, *n*=40 with 20 right side and 20 left side, #Nonsignificant, *$P$<0.05, **$P$<0.01. Statistical analysis – Independent *t*-test[10]

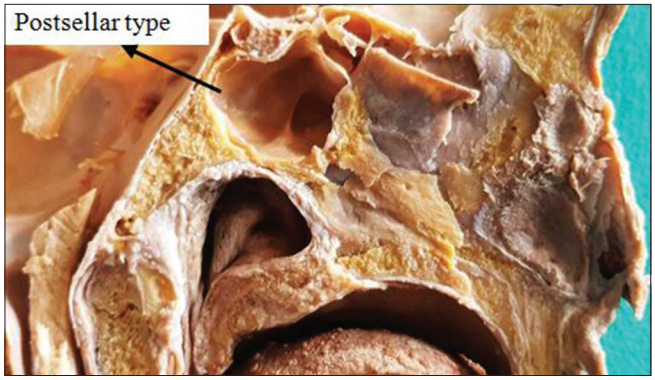


**Figure 2: Type of sphenoid air sinus**

## Shape of the sphenoid ostia

In a study done by D'Souza *et al*., the sphenoid sinus ostia were slit type in majority of the cases, followed by oval and round shape.[10] The round shape ostia were seen more on the left side compared to the right side. In another study, 70% of the ostia were found to be round in shape, whereas 28% were ovoid.[11] In the study, the sphenoid sinus ostia were predominantly round shape (16, 40%), followed by oval (12, 30%) and slit shape (12, 30%) irrespective of the sides.

## Morphometry of sphenoid air sinus

Ariji *et al*. and Ikeda *et al*. reported that the volume of paranasal air sinuses increases up to 20 years and then decreases as age advances.[20,21] Schatz and Becker observed that sphenoid sinus increases in size up to 15 years and thereafter maintains the same size and volume.[22] The sphenoid air sinus starts to develop rapidly after the age of 3 years and spreads back toward the sella turcica around the age of 7 years and reaches adult form at the age of 12 years. The maximum average of sphenoid sinus volume was 7.5 $cm^3$ and 8.2 $cm^3$ reported by Schatz *et al*.[23] In another study, the sphenoid sinus volume increased in both sexes up to 25 years (8.71 ± 2.44 $cm^3$) and decreased after the age of 25.[2] In the present study, the sphenoidal air sinus was measured and compared between the right and left sides [Table 1]; the volume was not measured as the study was done on specimen of sagittal section and hence only length and width were measured. The length of the sinus on the right side was less when compared to the left side. The width of the sinus showed a significant difference among the sides. When analyzed, the morphometric data of sphenoid air sinus were found to be statistically significant ($P$ < 0.01) [Table 1].

## Sphenoid ostium from various anatomical landmarks

The sphenoid sinuses are the most inaccessible paranasal sinuses when compared to all other sinuses.[24] The distance of the sphenoid ostium from various anatomical landmarks in comparison with other studies is tabulated [Table 3].

In the present study, the distance from ostium to superior concha was found to be significant, whereas other measurements were insignificant when compared between right and left. Kim *et al*.[25] suggested that the best anatomical reference that enables identification of the sphenoid ostium is the posteroinferior end of the superior turbinate, where each ostium is located medially and superiorly. The sphenoid ostium was identified at an average distance of 1.49 cm superior to the choana by Abuzayed *et al*.[26] In another study, the distance was 1.37 cm on the right side and 1.5 cm on the left side [Table 3].[10] In the present study, the distance between sphenoid ostium and choana was 2.30 cm on the right side and 2.46 cm on the left side and was considered to be the most reliable landmark to approach sphenoid ostium. The knowledge of the anatomical relationships of the sphenoid sinus is needed for the success of ESSs and to avoid the various intraoperative surgical complications.[27]

## Conclusion

During the endoscopic approach of the sphenoid sinus ostium, it is not always easy to locate the ostium. The present study will serve as a guideline for the endoscopic surgical approach of sinus ostium using the various anatomical landmarks. The four landmarks include choana, nasion, anterior end of the superior concha, and basisphenoid which will be helping to approach the sphenoid ostium. The study will be further extended in humans using CT scan. Accurate evaluation of the distance of the sphenoid ostium from the above landmarks will be possible with preoperative CT scans of the sinuses.

**Table 3: Comparison of distance of sphenoid ostium from various anatomical landmarks with previous studies**

| Mean distance (cm) | D'Souza *et al*.[10] | Present study |
|---|---|---|
| SO-C | | |
| Right | 1.37±0.33 | 2.30±0.10 |
| Left | 1.5±0.46 | 2.46±0.22 |
| SO-SC | | |
| Right | 1.52±0.30 | 1.80±0.15 |
| Left | 1.42±0.39 | 2.43±0.17 |
| SO-N | | |
| Right | 4.58±0.48 | 4.94±0.27 |
| Left | 4.49±0.25 | 5.00±0.31 |
| SO-BS | | |
| Right | 3.64±0.63 | 3.94±0.28 |
| Left | 3.62±0.60 | 4.07±0.21 |

SO: Sphenoid ostium, C: Choana, N: Nasion, SC: Anterior end of superior concha, BS: Basisphenoid

### Financial support and sponsorship

Nil.

### Conflicts of interest

There are no conflicts of interest.

## References

1. Miller AJ, Amedee RG. Functional anatomy of the paranasal sinuses. J La State Med Soc 1997;149:85-90.
2. Amedee R. Sinus anatomy and function. In: Bailey BJ, editor. Head and Neck Surgery- Otolaryngology. Vol. 1. Philadelphia: J.B. Lippincott Company; 1993. p. 342-9.
3. Kaluskar SK, Patil NP, Sharkey AN. The role of CT in functional endoscopic sinus surgery. Rhinology 1993;31:49-52.
4. Seirikci A, Bayazõt YA, Bayram M, Mumbu S, Güngör K, Kanlikama M. Variations of sphenoid and related structures. Eur Radiol 2000;10:844-8.
5. Jankowski R, Auque J, Simon C, Marchal JC, Hepner H, Wayoff M. Endoscopic pituitary tumor surgery. Laryngoscope 1992;102:198-202.
6. Stankiewicz JA. Complications of endoscopic nasal surgery. Occurrence and treatment. Am J Rhinol 1987;1:45-9.
7. Buus DR, Tse DT, Farris BK. Ophthalmic complications of sinus surgery. Ophthalmology 1990;97:612-9.
8. Cappabianca P, Cavallo LM, Colao A, Del Basso De Caro M, Esposito F, Cirillo S, *et al*. Endoscopic endonasal transsphenoidal approach: Outcome analysis of 100 consecutive procedures. Minim Invasive Neurosurg 2002;45:193-200.
9. Bolger WE, Butzin CA, Parsons DS. Paranasal sinus bony anatomic variations and mucosal abnormalities: CT analysis for endoscopic sinus surgery. Laryngoscope 1991;101:56-64.
10. D'Souza A, Ankolekar VH, Das A, Kotian SR, Hosapatna M, D'Souza AS. Surgical relevance of sphenoid sinus and its ostium: An anatomical study. J Clin Exp Res 2013;1:43-6.
11. Clemente MP. Anatomy of the paranasal sinuses. In: Levine HL, Clemente MP, editors. Sinus Surgery: Endoscopic and Microscopic Approaches. New York: Thieme; 1996. p. 25-8.
12. Jho HD, Carrau RL. Endoscopic endonasal transsphenoidal surgery: Experience with 50 patients. J Neurosurg 1997;87:44-51.
13. Teatini G, Simonetti G, Salvolini U, Masala W, Meloni F, Rovasio S, *et al*. Computed tomography of the ethmoid labyrinth and adjacent structures. Ann Otol Rhinol Laryngol 1987;96:239-50.
14. Hamid O, El Fiky L, Hassan O, Kotb A, El Fiky S. Anatomic variations of the sphenoid sinus and their impact on trans-sphenoid pituitary surgery. Skull Base 2008;18:9-15.
15. Sethi DS, Stanley RE, Pillay PK. Endoscopic anatomy of the sphenoid sinus and sella turcica. J Laryngol Otol 1995;109:951-5.
16. Gupta T, Aggarwal A, Sahni D. Anatomical landmarks for locating the sphenoid ostium during endoscopic endonasal approach: A cadaveric study. Surg Radiol Anat 2013;35:137-42.
17. Sareen D, Agarwal AK, Kaul JM, Sethi A. Study Of Sphenoid Sinus Anatomy In Relation To Endoscopic Surgery. Int. J. Morphol., 200;23:261-6.
18. Tan HK, Ong YK. Sphenoid sinus: An anatomic and endoscopic study in Asian cadavers. Clin Anat 2007;20:745-50.
19. Dyer EH, Civit T, Visot A, Delalande O, Derome P. Transsphenoidal surgery for pituitary adenomas in children. Neurosurgery 1994;34:207-12.
20. Lang J. Clinical Anatomy of the Nose, Nasal Cavity and Paranasal Sinuses. Translated by Stell PM. 1st ed. Stuttgart/New York: Thieme; 1989. p. 85-94.
21. Ariji Y, Ariji E, Yoshiura K, Kanda S. Computed tomographic indices for maxillary sinus size in comparison with the sinus volume. Dentomaxillofac Radiol 1996;25:19-24.
22. Ikeda A. Volumetric measurement of the maxillary sinus by coronal CT scan. Nippon Jibiinkoka Gakkai Kaiho 1996;99:1136-43.
23. Schatz CJ, Becker TS. Normal CT anatomy of the paranasal sinuses. Radiol Clin North Am 1984;22:107-18.
24. Karakas S, Kavakli A. Morphometric examination of the paranasal sinuses and mastoid air cells using computed tomography. Ann Saudi Med 2005;25:41-5.
25. Kim HU, Kim SS, Kang SS, Chung IH, Lee JG, Yoon JH. Surgical anatomy of the natural ostium of the sphenoid sinus. Laryngoscope 2001;111:1599-602.
26. Abuzayed B, Tanriöver N, Ozlen F, Gazioğlu N, Ulu MO, Kafadar AM, *et al*. Endoscopic endonasal transsphenoidal approach to the sellar region: Results of endoscopic dissection on 30 cadavers. Turk Neurosurg 2009;19:237-44.
27. Lakhani M, Sadiq M, Mukhtar S. Sphenoid sinus anatomical relations and their implications in endoscopic sinus surgery. Int J Med Res Health Sci 2017;6:162-6.

Original Article

# Anomalous Subaortic Left Brachiocephalic Vein: Prevalence and Associated Anomalies

**C.S. Ramesh Babu, Arjun Kumar[1], Om Prakash Gupta[1]**

*Department of Anatomy, Muzaffarnagar Medical College, Muzaffarnagar, [1]Dr. O.P. Gupta Imaging Centre, Meerut, Uttar Pradesh, India*

## Abstract

**Introduction:** Thoracic venous anomalies are very rare with an estimated prevalence of 0.7% in the general population. One of the rarest such anomaly is a subaortic course of the left brachiocephalic vein (LBV) commonly associated with congenital cardiac or aortic arch anomalies. **Material and Methods:** We retrospectively analyzed chest computed tomography scans of 710 participants and found incidentally two cases of anomalous subaortic course of the LBV in two females. **Results:** The observed prevalence of subaortic LBV is 0.28% (2/710 cases). Isolated subaortic LBV without any associated cardiac or aortic arch anomaly was observed in a female patient. Rare bilateral ectopic origin of bronchial arteries from corresponding subclavian arteries was also noted in this patient. In another female patient, right aortic arch anomaly was associated with subaortic LBV. The right-sided aortic arch had an aberrant retroesophageal left subclavian artery arising from a Kommerell's diverticulum as the last branch. **Discussion and Conclusion:** Extensive literature search has yielded only 15 cases of isolated anomalous subaortic LBV in subjects without any cardiac and aortic arch anomaly. Although this condition is asymptomatic, its presence, when detected, should alert the clinician to the possible presence of associated congenital cardiac and aortic arch anomalies. Accurate knowledge of these rare anomalies will enhance the diagnostic accuracy and proper interpretation of radiological images. Such thorough knowledge will avoid interpreting the anomalous vein as an enlarged lymph node, enlarged left superior intercostal vein, and reduce the chances of surgical complications.

**Keywords:** *Aberrant left subclavian artery, Kommerell's diverticulum, left innominate vein, right aortic arch, thoracic venous anomalies*

## Introduction

The left brachiocephalic (left innominate) vein (LBV) is formed by the union of the left internal jugular and subclavian veins at the level of the left sternoclavicular joint. Normally it passes through the prevascular space, from left to right, just above the arch of aorta and anterior to supra-aortic branches to join the right brachiocephalic vein (RBV) to form the superior vena cava (SVC). It is the most anteriorly placed vessel in the superior mediastinum. Anomalous subaortic or retroaortic LBV (ASLBV) is an extremely rare venous anomaly in which the LBV passes below the arch, above the pulmonary artery and behind the ascending aorta to join RBV at or below the level of joining of arch of azygos vein. In such cases, the SVC is short and azygos vein drains into RBV. When present this anomaly is usually associated with congenital heart disease (CHD) or aortic arch anomalies like right aortic arch (RAA). Anomalous subaortic LBV is seen in about 0.5%–1.7% of all children with CHD.[1] It is estimated that about 80% of cases with anomalous subaortic LBV have associated right ventricular outflow tract obstruction.[2,3] Another common association is the presence of right sided aortic arch.[4] Isolated subaortic LBV is tremendously rare (0.02% prevalence) with only a handful of reports available in the literature.[5] Since this anomaly is asymptomatic, its presence is detected incidentally at autopsy, surgery or radiological investigations. Incidental detection of anomalous LBV should alert the clinician of possible associated CHD or aortic arch anomalies. We report here incidental observation of two cases of anomalous subaortic LBV while retrospectively analysing contrast enhanced computed tomographic (CECT) chest scans.



**How to cite this article:** Babu CSR, Kumar A, Gupta OP. Anomalous subaortic left brachiocephalic vein: Prevalence and associated anomalies. J Anat Soc India 2020;69:XX-XX.

**Article Info**

**Received:** 17 July 2020
**Accepted:** 01 September 2020
**Available online:** ***

***Address for correspondence:***
*Prof. C.S. Ramesh Babu, Department of Anatomy, Muzaffarnagar Medical College, N.H. 58, Opp. Begrajpur Industrial Area, Muzaffarnagar - 251 203, Uttar Pradesh, India.*
*E-mail: csrameshb@gmail.com*

**Access this article online**

**Website:** www.jasi.org.in
**DOI:** 10.4103/JASI.JASI_111_20
**Quick Response Code:**

## Material and Methods

We retrospectively reviewed CT scans of 710 patients referred to the imaging center for CECT of the thorax for suspected pathologies of the lungs and mediastinum during the period September 2015 to March 2018. The imaging data were collected retrospectively from the archives of the imaging center. The study population included 435 males and 275 females (age ranging from 6 months to 86 years, mean age 51.28 ± 17.70 years). The scans of the patients with malignancies likely to distort the anatomy of aortic arch, poorly enhanced scans, and those with thoracic aortic disease were excluded from the study.

All patients underwent contrast-enhanced multidetector computed tomography by a 64 channel scanner (GE Optima 660, 2011, Tokyo, Japan) and received 90–100 mL of nonionic iohexol contrast (Omnipaque 350 mg I/mL; GE Healthcare, Shanghai, China) at the rate of 5 mL/s intravenously. Written informed consent was obtained by the imaging center from each patient before contrast injection. Sections of 0.625 mm thickness were obtained from the lower part of the neck to the upper part of the abdomen and analyzed in a separate work station (GE: AW Volume share 4.5). After analyzing axial, coronal, and sagittal scans, volume rendered and maximum intensity projections were obtained. The data were collected to study the variations in the branching pattern of arch of the aorta and incidentally two cases having anomalous subaortic LBV were detected.

## Results

Two cases of anomalous subaortic LBV were detected incidentally, both in females. Isolated subaortic LBV was detected in a female aged 32 years with a normal left-sided aortic arch. No congenital cardiac anomaly was reported. The anomalous vein was crossing the left lateral side of arch and then turning to the right below the arch and above the pulmonary artery [Figure 1a and b]. The anomalous vein coursed anterior to tracheal bifurcation and posterior to ascending aorta to join the RBV just below the insertion of azygos vein [Figures 1b and 2]. An early branch from the right pulmonary artery was also noted [Figure 1b]. Rare ectopic origin of bronchial arteries (BA) bilaterally from the corresponding subclavian arteries was also observed [Figure 1b] Ectopic right BA arose in the root of the neck from the right subclavian (RSA) while ectopic left BA originated from the left subclavian just above the arch [Figure 1b].

The second case of subaortic LBV was seen in a female aged 30 years and was associated with a high positioned right-sided aortic arch [Figures 3 and 4]. The subaortic LBV was passing below the right arch through the subaortic space, above the pulmonary artery and behind the ascending aorta to join the RBV at the level of insertion of azygos vein [Figures 5 and 6]. The anomalous vein was crossing anterior to the trachea [Figure 5c]. Type II RAA with the branching sequence of left common carotid artery, right common carotid artery, RSA, and Aberrant left subclavian artery (ALSA) was identified [Figure 4]. The aberrant left subclavian artery (ALSA) was arising from a retroesophageal Kommerell's diverticulum and was coursing behind the esophagus to reach the left side [Figures 6 and 7]. Descending thoracic aorta was present on the right side of the vertebral column. No cardiac anomaly was seen.

## Discussion

Thoracic venous anomalies are very rare with an estimated prevalence of 0.7% in the general population.[6] ASLBV is

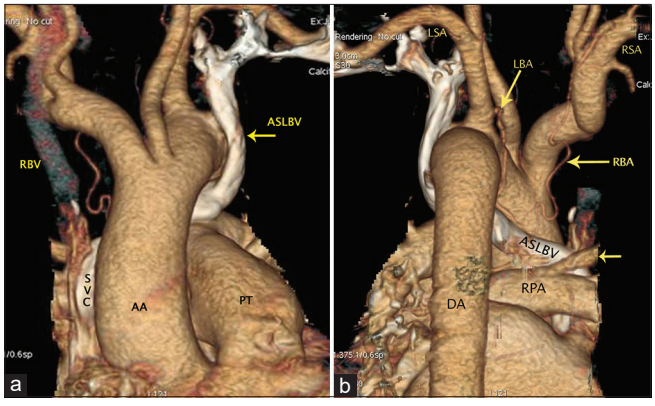


**Figure 1: Volume rendered image (a) anterior view. Isolated anomalous subaortic left brachiocephalic vein descending on the left side of arch and then below the arch and behind the ascending aorta to join right brachiocephalic vein to form the superior vena cava. (b) Posterior view. The ASLBV passes through aorto-pulmonary window above the right pulmonary artery which is giving an early branch (arrow). Note also the presence of ectopic origin of both left bronchial and right bronchial arteries from the corresponding subclavian arteries (LSA, RSA). AA: Ascending aorta, DA: Descending aorta, PT: Pulmonary trunk**

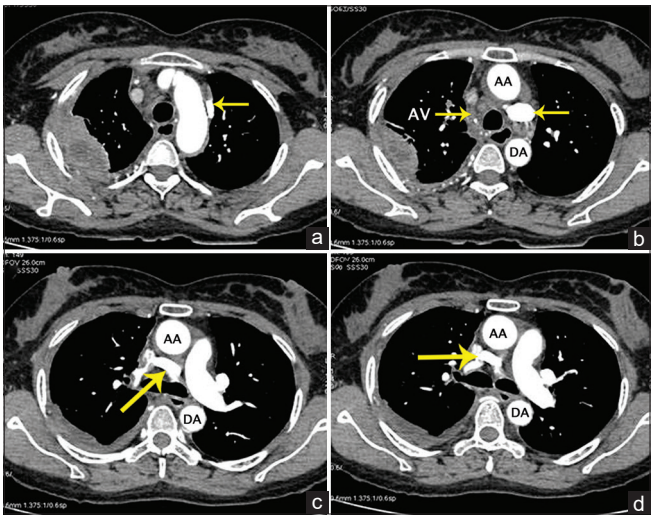


**Figure 2: (a-d) Serial axial sections depicting the course of anomalous subaortic left brachiocephalic vein (arrow) passing from the left side of the arch of aorta (a) then behind the ascending aorta and anterior to trachea (b and c) to form superior vena cava (d). DA: Descending aorta**

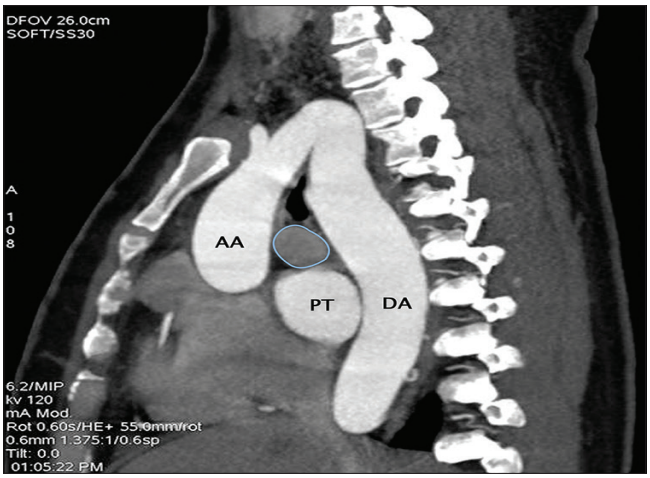


**Figure 3: Sagittal section. Higher position of right arch in the superior mediastinum with anomalous subaortic left brachiocephalic vein (blue circle) passing through a larger subaortic space above the pulmonary trunk. AA: Ascending aorta, DA: Descending aorta**

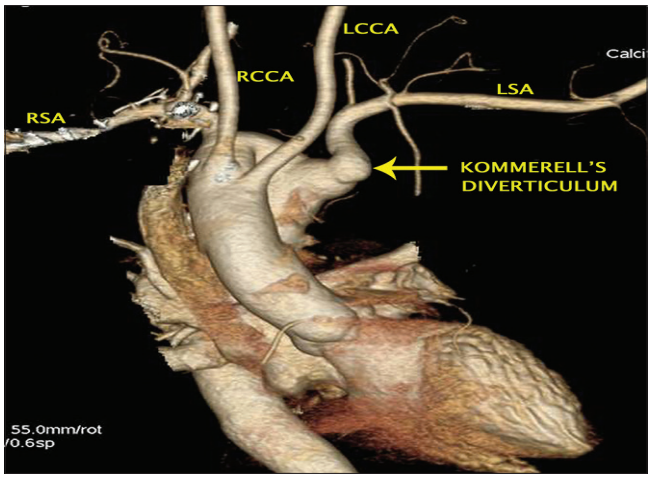


**Figure 4: VR image of the right sided arch of aorta with 4 branches – left common carotid artery, right common carotid artery, right subclavian and left subclavian in that order. The left subclavian artery has an aberrant retroesophageal course and exhibits a Kommerell's Diverticulum at its origin**

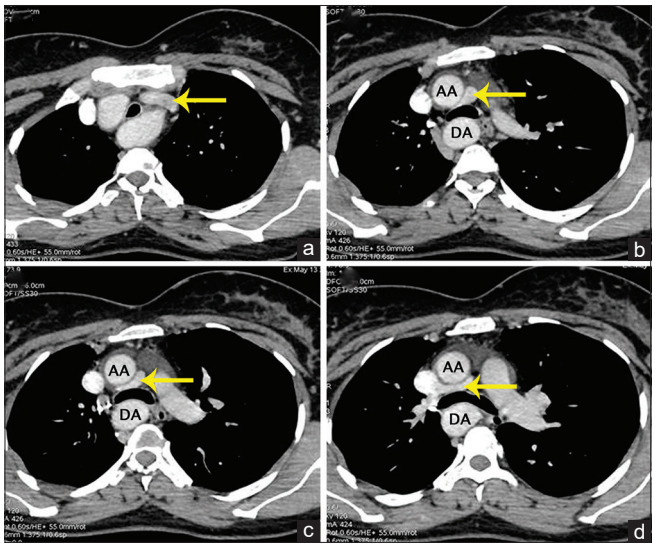


**Figure 5: (a-d) Serial axial sections showing the course of anomalous subaortic left brachiocephalic vein (arrow) which is sandwiched between ascending aorta and trachea. Note the position of descending aorta on the right side of the vertebra**

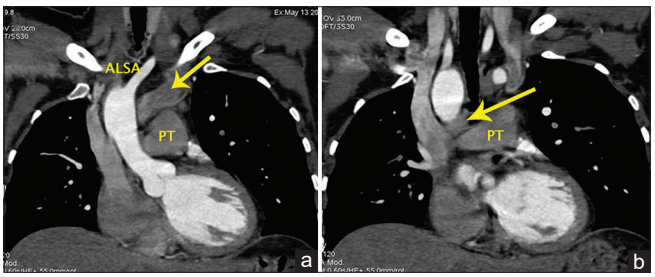


**Figure 6: Serial coronal sections showing the course of anomalous subaortic left brachiocephalic vein (arrow). Note the anomalous retroesophageal left subclavian artery is crossing the midline. PT: Pulmonary trunk**

one such uncommon systemic venous anomaly and when present, is usually associated with CHD, RAA, and other anomalies. It is present in about 0.5%–1.7% of all children with CHD.[1] The incidence of this venous anomaly associated with CHD was variously reported as 0.2% at necropsy,[7] 0.5%–0.98% by echocardiography,[2,8,9] 1.7% by CT,[4] and 0.57% of surgical cases.[10] It is estimated that the incidence in the general population is 0.06%–0.37%.[11] In a review of 1500 angiographic studies of the brachiocephalic veins, Roberts *et al*. reported only one case of subaortic LBV accounting for an incidence of 0.07%.[12] In a retrospective analysis of CT scans of 81,425 adult patients without CHD, Yamamuro *et al*. estimated an incidence of 0.03%–0.062% for anomalous LBV.[13] For evaluating the incidence of aberrant LBV and persistent left SVC without bridging vein, Kobayashi *et al*. recently reviewed CT scans of 49,494 patients and found an incidence of 0.055% and 0.15%, respectively, for these two venous anomalies in Japanese patients.[14] Out of 27 cases of ALBVs detected in their study, only one case had associated CHD, 14 patients had high aortic arches, and in 26 cases, the ALBVs had retroaortic course. Reported prevalence rates were largely derived by the retrospective analysis of the surgical, radiological, and autopsy records [Table 1]. Isolated ASLBV without any associated cardiac and aortic arch anomalies is still rarer,[5] and some of the adult cases reported since 1980 are summarised in Table 2.

Most commonly, the ASLBV was associated with conotruncal anomalies, aortic arch anomalies and deletion of chromosome 22q11.2. Most common associated finding is tetralogy of Fallot (TOF) reported to be present in 40%–93% cases of ASLBV.[8-10] Another associated anomaly with high frequency is the presence of right-sided aortic arch (RAA) in 46%–86% of cases.[2,10] Anomalous subaortic LBV was more common in those with RAA than those with the left aortic arch ($P < 0.0001$).[4] The presence of ASLBV in patients with deletion of chromosome 22q11.2 was also reported.[10,27] Ventricular septal defect (VSD) with

**Table 1: Reported prevalence of aberrant sub-aortic left brachiocephalic vein in cases with and without associated congenital heart disease**

| Author year | Modality of study | Cases associated with CHD | | Cases without CHD | |
|---|---|---|---|---|---|
| | | Total number | AS-LBV cases (%) | Total number | AS-LBV cases (%) |
| Sherman, 1963[15] | Necropsy | 503 | 2 | - | - |
| Gerlis and Ho, 1989[7] | Necropsy | 2000 | 3 | 5000 | None |
| Choi *et al*., 1990[8] | Echocardiography | 2457 | 24 (0.98) | - | - |
| Curtil *et al*., 1999[9] | Echocardiography and surgery | 5218 | 27 (0.5) | - | - |
| Chen *et al*., 2005[4] | CT | 1812 | 27 | - | - |
| Kulkarni *et al*., 2008[2] | Echocardiography | 1432 | 8 (0.55) | - | - |
| Nagashima *et al*., 2010[10] | Surgical | 2449 | 14 (0.57) | 4805 | 1 (0.02) |
| Ko *et al*., 2011[16] | CT/MRI | - | - | 25,940 | 4 (adult) |
| Kahkouee *et al*., 2017[1] | CT angio | 1372 | 22 | - | - |
| Yamamuro *et al* 2017[13] | CT Chest | - | - | 81,425 | 27 (0.033) |
| Kobayashi *et al*., 2018[14] | CT Chest | 49,494 | 1 | 49,494 | 26 |
| Present study | CECT Chest | - | - | 710 | 2 (0.28) |

CHD: Congenital heart disease, CT: Computed tomography, CECT: Contrast enhanced computed tomography, AS-LBV: Aberrant sub-aortic left brachiocephalic vein, MRI: Magnetic resonance imaging

**Table 2: Reports of isolated sub-aortic left brachiocephalic Vein in cases of situs solitus (with out any cardiac/aortic arch anomaly)**

| Author and year | Modality of study | Sex, age | Remarks |
|---|---|---|---|
| Kitamura *et al*., 1981[17] | Cadaveric | Male, 69 | Left arch |
| Webb *et al*., 1982[18] | CECT chest | | Left arch |
| Fujimoto *et al*., 1992[19] | MRI | Female, 54 | Left aortic arch, no cardiac anomaly |
| Gülsün *et al*., 2003[20] | CECT, MRA | | No cardiac anomaly |
| Yama *et al*., 2005[21] | CECT-chest | Male, 46 | High left aortic arch |
| Park *et al*., 2006[11] | TE Echo, CT | Male, 63 | Left aortic arch |
| Ko *et al*., 2008[22] | CECT Chest | Male, 74 | Normal heart, left arch |
| | | Male, 50 | Normal heart, left arch right lung cancer |
| Jayaprakasam *et al*., 2008[23] | MDCT | Male, 34 | No cardiac anomaly |
| Berko *et al*., 2009[6] | CT Angio Chest | Male, 50 (1 out of 1000) | Dysphagia, dyspnoea |
| Nagashima *et al*., 2010[10] | CT | Male, 70 | Normal heart, left arch distal arch aneurysm |
| Srinivasan *et al*., 2013[24] | CECT-Chest | Male, 68 | Left aortic arch |
| Hussain *et al*., 2014[25] | Organ donor | | Normal heart |
| Iimura *et al*., 2014[26] | Cadaveric | Male, 73 | Left aortic arch |
| Semionov and Kosiuk, 2017[5] | CECT-Thorax | Female, 48 | Left aortic arch, normal heart |
| Kahkouee *et al*., 2017[1] | CT Angio | Female, 40 (1 out of 1372) | Left arch |
| Present study | MDCT | Female, 32 (1 out of 710) | Left aortic arch |

CT: Computed tomography, CECT: Contrast enhanced computed tomography, MRI: Magnetic resonance imaging, MRA: Magnetic resonance angiography, MDCT: Multi-detector computed tomography

pulmonary atresia, persistent truncus arteriosus, atrial septal defect (ASD), coarctation of aorta, and persistent ductus arteriosus are rare associations observed.[1,3,10,28,29]

Nakamura *et al*. reported the case of ASLBV in a 62-year-old male with lung cancer and no cardiac anomaly. They emphasized the importance of recognition of this vein in lung cancer patients because misinterpretation as an enlarged superior mediastinal lymph node may cause serious complications.[30] Botha and Odell reported the case of a 19-day-old male neonate with ASLBV associated with persistence of truncus arteriosus, VSD, secundum type ASD, absence of arterial duct, and normal left-sided aortic arch.[28] They noted that Adachi classified ASLBV into two types-type-I anterior to ductus, type II posterior to ductus. Gerlis and Ho added a third type passing below the left pulmonary artery[7] and Botha's case is Type IV-with the absence of arterial ligament and ASLBV cephalad to the pulmonary artery.[28] Level of entry of ASLBV into SVC was higher than the insertion of azygos vein in seven cases, at the same level in four cases and lower in three cases out of 14 cases studied.[31] Hoshino *et al*. described a case of 22q11.2 deletion syndrome with hypoparathyroidism, levocardia, high RAA with aberrant left subclavian

artery (ALSA) arising from Kommerell's diverticulum in a 54 year old male.[27] Hara *et al*. discussed the difficulties encountered while resecting the enlarged lymph nodes in a lung cancer patient having ASLBV and RAA with ALSA.[32] Ohkubo *et al*. reported an anomalous retroaortic LBV with RAA and ALSA in a 49-year-old man.[33]

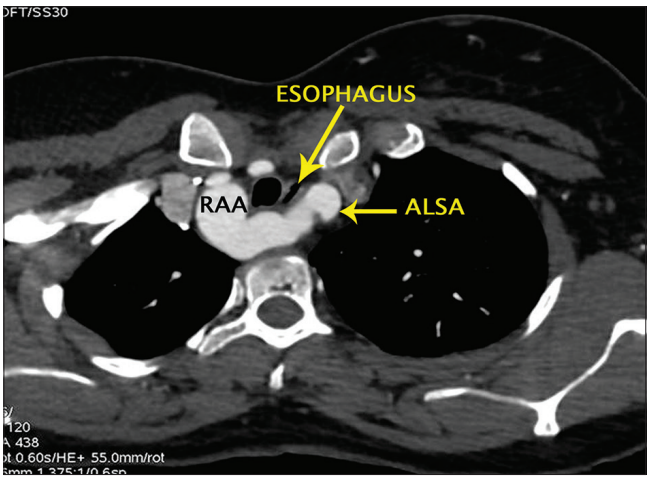


**Figure 7: Axial section showing the right aortic arch and the retroesophageal left subclavian artery arising from Kommerell's diverticulum**

Normally, the LBV develops from (a) left anterior cardinal (precardinal) vein and (b) transverse inter-precardinal anastomosis. The exact embryogenesis of the anomalous retro-aortic LBV remains uncertain. Adachi (1933) has suggested the presence of double precardinal anastomoses (ventral superior transverse and dorsal inferior transverse plexuses) around the primitive aorta.[34] Normally, the ventral superior transverse plexus develops into LBV, but the regression of superior and persistence of the inferior transverse plexus result in the development of anomalous LBV [Figure 8]. Takada *et al*. thought that this venous anomaly resulted from the precardinal anastomosis being situated posterior to the truncus arteriosus and double (circumaortic) LBV as a consequence of persistence of both cranial ventral and caudal dorsal precardinal anastomosis.[35] Minami *et al*. and Kim *et al*. believed that this anomaly can form secondarily when the elongation

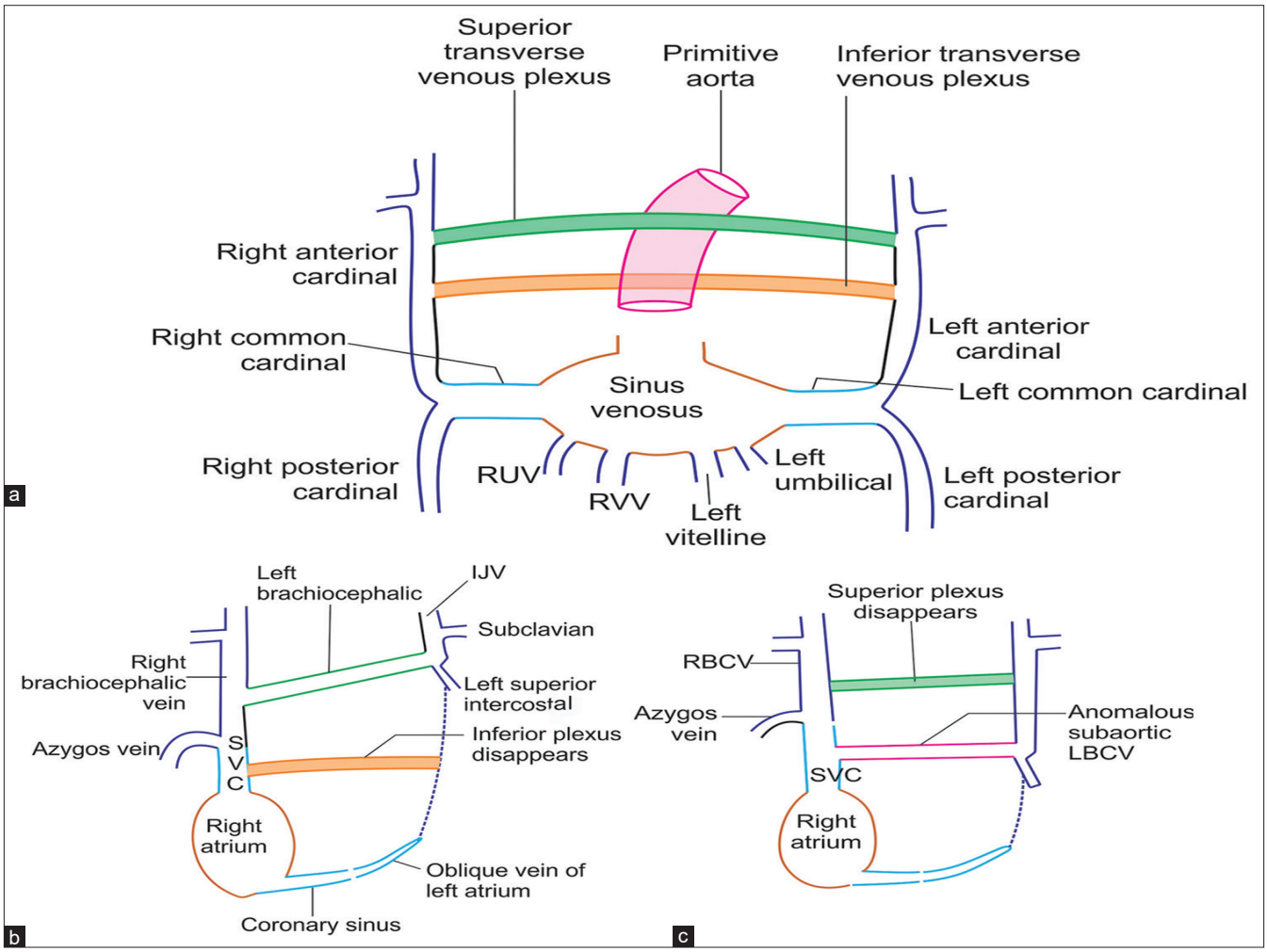


**Figure 8: Scheme showing the embryological basis of subaortic left brachiocephalic vein. (a) The developing aorta is surrounded by two venous plexuses connecting right and left anterior cardinal veins. (b) Persistence of ventral superior transverse plexus develops into normal left brachiocephalic vein passing anterior to supraaortic branches. (c) Instead persistence of dorsal inferior transverse plexus and involution of superior plexus gives rise to subaortic left brachiocephalic vein**

of the aortic arch prevents the normal cranial ventral precardinal anastomosis to develop.[36,37] Elongation of the aortic arch leads to narrowing of the prevascular space and widening of the subaortic space (aorticopulmonary window). This widening increases the chances for the persistence of caudal dorsal precardinal anastomosis posterior to the aorta and formation of anomalous LBV.

Arch of aorta and its supraaortic branches develop from paired pharyngeal arch arteries. Normally, the left fourth aortic arch artery develops into the arch of the aorta and right fourth arch artery and part of right dorsal aorta forms part of RSA artery. Distal portion of the right dorsal aorta disappears. RAA is formed due to the involution of left fourth arch artery and persistence of right fourth arch artery and right dorsal aorta. Along with this anomaly if the dorsal inferior transverse venous plexus persists, anomalous subaortic LBV is formed [Figure 9].

In one female patient, we observed anomalous LBV with RAA having aberrant retroesophageal LSA (ALSA) arising from Kommerell's diverticulum (Type II RAA). Right sided aortic arch is present in 0.05%–0.1% of radiology series and 0.04%–0.1% of autopsy series.[38] Edwards classified the RAA into three types. Type I is RAA with mirror image branching (left brachiocephalic trunk, right common carotid, and RSA), Type II is RAA with ALSA (left common carotid, right common carotid, RSA, and ALSA) and Type III is RAA with isolation of LSA. Type I and Type III are usually associated with some form of cyanotic CHD like TOF (conotruncal anomalies) but not Type II. Arazińska *et al*. reported that Type II RAA is the most common type of RAA observed in their retrospective analysis (11/20 patients).[38] Anomalous subaortic LBV combined with RAA and retroesophageal ALSA represented <0.005% in the prevalence of the adult population.

BA originate ectopically from the arch of aorta, subclavian arteries, thyrocervical trunk, and vertebral arteries. Ectopic origin of BA from subclavian arteries bilaterally is very rare.[39] We have observed bilateral ectopic origin of BA from corresponding subclavian arteries in a female patient.

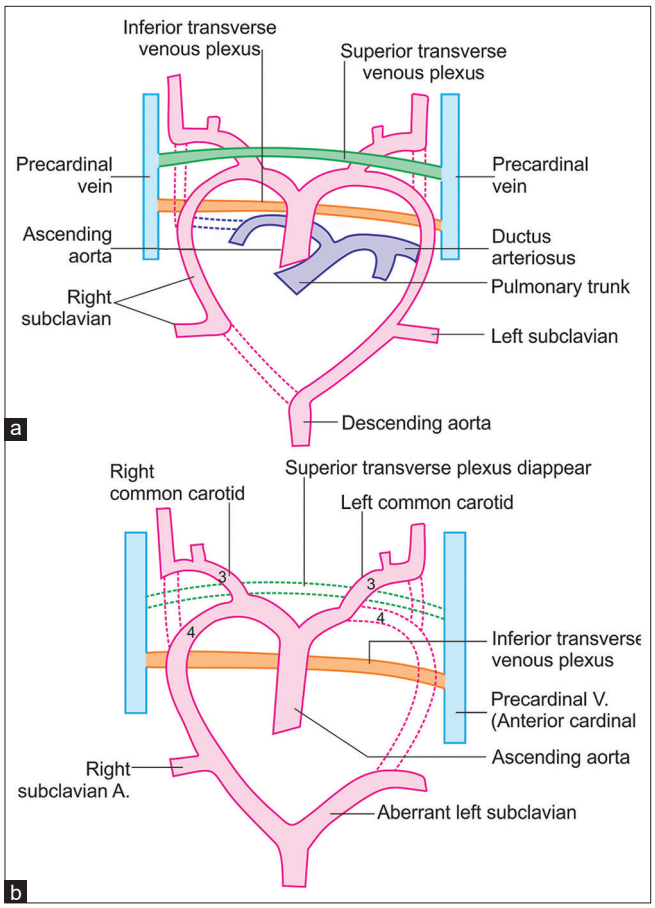


**Figure 9: Scheme showing the development of arch of aorta and its branches. (a) Normal development of arch of aorta from left fourth arch artery and left dorsal aorta. (b) Development of right aortic arch due to persistence of entire right dorsal aorta and involution of left dorsal aorta. Persistence of distal part of left dorsal aorta along with left seventh intersegmental artery develops into aberrant left subclavian artery. Anomalous subaortic left brachiocephalic vein develops due to persistence of dorsal inferior transverse plexus**

## Conclusion

Although this venous anomaly is asymptomatic having no pathophysiologic repercussions, it should alert the clinician to the possibility of associated CHD and aortic arch anomalies. This variant may mimic an enlarged lymph node resulting in the misinterpretation in imaging studies. This anomaly can cause difficulty during insertion of central venous catheter through a left-sided approach. It can cause difficulties by obstructing the surgical field during corrective surgeries for congenital cardiac anomalies. It can also be mistaken for a persistent left SVC, enlarged left superior intercostal vein or a vertical vein in cases of partial anomalous pulmonary venous return.

### Financial support and sponsorship

Nil.

### Conflicts of interest

There are no conflicts of interest.

## References

1. Kahkouee S, Sadr M, Pedarzadeh E, Fardin S, Borhani A, Gholami S, *et al*. Anomalous left brachiocephalic vein: Important vascular anomaly concomitant with congenital anomalies and heart diseases. Folia Morphol (Warsz) 2017;76:51-7.
2. Kulkarni S, Jain S, Kasar P, Garekar S, Joshi S. Retroaortic left innominate vein-Lncidence, association with congenital heart defects, embryology, and clinical significance. Ann Pediatr Cardiol 2008;1:139-41.
3. Sukulal K, Bijulal S, Tharakan JA. Differential diagnosis of vascular structures in relation to upper ascending aorta: The retro-aortic innominate vein. Ann Pediatr Cardiol 2013;6:97-8.
4. Chen SJ, Liu KL, Chen HY, Chiu IS, Lee WJ, Wu MH, *et al*. Anomalous brachiocephalic vein: CT, embryology, and clinical implications. AJR Am J Roentgenol 2005;184:1235-40.
5. Semionov A, Kosiuk J. Incidental retroaortic left innominate

vein in adult patient. Radiol Case Rep 2017;12:475-8.
6. Berko NS, Jain VR, Godelman A, Stein EG, Ghosh S, Haramati LB. Variants and anomalies of thoracic vasculature on computed tomographic angiography in adults. J Comput Assist Tomogr 2009;33:523-8.
7. Gerlis LM, Ho SY. Anomalous subaortic position of the brachiocephalic (innominate) vein: A review of published reports and report of three new cases. Br Heart J 1989;61:540-5.
8. Choi JY, Jung MJ, Kim YH, Noh CI, Yun YS. Anomalous subaortic position of the brachiocephalic vein (innominate vein): An echocardiographic study. Br Heart J 1990;64:385-7.
9. Curtil A, Tronc F, Champsaur G, Bozio A, Sassolas F, Carret JP, *et al*. The left retroaortic brachiocephalic vein: Morphological data and diagnostic ultrasound in 27 cases. Surg Radiol Anat 1999:21:251-4.
10. Nagashima M, Shikata F, Okamura T, Yamamoto E, Higaki T, Kawamura M, *et al*. Anomalous subaortic left brachiocephalic vein in surgical cases and literature review. Clin Anat 2010;23:950-5.
11. Park CK, Kim KJ, Park MK, Yang HJ, Cho JM, Jeon DS, *et al*. Subaortic left brachiocephalic vein. Korean Circ J 2006;36:605-7.
12. Roberts JR, Dotter CT, Steinberg I. Superior vena cava and innominate veins: Angiographic study. Am J Roentgenol 1951;66:341-52.
13. Yamamuro H, Ichikawa T, Hashimoto J, Ono S, Nagata Y, Kawada S, *et al*. Congenital anomalies of the left brachiocephalic vein detected in adults on computed tomography. Jpn J Radiol 2017;35:597-605.
14. Kobayashi M, Ichikawa T, Koizumi J, Hashimoto J, Yamamuro H, Hara T, *et al*. Aberrant left brachiocephalic vein versus persistent left superior vena cava without bridging vein in adults: Evaluation on computed tomography. Ann Vasc Dis 2018;11:535-41.
15. Sherman FE. An Atlas of Congenital Heart Disease. London: Henry Kimpton; 1963.
16. Ko SF, Sun CK, Liang CD, Yip HK, Sheu JJ, Hsieh MJ, *et al*. Double precardinal anastomoses with interconnecting venous plexus hypothesis in the embryogenesis of anomalous brachiocephalic veins: Computed tomography and magnetic resonance findings. J Thorac Imaging 2011;26:240-6.
17. Kitamura S, Sakai A, Nishiguchi T. A case of the left innominate vein passing behind the ascending aorta. Anat Rec 1981;201:567-72.
18. Webb WR, Gamsu G, Speckman JM, Kaiser JA, Federle MP, Lipton MJ. Computed tomographic demonstration of mediastinal venous anomalies. Am J Roentgenol 1982;139:157-61.
19. Fujimoto K, Abe T, Kumabe T, Hayabuchi N, Nozaki Y. Anomalous left brachiocephalic (innominate) vein: MR demonstration. Am J Roentgenol 1992;159:479-80.
20. Gülsün M, Gökoğlu A, Ariyürek M, Demirkazik FB, Hazirolan T. Subaortic left brachiocephalic vein: Computed tomography and magnetic resonance angiography findings. Surg Radiol Anat 2003;25:335-8.
21. Yama N, Nara S, Itoh Y, Kurimoto Y, Narimatsu E, Asai Y, *et al*. A case of anomalous subaortic left brachiocephalic vein mimicking mediastinal hematoma. J Trauma 2005;58:419-20.
22. Ko SF, Huang CC, Ng SH, Hsieh MJ, Lee CC, Wan YL, *et al*. Imaging of the brachiocephalic vein. Am J Roentgenol 2008;191:897-907.
23. Jayaprakasam VS, Gurudev S, Irion K, Khan AN, Pettit AR. Anomalous subaortic left brachiocephalic vein: A case report. Radiol Bras 2008;41:135-7.
24. Srinivasan S, Kannivelu A, Ali SZ, See PP. Isolated retroaortic left innominate vein in an adult without cardiac or aortic anomalies. Indian J Radiol Imaging 2013;23:308-9.
25. Hussain ST, Vivacqua A, Keshavamurthy S, Soltesz EG. Isolated anomalous retroaortic left brachiocephalic vein in an adult organ donor. Ann Thorac Surg 2014;98:115.
26. Iimura A, Oguchi T, Matsuo M, Hayashi S, Moriyama H, Itoh M. Anatomical study of the coexistence of the postaortic left brachiocephalic vein with the postaortic left renal vein with a review of the literature. Okajimas Folia Anat Jpn 2014;91:73-82.
27. Hoshino Y, Machida M, Shimano SI, Taya T. An adult case of chromosome 22q11.2 deletion syndrome associated with a high-positioned right aortic arch. Intern Med 2017;56:865-72.
28. Botha CA, Odell JA. Anomalous subaortic position of the left brachiocephalic (innominate) vein. A second case associated with truncus arteriosus. Cardiovasc J S Afr 1993;4:20-1.
29. Patel S, Makhija P, Sernich S. Rare association of retroaortic innominate vein and coarctation of aorta with hypoplastic leftb aortic arch. Embryology review of retroaortic innominate vein. Congenit Cardiol Today 2015;13:1-6.
30. Nakamura R, Yoshihisa I, Iwasaki K, Yumoto T, Yuzawa K, Ueki H. Left anomalous brachiocephalic vein in a patient with right lung cancer. Ann Thorac Surg 2013;96:307-9.
31. Chern MS, Ko JS, Tsai A, Wu MH, Teng MM, Chang CY. Aberrant left brachiocephalic vein: CT imaging findings and embryologic correlation. Eur Radiol 1999;9:1835-9.
32. Hara M, Matsuzaki Y, Shinuzu T, Tomita M, Ayabe T, Onitsuka T. Right lung cancer with right aortic arch and posterior aortic left innominate vein. J Jpn Assoc Chest Surg 2006;20:166-70.
33. Ohkubo Y, Okano T, Saijyo A, Takei S, Kurashina N, Wagai F, *et al*. A case report of anomalous left brachiocephalic vein. Jpn J Thorac Dis 1991;29:758-63.
34. Adachi B. Das Venensystem der Japaner. Anatomie der Japaner II. Tokyo: Kenkyusha; 1933. p. 83-7.
35. Takada Y, Narimatsu A, Kohno A, Kawai C, Hara H, Harasawa A, *et al*. Anomalous left brachiocephalic vein: CT findings. J Comput Assist Tomogr 1992;16:893-6.
36. Minami M, Noda M, Kawauchi N, Shirouzu I, Nakajima J, Araki T, *et al*. Postaortic left innominate vein: Radiological assessment and pathogenesis. Clin Radiol 1993;48:52-6.
37. Kim SH, Chung JW, Im JG, Choi YW, Choe YH, Han MC. Subaortic left innominate vein: Radiological findings and consideration of embryogenesis. J Thorac Imaging 1999:14:142-6.
38. Arazińska A, Polguj M, Szymczyk K, Kaczmarska M, Trębiński Ł, Stefańczyk L. Right aortic arch analysis – Anatomical variant or serious vascular defect? BMC Cardiovasc Disord 2017;17:102.
39. Amrhein TJ, Kim C, Smith TP, Washington L. Bronchial artery arising from the left vertebral artery: Case report and review of the literature. J Clin Imaging Sci 2011;1:62.

Original Article

# The Measurement Indexes and the Relationships with Adjacent Structures of Vidian Canal and Foramen Rotundum using Computed Tomography

**Gozde Serindere, Kaan Gunduz[1], Hakan Avsever [2]**

*Department of Dentomaxillofacial Radiology, Faculty of Dentistry, Hatay Mustafa Kemal University, Hatay, [1]Department of Dentomaxillofacial Radiology, Faculty of Dentistry, Ondokuz Mayıs University, Samsun, [2]Department of Dentomaxillofacial Radiology, Gulhane Faculty of Dentistry, Health Sciences University, Ankara, Turkey*

## Abstract

**Introduction:** The aim of this study was to evaluate vidian canal (VC) and foramen rotundum (FR) and their anatomical relationships with adjacent structures using computed tomography (CT) in a Turkish subpopulation. **Material and Methods:** CT images of 150 patients were retrospectively evaluated**.** Various morphometric measurements (distance from FRs to midline, distance from FR to VC, position and angle of FR, and types of FR and VC) were performed from both left and right sides on CT scans. **Results:** One hundred and fifty patients with a mean age of 41.06 ± 17.812 years were included in this study. The mean distance from midline to right FR was 17.89 ± 1.94 and 18 ± 1.83 in females and males, respectively. The mean distance from midline to left FR was 18.33 ± 1.94 and 19 ± 2.18 in females and males, respectively. Twenty-three cases had Type 1 VC and 40 and 112 cases had Type 2 and 3 VCs, respectively. Three patients had Type I FR, 25 and 57 patients had Type IIa and IIb, respectively, and 93 patients had Type III FR. The position of FRs regarding the base of lateral pterygoid plate was online in 77 patients, medially placed in 92 patients, and laterally placed in 12 patients. **Discussion and Conclusion:** It is important to know sphenoid sinus and neighboring anatomical structures for planning of endoscopic skull base surgery because it is located close to some important anatomical structures such as internal carotid arteries, optic nerve, and cranial nerves. Surgeons should be careful in preoperative treatment planning and also during the operation.

**Keywords:** *Computed tomography, foramen rotundum, sphenoid sinus, vidian canal*

## Introduction

The sphenoid sinus has important anatomy during surgical operations of the ventral skull base that is not only the route for reaching the sellar, parasellar, suprasellar, and clival areas but also a way to Meckel's cave and the midcranial fossa. It is located close to various vital anatomical structures such as the internal carotid artery, optic nerve, and cranial nerves. The location of surgical window to the midcranial fossa is in the pterygoid body of the sphenoid bone.[1]

The foramen rotundum (FR) is a round opening of the sphenoid bone greater wing that anteriorly locates into the pterygopalatine fossa and includes the maxillary nerve;[2] it locates above and lateral to the pterygoid canal.[3] The maxillary branch of the trigeminal nerve passes through the FR[3] after crossing the midcranial fossa where it is in relation to the cavernous sinus lateral wall.[4]

The vidian canal (VC), nerve, and artery are named after Vidius. Vidius was a Medicine Professor at the College of France, and he was a physician to the King of France in the middle of the 16th century.[5,6] The VC may be observed at the skull base at the anterior border of the foramen lacerum and may locate above and between the pterygoid plates of the sphenoid bone. It enters the pterygopalatine fossa and contains the Vidian nerve, artery, and vein. The Vidian nerve arises from the union of postganglionic sympathetic fibers of the deep petrosal nerve of the carotid plexus and preganglionic parasympathetic fibers from the greater petrosal nerve. After entering the pterygopalatine fossa through the VC, the Vidian nerve enters the posterior area of the pterygopalatine ganglion. The sympathetic fibers provide the vascular constriction in the nasal cavity, and the parasympathetic fibers are responsible for the mucosal secretions in the oral and nasal cavity and the pharynx.[7,8]

The sphenoid sinus is the most difficult to reach the paranasal sinuses.[9] In close



**How to cite this article:** Serindere G, Gunduz K, Avsever H. The measurement indexes and the relationships with adjacent structures of vidian canal and foramen rotundum using computed tomography. J Anat Soc India 2020;69:XX-XX.

**Article Info**

**Received:** 06 April 2020
**Accepted:** 22 May 2020
**Available online:** ***

***Address for correspondence:***
*Dr. Gozde Serindere, Department of Dentomaxillofacial Radiology, Faculty of Dentistry, Hatay Mustafa Kemal University, 31060 Hatay, Turkey.*
*E-mail: gozdeserindere@mku.edu.tr*

**Access this article online**

**Website:** www.jasi.org.in
**DOI:** 10.4103/JASI.JASI_56_20
**Quick Response Code:**

relationship, there are several vital anatomical structures such as internal carotid artery, optic nerve, and VC. Physicians dealing with skull base surgery must know the important anatomical structures in the skull base. In surgical procedures performed with insufficient anatomical information, complications are inevitable.[10,11] Imaging modalities are important for the treatment of skull base disorders because clinical evaluation of this region is frequently difficult. Computed tomography (CT) is an ideal choice to evaluate anatomy and is frequently combined with magnetic resonance imaging.[12]

The aim of this study was to evaluate the measurement indexes of FR and VC and also their relationships with the adjacent structures on CT scans.

## Material and Methods

### Study design

Before starting the study, ethical approval was obtained from the Local Ethics Committee of Hatay Mustafa Kemal University (Decision date: January 16, 2020, decision number: 07). Images of 150 patients (71 females and 79 males; mean age: 41.06) who applied to the Department of Dentomaxillofacial Radiology were selected from the database. Patients under 18 years of age, or patients with known skull base pathology, remarkable rhinosinusitis (inflammatory changes that prevent the visualization of the skull base anatomy), maxillofacial fractures, sinonasal tumors, or polyposis, were excluded from the study. One hundred and fifty CT images that met the inclusion criteria were evaluated retrospectively.

CT machine (Toshiba Aquilion, Toshiba Medical Systems, Otawara, Japan) was used for all the CT procedures. A routine protocol was performed. All evaluations were performed by a 15.6-inch full HD notebook with resolution of 1920 × 1080 pixels and by a single observer (GS) who had 6 years. Undecided situations were solved by consensus with KG who had nearly 15 years of clinical experience.

Evaluations were performed using the hospital information system (ENLIL and PACS). For standardization, the first coronal section with VC and FR seen together was selected.

### The measurements of this study

An imaginary midline line perpendicular to the rostrum was identified. Various morphometric parameters were studied according to this midline [Figure 1].

These measurements were performed based on the studies of Mohebbi *et al*. as follows:[13]

- Distance from the midline to the right and left FRs
- Direct distance between VC and FR on both sides
- Horizontal distance between VC and FR on each side (distance between two vertical lines intersecting FR and VC)

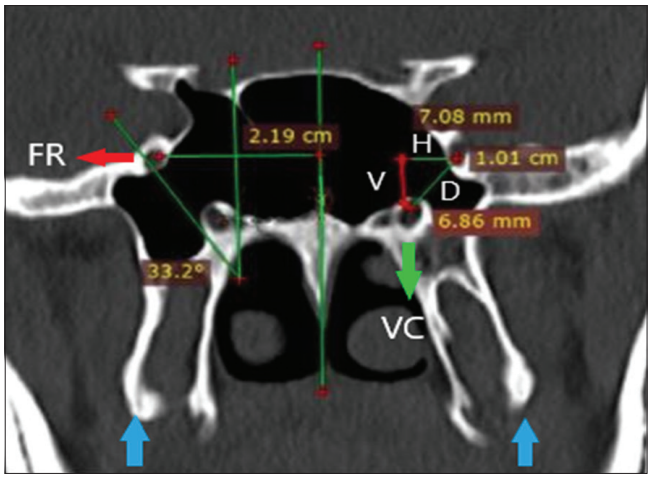


**Figure 1: The demonstration of various morphometric parameters (red arrow: foramen rotundum, green arrow: vidian canal, and blue arrow: lateral pterygoid plates; V: Vertical distance, H: Horizontal distance, and D: Direct distance) on the coronal computed tomography scan based on the study of Mohebbi *et al*.[13]**

- Vertical distance between VC and FR on each side (distance between two horizontal lines intersecting VC and FR)
- Right and left rotundum angles (were calculated as the angle between the imaginary line connecting FR to VC and the vertical line that crosses VC).

FR's position relative to the base of lateral pterygoid plate as reported by Mohebbi *et al*.[13] [Figure 2] was as follows:

- Located online: When FR is tangent to the lateral pterygoid plate
- Medially located: If FR is in the medial position relative to the lateral pterygoid plate
- Laterally located: FR is lateral to the lateral pterygoid plate.

The types of FR and VC based on the study of Mohebbi *et al*.[13] and Lee *et al*.[10] [Figure 3] were as follows:

- VC was divided into three types on CT:
  - Type 1 – VC is completely in the sphenoid sinus
  - Type 2 – When the VC is on the floor of the sphenoid sinus or partially protrudes into the sphenoid sinus
  - Type 3 – VC fully embedded in the sphenoid corpus.
- FR was divided into three types on CT:
  - Type I – FR is completely localized in the sinus cavity
  - Type IIa – FR is partially localized in the sinus cavity or partially protruding into the sphenoid sinus
  - Type IIb – When FR is tangent to the sinus wall
  - Type III – FR is completely inside the sphenoid bone.

### Statistical analysis

SPSS version 22 software (SPSS Inc., Chicago, IL, USA) was used to enter and analyze data. All analyses have been done with SPSS version 22 software at an error level of

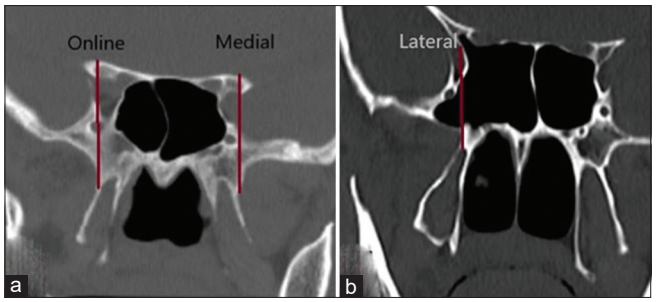


**Figure 2: Coronal computed tomography scan shows foramen rotundum localization with respect to the base of lateral pterygoid plate. (a) Online (right side) and medial (left side) (b) lateral**

0.05. The quantitative variables which included distances were expressed as standard deviation and mean. Statistical significance between right and left distances was determined using paired *t*-test and Student's *t*-test. According to the null hypothesis, there was no difference between the groups tested. $P < 0.05$ was defined as significant.

To study relationship between three qualitative variables of FR-online located, FR-medial, and FR-lateral, the Chi-squared test and Fisher's exact test was used. The relationship between variable of age and all individual quantitative variables was examined with Pearson correlation test. Since the sample size was below 30 at some levels of the qualitative variables and also reached below 5 at some levels of qualitative variables, the age variable distribution was not normal at some levels of qualitative variables with the sample size of below 30. Therefore, the Kruskal–Wallis nonparametric test was used to study the relationship between variable of age and all individual qualitative variables. An Independent *t*-test was used to examine the difference in the variables measuring the right and left sides according to gender. The Chi-squared test was used to examine the relationship between gender and all qualitative variables.

Due to the large sample size and based on the central limit theorem, the average distribution of quantitative variables is approximately normal.

## Results

The research participants have a mean age of 41.06 ± 17.812. Seventy-one (47.3%) females and 79 (52.7%) males were included in this study. Tables 1 and 2 report the descriptive statistics for the quantitative and qualitative variables according to gender, respectively. There was a significant difference in the distance from midline to right and left FR, horizontal, vertical, and direct distances from the right and left FRs to VCs ($P < 0.05$). There was no difference between the variables FR-online located and FR-medial ($P > 0.05$). There was a significant difference between the variables Type 1 VC and Type 3 VC. There was a significant relationship between the variables Type 2 VC and Type 3 VC ($P < 0.05$). There was a significant difference between the variables Type IIb FR and Type III FR ($P < 0.05$) [Table 3]. *P* value between some variables, as shown in Table 3, could not be calculated because the cells of the Chi-squared test were all zero.

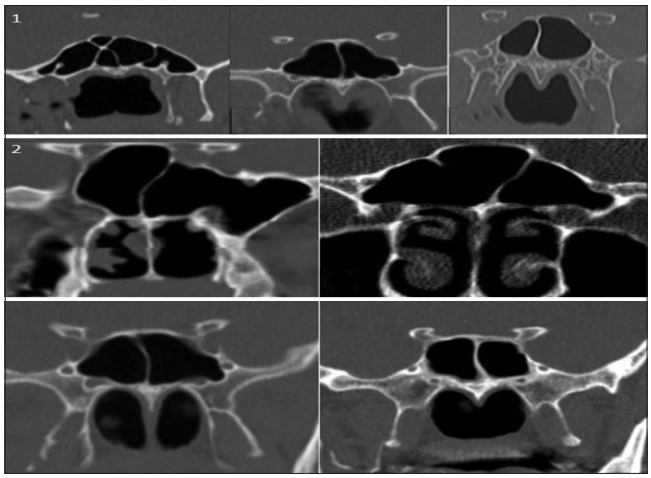


**Figure 3: (1) The types of vidian canal (a) Type 1 (b) Type 2 (c) Type 3 (2) the types of foramen rotundum (a) Type I (b) Type IIa (c) Type IIb (d) Type III**

**Table 1: Descriptive statistics for the quantitative variables according to gender**

| Variables | Mean±SD | |
|---|---|---|
| | Female | Male |
| Age | 43.70±15.50 | 38.68±19.45 |
| The distance from midline to right FR | 17.89±1.94 | 18±1.83 |
| The distance from midline to left FR | 18.33±1.94 | 19±2.18 |
| Direct distance between VK-FR right | 6.36±2.42 | 5.89±2 |
| Direct distance between VK-FR left | 6.54±2.17 | 6.54±1.75 |
| Horizontal distance between VK-FR right | 4.46±2.01 | 4.08±1.76 |
| Horizontal distance between VK-FR left | 4.73±1.83 | 4.75±1.56 |
| Vertical distance between VK-FR right | 4±1.84 | 3.8±1.54 |
| Vertical distance between VK-FR left | 3.97±1.64 | 4.05±1.59 |
| Right rotundum angle | 40.66±7.48 | 37.88±7.16 |
| Left rotundum angle | 40.07±6.75 | 38.89±6.48 |

FR: Foramen rotundum, VK: Vitek-Kent, SD: Standard deviation

Pearson correlation test and Kruskal–Wallis test results are reported in Table 3. There was no significant relationship between age and all individual quantitative variables ($P > 0.05$).

Table 3 shows that there was a significant difference in age among three levels of left, right, and bilateral localizations of qualitative variables of FR-online, FR-medial, Type 2 VC, Type 3 VC, Type IIb FR, and Type III FR. No significant difference was found in age at levels of other qualitative variables ($P > 0.05$).

There was a significant difference between gender and the distance from midline to left FR and right rotundum angle ($P < 0.05$), and no significant difference was found between the other parameters and gender ($P > 0.05$).

**Table 2: Descriptive statistics for the qualitative variables according to gender**

| Variables | Female, *n* (%) | Male, *n* (%) |
|---|---|---|
| FR-online located | | |
| Left | 5 (7) | 10 (12.7) |
| Right | 7 (9.9) | 6 (7.6) |
| Bilateral | 22 (31) | 27 (34.2) |
| Missing | 37 (52.1) | 36 (45.6) |
| FR-medial | | |
| Left | 7 (9.9) | 4 (5.1) |
| Right | 4 (5.6) | 10 (12.7) |
| Bilateral | 35 (49.3) | 32 (40.5) |
| Missing | 25 (35.2) | 33 (41.8) |
| FR-lateral | | |
| Left | 1 (1.4) | 4 (5.1) |
| Right | 2 (2.4) | 2 (2.5) |
| Bilateral | 1 (1.4) | 2 (2.5) |
| Missing | 67 (94.4) | 71 (89.9) |
| Type 1 VC | | |
| Left | 2 (2.8) | 4 (5.1) |
| Right | 5 (7) | 2 (2.5) |
| Bilateral | 4 (5.6) | 6 (7.6) |
| Missing | 60 (84.5) | 67 (84.8) |
| Type 2 VC | | |
| Left | 6 (8.5) | 3 (3.8) |
| Right | 4 (5.6) | 3 (3.8) |
| Bilateral | 16 (22.5) | 8 (10.1) |
| Missing | 45 (63.4) | 65 (82.3) |
| Type 3 VC | | |
| Left | 6 (8.5) | 5 (6.3) |
| Right | 5 (7) | 5 (6.3) |
| Bilateral | 37 (52.1) | 54 (68.4) |
| Missing | 23 (32.4) | 15 (19) |
| Type I FR | | |
| Left | 1 (1.4) | 1 (1.3) |
| Right | 0 | 0 |
| Bilateral | 1 (1.4) | 0 |
| Missing | 69 (97.2) | 78 (98.7) |
| Type IIa FR | | |
| Left | 2 (2.8) | 0 |
| Right | 5 (7) | 7 (8.9) |
| Bilateral | 6 (8.5) | 5 (6.3) |
| Missing | 58 (81.7) | 67 (84.8) |
| Type IIb FR | | |
| Left | 4 (5.6) | 5 (6.3) |
| Right | 4 (5.6) | 4 (5.1) |
| Bilateral | 15 (21.1) | 25 (31.6) |
| Missing | 48 (67.6) | 45 (57) |
| Type III FR | | |
| Left | 6 (8.5) | 9 (11.4) |
| Right | 4 (5.6) | 4 (5.1) |
| Bilateral | 36 (50.7) | 34 (43) |
| Missing | 25 (35.2) | 32 (40.5) |

FR: Foramen rotundum, VC: Vidian canal

There was no difference between each of the variables and gender ($P > 0.05$) [Table 3].

## Discussion

Although there are some studies on VC in the literature, to our knowledge, no such detailed studies about the radioanatomic relationship of VC and FR with adjacent anatomical structures have been found except one study reported by Mohebbi *et al*.[13]

Measurement values in our study were lower than those of Mohebbi *et al*.[13] It was reported by Mohebbi *et al*.[13] that the position of FRs was online in 50% of cases, medially placed in 47%, and laterally placed in 3% of cases. In our study, the case numbers of medially placed FR were higher than online placed, and the incidence of laterally placed FR was higher according to the study of Mohebbi *et al*.[13] In addition, in their study, it was found that 28 cases (28%) had Type 1 VC and 48% and 24% had Type 2 and 3 VCs, respectively. Four patients (4%) had Type I FR, 28% and 44% had Type IIa and IIb, respectively, and 24% had Type III FR.[13] In our study, all percentages were found to be lower except the percentage of Type 3 VC and FR. Furthermore, they reported the distance from FR to midline as 19.00 ± 2.07 mm in the right side and 19.34 ± 2.17 mm in the left side. In the right side, horizontal, vertical, and direct distances from FR to VC were reported as 5.89 ± 2.4 mm, 5.06 ± 2.03 mm, and 8.16 ± 2.27 mm, respectively. In the left side, horizontal, vertical, and direct distances from FR to VC were reported as 5.93 ± 2.13 mm, 5.49 ± 2.13 mm, and 9.20 ± 2.15 mm, respectively. Right and left FR angles were reported as 46.76 ± 12.32 and 46.40 ± 10.67, respectively.[13] All values of this study were lower than the study of Mohebbi *et al*.[13]

Kasemsiri *et al*.[11] reported the average distance from midline to left FR 19.11 mm and to right FR 17.67 mm. Close results were found in this study. Mohebbi *et al*.[13] reported that the average distance of midline to left FR was found to be significantly more than to right FR. The average horizontal and vertical distances from FR to VC in Kasemsiri's study[11] showed no significant difference between right and left sides, as the same result in the study of Mohebbi *et al*.[13] In our study, there was a significant difference in the distance from midline to right and left FR and horizontal, vertical, and direct distances from the right and left FRs to VCs.

Yeğin *et al*.[14] reported that VC in females was found in 31.5%, 32%, and 36.5% belonging to Types 1, 2, and 3, respectively. VC in males was found in 32.2%, 28.6%, and 39.1% belonging to Types 1, 2, and 3, respectively. In our study, VC in females was found in 15.5%, 36.6%, and 67.6% belonging to Types 1, 2, and 3, respectively. VC in males was found in 15.2%, 17.7%, and 81% belonging to Types 1, 2, and 3, respectively. The reason for some high results in our study may be the calculation of percentages of men and women among themselves, not by total number.

**Table 3: Relationships between variables analyzed by different statistical tests stated in the results section of the article**

| Variables | *P* |
|---|---|
| The distance from midline to right FR | 0.000 |
| The distance from midline to left FR | |
| Direct distance between VK-FR right | 0.001 |
| Direct distance between VK-FR left | |
| Horizontal distance between VK-FR right | 0.000 |
| Horizontal distance between VK-FR left | |
| Vertical distance between VK-FR right | 0.304 |
| Vertical distance between VK-FR left | |
| Right rotundum angle | 0.692 |
| Left rotundum angle | |
| FR-online located and FR-medial | 0.000 |
| FR-online located and FR-lateral | 0.1 |
| FR-medial and FR-lateral | 0.333 |
| Type 1 VC and Type 2 VC | 0.250 |
| Type 1 VC and Type 3 VC | 0.012 |
| Type 2 VC and Type 3 VC | 0.01 |
| Type I FR and Type IIa FR | Not calculated |
| Type I FR and Type IIb FR | Not calculated |
| Type I FR and Type III FR | Not calculated |
| Type IIa FR and Type IIb FR | 0.333 |
| Type IIa FR and Type III FR | Not calculated |
| Type IIb FR and Type III FR | 0.001 |
| Age and the distance from midline to right FR | 0.395 |
| Age and the distance from midline to left FR | 0.803 |
| Age and direct distance between VC-FR right | 0.372 |
| Age and direct distance between VC-FR left | 0.905 |
| Age and horizontal distance between VC-FR right | 0.143 |
| Age and horizontal distance between VC-FR left | 0.859 |
| Age and vertical distance between VC-FR right | 0.410 |
| Age and vertical distance between VC-FR left | 0.409 |
| Age and right rotundum angle | 0.866 |
| Age and left rotundum angle | 0.336 |
| Age and FR-online located | 0.023 |
| Age and FR-medial | 0.022 |
| Age and FR-lateral | 0.442 |
| Age and Type 1 VC | 0.897 |
| Age and Type 2 VC | 0.035 |
| Age and Type 3 VC | 0.021 |
| Age and Type I FR | 0.667 |
| Age and Type IIa FR | 0.711 |
| Age and Type IIb FR | 0.038 |
| Age and Type III FR | 0.049 |
| Gender and the distance from midline to right FR | 0.734 |
| Gender and the distance from midline to left FR | 0.048 |
| Gender and direct distance between VC-FR right | 0.202 |
| Gender and direct distance between VC-FR left | 0.984 |
| Gender and horizontal distance between VC-FR right | 0.217 |
| Gender and horizontal distance between VC-FR left | 0.934 |
| Gender and vertical distance between VC-FR right | 0.453 |
| Gender and vertical distance between VC-FR left | 0.738 |
| Gender and right rotundum angle | 0.021 |
| Gender and left rotundum angle | 0.275 |
| Gender and FR-online located | 0.570 |
| Gender and FR-medial | 0.150 |
| Gender and FR-lateral | 0.758 |
| Gender and Type1 VK | 0.376 |
| Gender and Type2 VK | 0.901 |
| Gender and Type3 VK | 0.631 |
| Gender and Type I FR | 1 |
| Gender and Type IIa FR | 0.512 |
| Gender and Type IIb FR | 0.768 |
| Gender and Type III FR | 0.731 |

FR: Foramen rotundum, VC: Vidian canal, VK: Vitek-Kent

According to the cone-beam CT study of Bahşi *et al*.,[15] it was reported that VC totally protruded into the sphenoid sinus (19.75%), partially protruded into the sphenoid sinus (44.37%), and embedded inside bony tissue of the body of sphenoid bone (35.87%). We can say that there are lower results in our study except the incidence of Type III FR.

Yazar *et al*.[16] reported the mean distance from FR to VC as 7.2 mm. As can be seen, the results of this study were lower than the results in the studies we discussed. We think that this result depends on the subpopulation we are working on.

Nowadays, less invasive endoscopic surgery is frequently performed for treating several diseases of paranasal sinuses.[14] Surgical excision of pituitary tumors is frequently performed with endoscopic transsphenoidal approach.[17] The paranasal sinuses have several anatomical variations. Appropriate information of these variations before the surgical operations using CT is fundamental to decrease the complications and to prevent the injury of important structures.[18] Several vital anatomical structures have a relationship with sphenoid sinus such as VC and FR.[9]

## Conclusion

Although there are studies related to the anatomical and radiological evaluation of VC in the literature, there is no comprehensive radiographic anatomical study in which VC and FR were evaluated together, except for the study of Mohebbi *et al*.[13] We think that this situation will increase the value of our study, can be a motivation source for other authors who are interested in this subject, and can make useful contributions to the literature.

### Financial support and sponsorship

Nil.

## Conflicts of interest

There are no conflicts of interest.

## References


1. Vaezi A, Cardenas E, Pinheiro-Neto C, Paluzzi A, Branstetter BF 4th, Gardner PA, *et al*. Classification of sphenoid sinus pneumatization: Relevance for endoscopic skull base surgery. Laryngoscope 2015;125:577-81.
2. Feneis H, Dauber W. Pocket Atlas of Human Anatomy-Based on the İnternational Nomenclature. 4th ed. Stuttgart: Thieme; 2000.
3. Berkovitz BK, Moxham BJ, Langdon JD. The temporomandibular joint and pterygopalatine fossa. In: Langdon JD, Berkovitz BK Moxham BJ, editors. Surgical Anatomy of the İnfratemporal Fossa. London: Martin Dunitz; 2003. p. 49-52.
4. Tubbs RS, Hill M, May WR, Middlebrooks E, Kominek SZ, Marchase N, *et al*. Does the maxillary division of the trigeminal nerve traverse the cavernous sinus? An anatomical study and review of the literature. Surg Radiol Anat 2008;30:37-40.
5. Tubbs RS, Salter EG. Vidius vidius (Guido Guidi): 1509-1569. Neurosurgery 2006;59:201-3.
6. Üstün Ç. Guido Guidi's short biography and his eponyms (the vidian artery, nerve and canal). Inönü Üniversitesi Tıp Fakültesi Dergisi 2003;10:51-3.
7. Standring S. Gray's anatomy E-Book: the anatomical basis of clinical practice. 41th ed. London: Elsevier Health Sciences; 2016.
8. Bahşi İ, Orhan M, Kervancıoğlu P, Yalçın ED. Morphometric evaluation and clinical implications of the greater palatine foramen, greater palatine canal and pterygopalatine fossa on CBCT images and review of literature. Surg Radiol Anat 2019;41:551-67.
9. Kazkayasi M, Karadeniz Y, Arikan OK. Anatomic variations of the sphenoid sinus on computed tomography. Rhinology 2005;43:109-14.
10. Lee JC, Kao CH, Hsu CH, Lin YS. Endoscopic transsphenoidal vidian neurectomy. Eur Arch Otorhinolaryngol 2011;268:851-6.
11. Kasemsiri P, Solares CA, Carrau RL, Prosser JD, Prevedello DM, Otto BA, *et al*. Endoscopic endonasal transpterygoid approaches: Anatomical landmarks for planning the surgical corridor. Laryngoscope 2013;123:811-5.
12. Chong VF, Khoo JB, Fan YF. Imaging of the nasopharynx and skull base. Neuroimag Clin N Am 2004;14:695-719.
13. Mohebbi A, Rajaeih S, Safdarian M, Omidian P. The sphenoid sinus, foramen rotundum and vidian canal: A radiological study of anatomical relationships. Braz J Otorhinolaryngol 2017;83:381-7.
14. Yeğin Y, Çelik M, Altıntaş A, Şimşek BM, Olgun B, Kayhan FT. Vidian canal types and dehiscence of the bony roof of the canal: An anatomical study. Turk Arch Otorhinolaryngol 2017;55:22-6.
15. Bahşi İ, Orhan M, Kervancıoğlu P, Yalçın ED. The anatomical and radiological evaluation of the Vidian canal on cone-beam computed tomography images. Eur Arch Otorhinolaryngol 2019;276:1373-83.
16. Yazar F, Cankal F, Haholu A, Kiliç C, Tekdemir I. CT evaluation of the vidian canal localization. Clin Anat 2007;20:751-4.
17. Unal B, Bademci G, Bilgili YK, Batay F, Avci E. Risky anatomic variations of sphenoid sinus for surgery. Surg Radiol Anat 2006;28:195-201.
18. Kaplanoglu H, Kaplanoglu V, Dilli A, Toprak U, Hekimoğlu B. An analysis of the anatomic variations of the paranasal sinuses and ethmoid roof using computed tomography. Eurasian J Med 2013;45:115-25.

Original Article

# Prevalence and Pattern of Molar Incisor Hypomineralization in Delhi Region

**Rashi Singh, Binita Srivastava, Nidhi Gupta**

*Department of Paediatric and Preventive Dentistry, Santosh Deemed to be University, Ghaziabad, Delhi NCR, India*

## Abstract

**Introduction:** Molar incisor hypomineralisation (MIH) is currently the most prevalent of developmental defects of enamel among children. Molar incisal hypomineralisation presents itself as a serious clinical dilemma for pediatric dentists and clinical practitioners. It is a global endemic. However, its prevalence in India remains uncertain to find prevalence and pattern of MIH in Delhi Region. **Material and Methods:** A total of 649 children aged between 7 and 10 years were randomly selected from various schools in Delhi National Capital Region (NCR). The teeth were examined moist under natural light. The developmental defects of enamel were graded using the modified European Academy of Pediatric Dentistry judgment Criteria given by Ghanim *et al*. 2015. **Results:** A total of 97 subjects presented with MIH of 649 subjects examined. MIH presented with a prevalence of 15%. Creamy white opacities were the most common of defects present, followed by yellowish-brown opacities. **Discussion and Conclusion:** The prevalence of MIH in the Delhi NCR region is 15%.

**Keywords:** *Demarcated opacities, developmental defects of enamel, European Academy of Pediatric Dentistry, hypomineralized second primary molar, molar-incisor hypomineralization*

## Introduction

Molar incisor hypomineralisation (MIH) is defined as the clinical appearance of morphological enamel defects involving the occlusal and/or incisal third of one or more permanent molars and is frequently associated with similar defects in permanent incisors. MIH is as a result of the hypomineralization of systematic origin. The term MIH was first cited by Weerheijm *et al*. 2001.[1,2]

Any insult or injury to ameloblasts during the formative stage of enamel may lead to qualitative or quantitative defects of enamel. The earlier focus of the research was mainly on developmental defects like amelogenesis imperfect or dental fluorosis, but currently, it has been shifted to MIH due to an increase in the number of cases being reported.[3]

MIH is a chronological qualitative defect of enamel affecting first permanent molars and being associated with permanent incisors usually presenting as well-demarcated creamy white or yellowish enamel defects, which may or may not be associated with posteruptive breakdown (PEB).[4]

There has been a wide disparity in the prevalence reports of MIH. In national epidemiological surveys on caries prevalence, children are normally not screened for the presence of MIH, so little is known about its occurrence. Various studies done worldwide have shown the prevalence of MIH, ranging from 2.4% to 40.2% due to the different criteria used.[5]

With the introduction of the terminology of MIH, European Academy of Paediatric Dentistry (EAPD) gave the first index for specific reporting of MIH in 2003. Other Non-European criteria have also reported with wide variations in the prevalence ranging from as high as 40.2% in Brazilian children (Weerheijm *et al*. 2003) to as low as 2.8% in Hongkong (Cho *et al*. 2008).[6,7]

FDI commission on oral health, research, and epidemiology in 1992 classified enamel defects into two distinct categories: hypomineralized enamel or opacities and-enamel hypoplasia. The first judgment criterion for MIH was given by EAPD in 2003 further modified in 2008.[8,9]

In 2015 Ghanim *et al*. proposed a charting method for the purpose of using single unified criteria for reporting of MIH cases,

**How to cite this article:** Singh R, Srivastava B, Gupta N. Prevalence and pattern of molar Incisor hypomineralization in Delhi region. J Anat Soc India 2020;69:XX-XX.



**Article Info**

**Received:** 30 May 2020
**Accepted:** 31 August 2020
**Available online:** ***

***Address for correspondence:***
*Dr. Rashi Singh, Department of Paediatric and Preventive Dentistry, Santosh Deemed to be University, Ghaziabad, Delhi NCR, India. E-mail: drsinghrashi@gmail.com*

**Access this article online**

**Website:** www.jasi.org.in
**DOI:** 10.4103/JASI.JASI_101_20
**Quick Response Code:**

which may help preventing the disparity encountered during data compilation due to different coding criteria being used by different researchers, thus provide a better picture of MIH worldwide.[10]

There have not been any reported studies in India with the new unified criteria to determine the prevalence of MIH; therefore, studies are needed for improved understanding of MIH and its presentation in this region.

The aim of the present study was to determine the prevalence and pattern of MIH in the Delhi Region.

## Material and Methods

### Study design

*Sample size*

The present study was conducted on a total of 649 children. Children aged 7–12 years were randomly selected from different schools in the Delhi region.

### Inclusion criteria

Normal healthy co-operative children aged 7–12 years, with proper consent duly signed by the parents, were randomly selected for the study.

### Exclusion criteria

Children having other enamel defects such as amelogenesis imperfecta, dentinogenesis imperfecta, hypoplastic diffused enamel defects, tetracycline stains on index teeth were excluded from the study.

Furthermore, noncooperative children or children affected by any systemic diseases were excluded from the study.

### Examination of index teeth

Clinical examination for MIH was conducted in the school itself. Each child was examined by a single examiner under natural light, while seated on a school chair. A trained assistant helped record the findings during intra-oral examination.

The teeth were examined moist. Any debris, if present-were removed with a gauze swab. Four first permanent molar and permanent incisors were examined in each child and evaluated according to base on the modified EAPD charting and recording criteria given by Ghanim *et al*. 2015.

Children with lesions smaller than 2 mm were excluded from further evaluation [Figures 1 and 2]. Teeth which

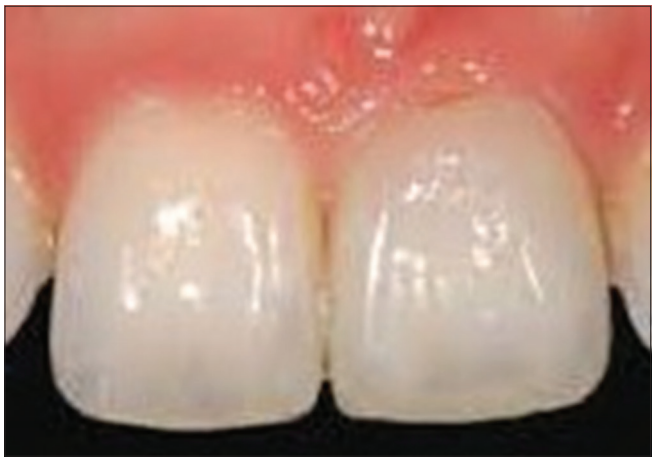

**Figure 1: Normal Incisors**

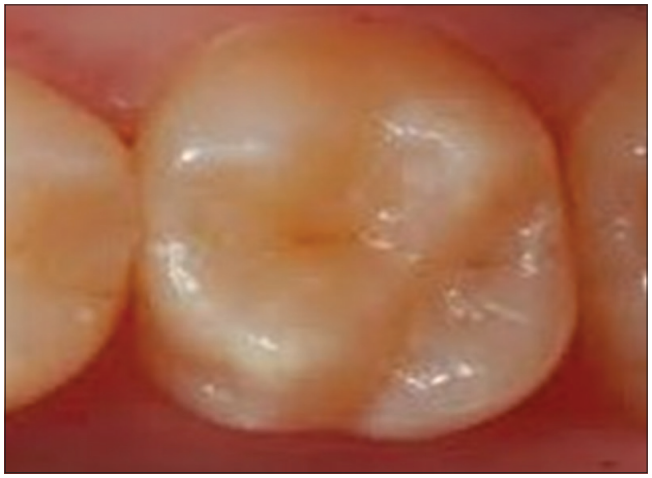

**Figure 2: Normal molar**

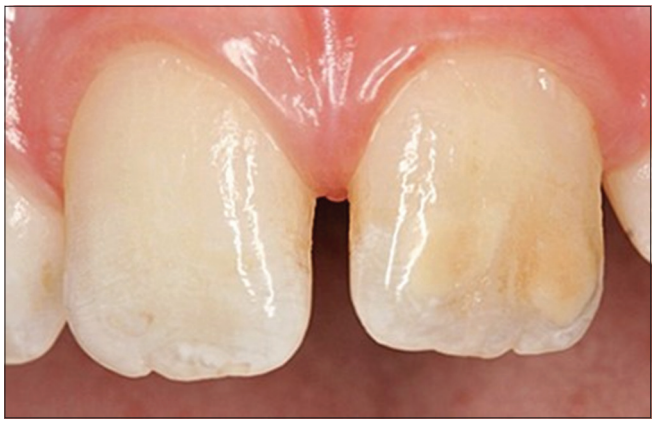

**Figure 3: Molar incisor hypomineralisation lesion in incisors**

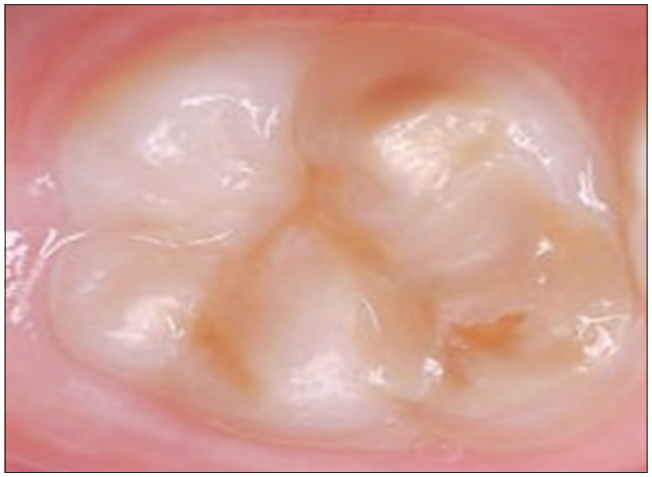

**Figure 4: Molar incisor hypomineralisation lesion in molar**

were currently erupting or erupted <2/3rd were considered to be unerupted. A child was diagnosed positive for MIH if at least one of the erupted first permanent molars presented with a demarcated defect on enamel >2 mm in diameter [Figures 3 and 4].

The data of patients was recorded on a preprinted pro formas with subject's demographic details.

Data were collected manually, tabulated in MS windows excel sheet and analyzed using SPSS software version 17.0 (Inc., Chicago, USA). Data were assessed using Pearson's Chi-square test, Spearman's co-efficient, Fisher's extract, McNemara's test, etc.

## Results

A total of 649 subjects were examined, of which 97 subjects (15%) reported with the presence of MIH. No significant differences were found between males and females in MIH prevalence.

Number of subjects with only molars involved were 40 (6.22%), whereas subjects who showed involvement of both molars and incisors affected were 57 (8.78%).

Of the entire subjects involved total number of molars affected were 244/388 (62.89%).

Table 1 shows the distribution of MIH in molars. There was no significant predilection towards right or left side. Mandibular molars were more commonly affected than the maxillary molars.

Of all the teeth involved, a total of 131/776 incisors were affected (16.88%).

Table 2 shows the distribution of MIH in incisors. There was no right or left predilection. Maxillary incisors appeared to be more commonly affected than mandibular incisors.

Table 3 shows the presentation of MIH in molars. Two molars were the most commonly affected followed by the involvement of both maxillary and mandibular molars of both arches simultaneously. Single molar involvement was less common.

Table 4 shows the presentation of MIH in Incisors. Single incisor involvement was the most common, and usually, the maxillary incisors were most involved.

Table 5 shows surface involvement in molars. About 48% of the molars surfaces were affected. Buccal and occlusal surfaces were the most commonly affected. Lingual or palatal surface involvement was less.

- Total number of surfaces-732
- Total number of surfaces affected-352 (48.09%).

Coming to defect characteristics in molars, Creamy white opacities were the most usually encountered in about 81.53% of surfaces involved, followed by yellowish-brown opacities in 18.46%. PEB was also seen in 5.97% of surfaces.

**Table 1: Number of molars affected**

| | Right | Left | Total |
|---|---|---|---|
| Max | 55 | 52 | 107 |
| Mand | 68 | 69 | 137 |

**Table 2: Number of incisors affected**

| Tooth | Right | | Left | |
|---|---|---|---|---|
| | LI | CI | CI | LI |
| Max | 8 | 27 | 31 | 8 |
| Mand | 8 | 21 | 21 | 7 |

**Table 3: Number of molar teeth affected as per subjects**

| | Subjects (*n*=97) | Molars (%) |
|---|---|---|
| 1 molar | 14 | 14 (5.74) |
| 2 molars | 48 | 96 (39.34) |
| 3 molars | 6 | 18 (7.38) |
| 4 molars | 29 | 116 (47.54) |

**Table 4: Number of incisor teeth affected as per subjects**

| | Subjects (*n*=57), *n* (%) |
|---|---|
| 1 incisor | 24 (24.74) |
| 2 incisors | 11 (11.34) |
| 3 incisors | 13 (13.40) |
| ≥4 incisors | 9 (9.27) |

**Table 5: Number of surfaces affected in molars**

| Surfaces | *n*=352, *n* (%) | Surfaces |
|---|---|---|
| Occlusal | 147 (41.76) | Occlusal |
| Buccal | 148 (42.05) | Buccal |
| Lingual/palatal | 57 (16.19) | Lingual |

## Discussion

MIH is a term used to describe hypoplastic developmental defects in enamel. The term was first introduced by Weerhejeim *et al.* in 2003. It describes a special pattern of enamel defects affecting the permanent first molars and incisors. The defects present as clearly demarcated opacities ranging from white to yellow to yellowish-brown which may be associated with PEB.

MIH is very frequent in populations across the world. The European academy has long recognized MIH as a global phenomenon necessitating further research and knowledge to have full understanding of the defect. Furthermore, the EAPD had announced criteria specifically for MIH evaluation.

However, there was a wide variation in defect prevalence due to the use of different criteria and indices across the globe; cross comparison of data are difficult. Other non-European countries also showed a wide disparity in the prevalence of MIH, ranging from a low of 2.8% in Hong Kong to a high of 40.2% in Brazil.

Considering this, a unified diagnostic criterion was proposed by Ghanim *et al*. in 2015. This criteria proposed a grading method that allowed separate classification for hypomineralized demarcated lesions of the enamel (MIH) and also differentiated it from other similar defects. It also aids in grading the severity of the lesion.

In this study, permanent molars and incisors were scored based on the same criteria. The study reported a prevalence of MIH was 15%, which was in sync with studies done by Kusku *et al*. 14.9%, Laisi *et al*. 16.3%, and Balmer *et al*. 15.9%.[11,12] It was moderately prevalent than studies done by Bhaskar *et al*. 9.46%, Parikh *et al*. 9.2%.[13,14] This study showed that MIH in Delhi was moderately prevalent in comparison with data from other cities and countries.

There were differences found between investigations in regard to MIH. This may be because of the reason that the criteria used for investigations were different or self-made at time.[15] In this study a criterion strictly for MIH was applied and not adapted from other criteria. The modified DDE index does not differentiate clearly between hypomineralisation and certain other enamel defects.

With the standardization of criteria, the prevalence of MIH has shown a gradual increase due to proper diagnosis of lesion and more cases being reported; thus has become a significant concern which needs to be taken care of.

The introduction of EAPD criteria for the evaluation and diagnosis of MIH was considered due to its simplicity which allows easy clinical reproducibility for recording defects. The criterion was standardized by Ghanim *et al*. in 2015, which was used in the present study.

The following study was done in the school campus itself in daylight conditions without using artificial light, which was in accordance with other studies conducted. Given the similarity in age group among different studies, the difference in results may be contributed to differences in criteria used, geographical locations, and other environmental factors.

Of the total subjects affected, about 63% had one or more molars affected. Incisors affected were less commonly affected, about 17% of cases. Although few studies have found a high prevalence of MIH in girls compared to boys, there was no significant gender prevalence in the present study.[16,17]

Mandibular molars were more commonly affected than maxillary molars. In incisors, there was no significant arch prevalence; it was more or less the same for both arches. The right side appeared to be more commonly effected than the left arch for MIH though the results were not statistically significant.[18]

Coming to lesion characteristics, white spot lesions were the most common in molars, followed by yellowish-brown lesions. PEB was most commonly associated with yellowish-brown lesions. The results showed a positive association between the change in color of enamel from white to yellowish-brown and the severity of the lesion. This remained constant for all ages. Also with an increase in the number of surfaces involved, there was an increase in the severity of the lesion.

In incisors, central incisors were most affected followed by mandibular central incisors then lateral incisors. The defect was almost 100% confined to the buccal surface and more common in the maxillary arch though not statistically significant. Other studies also reported similar findings where the subjects with an increased no of affected teeth reported with an increase in the severity and extent of lesions Jalevik *et al*. 2001, Leppaneimi *et al*. 2001, Lygidakis *et al*. 2008, Ghanim *et al*. 2011, Parikh *et al*. 2012.[19-21]

The incisors affected by MIH exhibited demarcated opacities with enamel loss. This was in line with other studies which stated that incisors rarely exhibit postoperative breakdown due to the absence of masticatory forces upon these surfaces.[22]

In epidemiological studies reporting of the severity of the defect is of greater importance as it reflects upon the treatment needs required by the children affected.

There is a lack of a demarcated classification for MIH lesions, which makes it difficult to diagnose the condition and provide solutions needed.

## Conclusion

MIH is the most prevalent current endemic faced by pediatric dentists and clinicians today, which needs to be attended as early as possible.

Further studies are needed in various regions of India to establish the exact current status of MIH in India using the recently standardized modified coding criteria.

### Financial support and sponsorship

Nil.

### Conflicts of interest

There are no conflicts of interest.

## References

1. Weerheijm KL, Jälevik B, Alaluusua S. Molar-incisor hypomineralisation. Caries Res 2001;35:390-1.
2. Weerheijm KL, Groen HJ, Beentjes VE, Poorterman JH. Prevalence of cheese molars in eleven-year-old Dutch children. ASDC J Dent Child 2001;68:259-62.
3. Elfrink ME, Schuller AA, Weerheijm KL, Veerkamp JS. Hypomineralized second primary molars: Prevalence data in Dutch 5-year-olds. Caries Res 2008;42:282-5.
4. Jeremias F, de Souza JF, Silva CM, Cordeiro Rde C, Zuanon AC, Santos-Pinto L. Dental caries experience and molar-incisor hypomineralization. Acta Odontol Scand 2013;71:1-7.

5. Muratbegovic A, Zukanovic A, Markovic N. Molar-incisor-hypomineralisation impact on developmental defects of enamel prevalence in a low fluoridated area. Eur Arch Paediatr Dent 2008;9:228-31.
6. Weerheijm KL, Duggal M, Mejàre I, Papagiannoulis L, Koch G, Martens LC, *et al*. Judgement criteria for molar incisor hypomineralisation (MIH) in epidemiologic studies: A summary of the European meeting on MIH held in Athens, 2003. Eur J Paediatr Dent 2003;4:110-3.
7. Cho SY, Ki Y, Chu V. Molar incisor hypomineralization in Hong Kong Chinese children. Int J Paediatr Dent 2008;18:348-52.
8. Weerheijm KL. Molar incisor hypomineralisation (MIH). Eur J Paediatr Dent 2003;4:114-20.
9. Lygidakis NA, Dimou G, Briseniou E. Molar-incisor -hypomineralisation (MIH). Retrospective clinical study in Greek children. I. Prevalence and defect characteristics. Eur Arch Paediatr Dent 2008;9:200-6.
10. Kusku OO, Caglar E, Sandalli N. The prevalence and aetiology of molar-incisor hypomineralisation in a group of children in Istanbul. Eur J Paediatr Dent 2008;9:139-44.
11. Balmer RC, Laskey D, Mahoney E, Toumba KJ. Prevalence of enamel defects and MIH in non-fluoridated and fluoridated communities. Eur J Paediatr Dent 2005;6:79-83.
12. Ghanim A, Elfrink M, Weerheijm K, Mariño R, Manton D. A practical method for use in epidemiological studies on enamel hypomineralisation. Eur Arch Paediatr Dent 2015;16:235-46.
13. Lygidakis NA, Wong F, Jälevik B, Vierrou AM, Alaluusua S, Espelid I. Best clinical practice guidance for clinicians dealing with children presenting with Molar-Incisor-Hypomineralisation (MIH): An EAPD Policy document. Eur Arch Paediatr Dent 2010;11:75-81.
14. Parikh DR, Ganesh M, Bhaskar V. Prevalence and characteristics of Molar Incisor Hypomineralisation (MIH) in the child population residing in Gandhinagar, Gujarat, India. Eur Arch Paediatr Dent 2012;13:21-6.
15. Oliver K, Messer LB, Manton DJ, Kan K, Ng F, Olsen C, *et al*. Distribution and severity of molar hypomineralisation: Trial of a new severity index. Int J Paediatr Dent 2014;24:131-51.
16. Elfrink ME, Ten Cate JM, Jaddoe VW, Hofman A, Moll HA, Veerkamp JS. Deciduous molar hypomineralization and molar incisor hypomineralization. J Dent Res 2012;91:551-5.
17. Chawla N, Messer LB, Silva M. Clinical studies on molar-incisor-hypomineralisation part II: Development of a severity index. Eur Arch Paediatr Dent 2008;9:191-9.
18. Weerheijm KL. Molar incisor hypomineralization (MIH): Clinical presentation, aetiology and management. Dent Update 2004;31:9-12.
19. Jälevik B, Klingberg GA. Dental treatment, dental fear and behaviour management problems in children with severe enamel hypomineralization of their permanent first molars. Int J Paediatr Dent 2002;12:24-32.
20. Seow WK. Clinical diagnosis of enamel defects: Pitfalls and practical guidelines. Int Dent J 1997;47:173-82.

Original Article

# Global Research Output of the Cerebellum: Yesterday, Today, and Tomorrow

**Murat Golpinar, Emre Demir[1]**

*Departments of Anatomy and [1]Biostatistics, Faculty of Medicine, Hitit University, Çorum, Turkey*

## Abstract

**Introduction:** The cerebellum has been regarded as a valuable research topic over the years because of its numerous roles in motor and nonmotor functions. The aim of the current study was to provide a comprehensive and holistic evaluation of publications concerning the cerebellum over the last 40 years which can be a potential guide for future research related to the cerebellum. **Material and Methods:** The Web of Science database was used to identify the publications relating to the cerebellum between 1980 and 2019. The identified publications were analyzed using the bibliometric approaches. The number of the publications concerning the cerebellum to be published between 2020 and 2028 was predicted using the linear regression analysis. **Results:** The literature review revealed a total of 33,186 publications. The top three active countries were found to be the USA (7362), Japan (2987), and the UK (1994). A positive and significant correlation was found between the number of cerebellum articles produced by the countries and the development indexes of the countries ($r = 0.743$, $P < 0.001$; $r = 0.676$, $P < 0.001$, $r = 0.656$, $P < 0.001$). The top three productive journals were found to be the Journal of Neuroscience, Brain Research, and Cerebellum. The total number of cerebellum publications is expected to continue in an increasing trend and reach a total of 891 publications at the end of 2028. **Discussion and Conclusion:** Recent studies on the cerebellum have mostly focused on the cerebellar degeneration, functional connections of the cerebellum, and its relationship with various diseases such as ataxia, schizophrenia, Parkinson's disease, autism, and aneurysms.

**Keywords:** *Bibliometric analysis, cerebellum, neuroanatomy, scientometric analysis, trends*

## Introduction

The cerebellum, which contains more than 50% of the neurons in the human brain, is a crucial component in the central nervous system. For many years, the cerebellum has been considered as primarily responsible for the coordination of movement and the maintenance of posture and balance. However, recent studies have indicated its contribution to a huge variety of cognitive, emotional, and behavioral functions.[1-3] Due to its extensive reciprocal connectivity with sensorimotor and association areas of the cerebral cortex, thalamus, and spinal cord, the cerebellum performs various vital functions in humans.[4] Studies have also shown that structural and functional cerebellar abnormalities are closely related to a wide range of neurodegenerative and psychiatric disorders, including Alzheimer's disease, Schizophrenia, Parkinson's disease, and Multiple sclerosis.[5-8] Due to its vital and different roles in motor and nonmotor functions, the cerebellum has been regarded as a valuable research topic over the past years.

Bibliometrics, based on the application of mathematical and statistical methods, is a commonly used approach for the descriptive analysis of the quality of scientific outputs such as books, articles, and reviews.[9,10] It provides an objective and effective way for a detailed evaluation of the history, current state and future of scientific publications in a particular field or specific topic, both qualitatively and quantitatively. In bibliometrics, specific features of the scientific documents and publications are analyzed to determine the level of scientific communication. Bibliometric analysis also allows the comparisons to reveal the efficiency of the researchers, institutions, organizations, and countries in various research areas. In this way, bibliometric information enables the identification of global research patterns, dynamics, and trends in a scientific field or topic during a certain period. Therefore, the bibliometric approach reveals valuable and useful information for the comprehensive



**How to cite this article:** Golpinar M, Demir E. Global research output of the cerebellum: Yesterday, today, and tomorrow. J Anat Soc India 2020;69:XX-XX.

**Article Info**

**Received:** 19 June 2020
**Accepted:** 13 August 2020
**Available online:** ***

***Address for correspondence:***
*Dr. Murat Golpinar, Department of Anatomy, Faculty of Medicine, Hitit University, Çorum, Turkey.*
*E-mail: golpinarmurat@hotmail.com*

**Access this article online**

**Website:** www.jasi.org.in
**DOI:** 10.4103/JASI.JASI_114_20
**Quick Response Code:**

evaluation of the scientific outputs for both researchers and organizations.[11,12] There have been many scientific papers concerning the cerebellum over the years, and studies on the cerebellum are still growing rapidly. However, there has been no detailed analysis performed on the scientific output in respect of the cerebellum to date. The aim of the present research was to perform a comprehensive and holistic analysis of the publications concerning the cerebellum published during the period from 1980 to 2019 through bibliometric approaches and to determine the evolving research trends on the cerebellum topic over the 40 years.

## Material and Methods

Articles about the cerebellum were accessed through the Web of Science (WoS) database, using the keywords of "cerebellum, cerebellar, cerebelli, and cerebello" in the titles section of the articles *(Search codes for repeatability were Title: [cerebellum] or Title: [cerebellar] or Title: [cerebelli] or Title: [cerebello] Refined by: Document Types: [Article] Timespan: 1980–2019. Indexes: SCI-Expanded, SSCI, A and HCI, CPCI-S, CPCI-SSH, BKCI-S, BKCI-SSH, ESCI)*. All the articles on the cerebellum in WoS downloaded through this search method (accession date: January 15, 2019; the number of publications may vary according to the date of search) were analyzed bibliometrically. A web site (http://lert.co.nz/map/) was used to generate the world map. VOSviewer (Version 1.6.13, Leiden University: Centre for Science and Technology) package program was utilized for bibliometric web visualizations.[13]

Statistical data analyses were performed using the SPSS software version 22.0 (SPSS Inc., Chicago, IL, USA, license: Hitit University). The normality of the data distribution was tested using the Kolmogorov–Smirnov test. According to the data distribution, the correlation analysis between the number of articles about the cerebellum and the Gross Domestic Products (GDP), GDP (at purchasing power parity) per capita (GDP PPP), and Human Development Index (HDI) were analyzed using the Spearman correlation test. The number of publications to be published in the following years was predicted using the linear regression analysis. Statistical significance was taken as $P < 0.05$.

## Results

The literature review revealed in a total number of 33,186 publications. Of these publications, 22,084 (66.5%) were articles, 6070 (18.291%) were meeting abstracts, 1271 (3.830%) were reviews, 1221 (3.679%) were proceedings papers, 1070 (3.224%) were letters, and the rest were editorial materials (963), notes (824), corrections (181), book chapters (163), early access (38), correction additions (17), discussions (15), news items (13), book reviews (12), reprints (12), books (5), bibliography (1), biographical item (1), hardware review (1), item about an individual (1), and retraction (1). This study performed the bibliometric analysis of only 22084 publications that were in the article category. Of these articles, 97.2% (21,460) were written in English. Other articles were written in French (184), German (114), Spanish (97), Russian (93), Japanese (51), Portuguese (24), Italian (17), Czech (14), Chinese (9), Turkish (7), Polish (5), Dutch (2), Hungarian (2), Serbian (2), Croatian (1), Slovak (1), and Ukrainian (1).

### Development of publications

The annual distribution of the 22,084 articles published between 1980 and 2019 is shown in Figure 1. The figure also displays the regression analysis results indicating the future predictions of expected publication numbers. According to the regression analysis results, it is estimated that 792 (CI 95%: 709–875) articles will be published in the year 2020 and 891 (695–1087) articles in the year 2028 [Figure 1].

### Active countries

A total of 142 countries had produced publications. The publication distribution of the countries was displayed on the World Map in Figure 2. The active countries that produced more than 100 articles were the USA (7362), Japan (2987), the UK (1994), Germany (1812), Italy (1771), France (1492), Canada (991), Spain (880), China (854), Netherlands (621), Switzerland (490), Australia (458), South Korea (431), Belgium (361), India (350), Turkey (343), Sweden (319), Brazil (294), Taiwan (274), Denmark (236), Israel (229), Norway (208), Russia (208), Finland (176), Mexico (175), Poland (175), Austria (159), Hungary (135), Greece (112), New Zealand (107), and Iran (100), respectively [Figure 3].

### Correlation analysis

A significant positive correlation was found between the number of articles about the cerebellum and GDP, GDP PPP, and HDI development indicators of the countries ($r = 0.743$, $P < 0.001$; $r = 0.676$, $P < 0.001$, $r = 0.656$, $P < 0.001$, respectively).

### Active authors

The top ten authors who produced the highest number of articles concerning the cerebellum were as fallow; Timmann D (161), Watanabe M (117), De Zeeuw CI (96), Kano M (94), D'angelo E (91), Hawkes R (90), Schousboe A (75), Mariani J (67), Mikoshiba K (58), and Linden DJ (57), respectively.

### Active institutions

The organizations and organizations enhanced that produced the highest number of articles on the cerebellum are listed in Table 1.

### Active research areas

In the past 40 years, the top ten research fields of

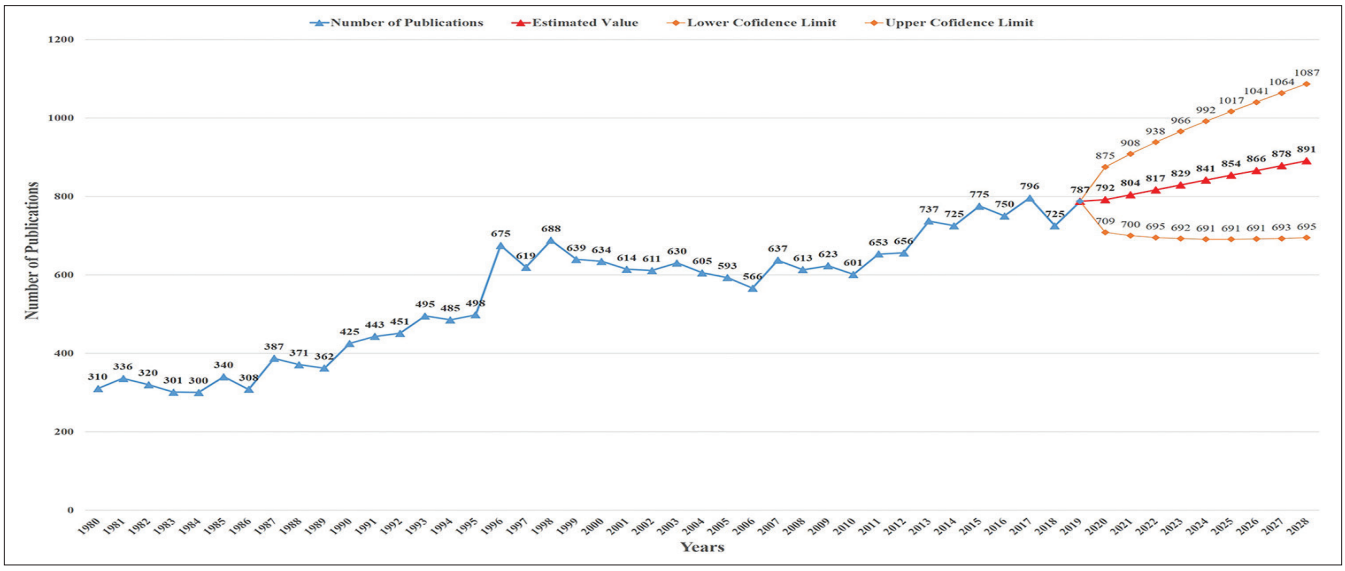


**Figure 1: Number of publications by years on the cerebellum**

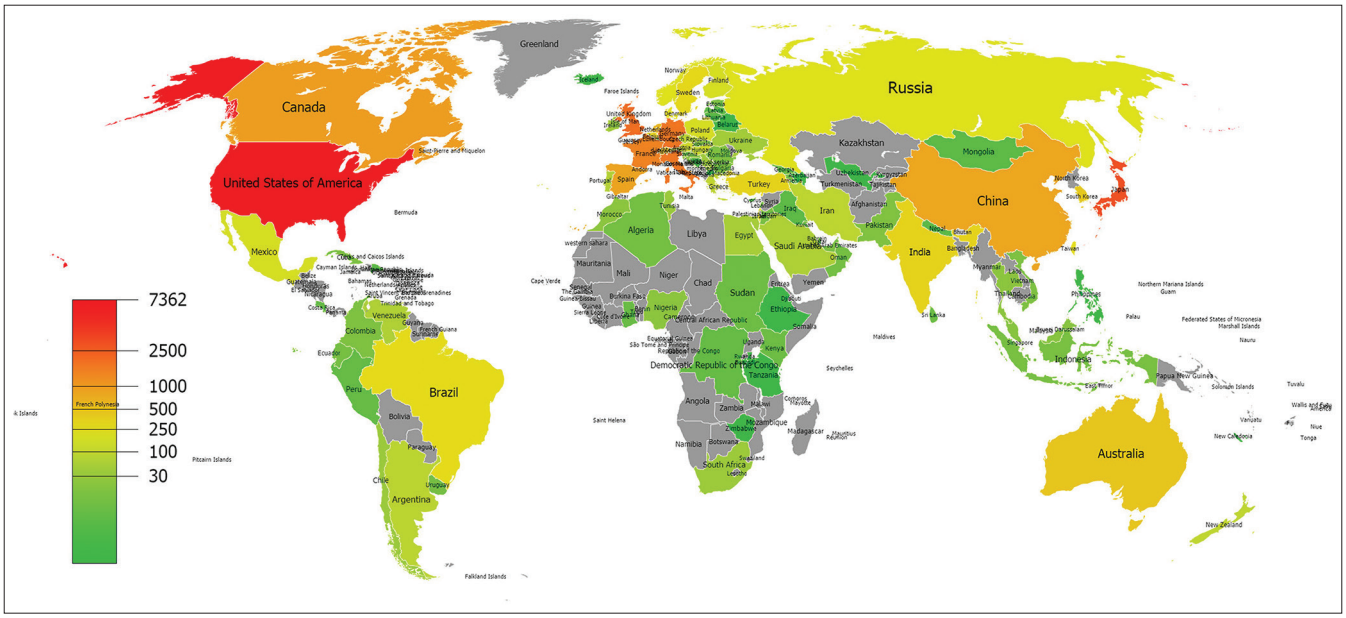


**Figure 2: The distribution of the most productive countries on the cerebellum**

cerebellum studies were found to include as follows: Neurosciences (11383; 51.5%), Clinical Neurology (4425; 20.037%), Biochemistry Molecular Biology (1785; 8.083%), Surgery (1410; 6.385%), Pharmacology Pharmacy (991; 4.487%), Physiology (969; 4.388%), Radiology Nuclear Medicine Medical Imaging (915; 4.143%), Cell Biology (899; 4.071%), Multidisciplinary Sciences (890; 4.030%), and Developmental Biology (819; 3.709%), respectively.

## Active journals

Articles related to the cerebellum were published in a total of 2327 journals. Of them, 52 were published more than 75 articles [Table 2]. The total number of citations and the mean number of citations per article are also given in Table 2. In addition, the top 10 most active journals that published the articles on cerebellum topic and the top 10 journals with the most citation per article are presented in Figure 4a and b, respectively.

## Citation analysis

Table 3 lists the 15 top-cited articles out of the total number of 22,084 articles on the cerebellum. The last column in Table 3 shows the average number of citations per year.

## Co-citation analysis

A total number of 343,238 different publications were cited in the references sections of the 22084 articles. The 10 most-cited publications that received more than 400 citations were the studies conducted by Ito, Lowry *et al*.,

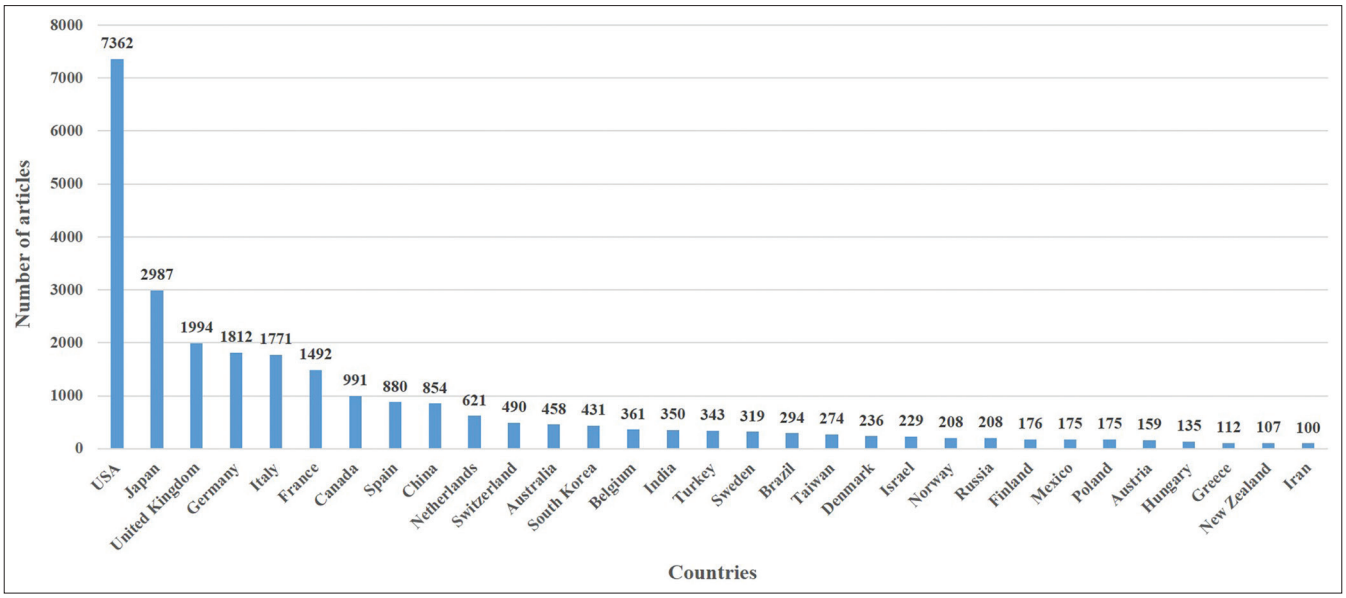


**Figure 3: The active countries that produced more than 100 articles on the cerebellum**

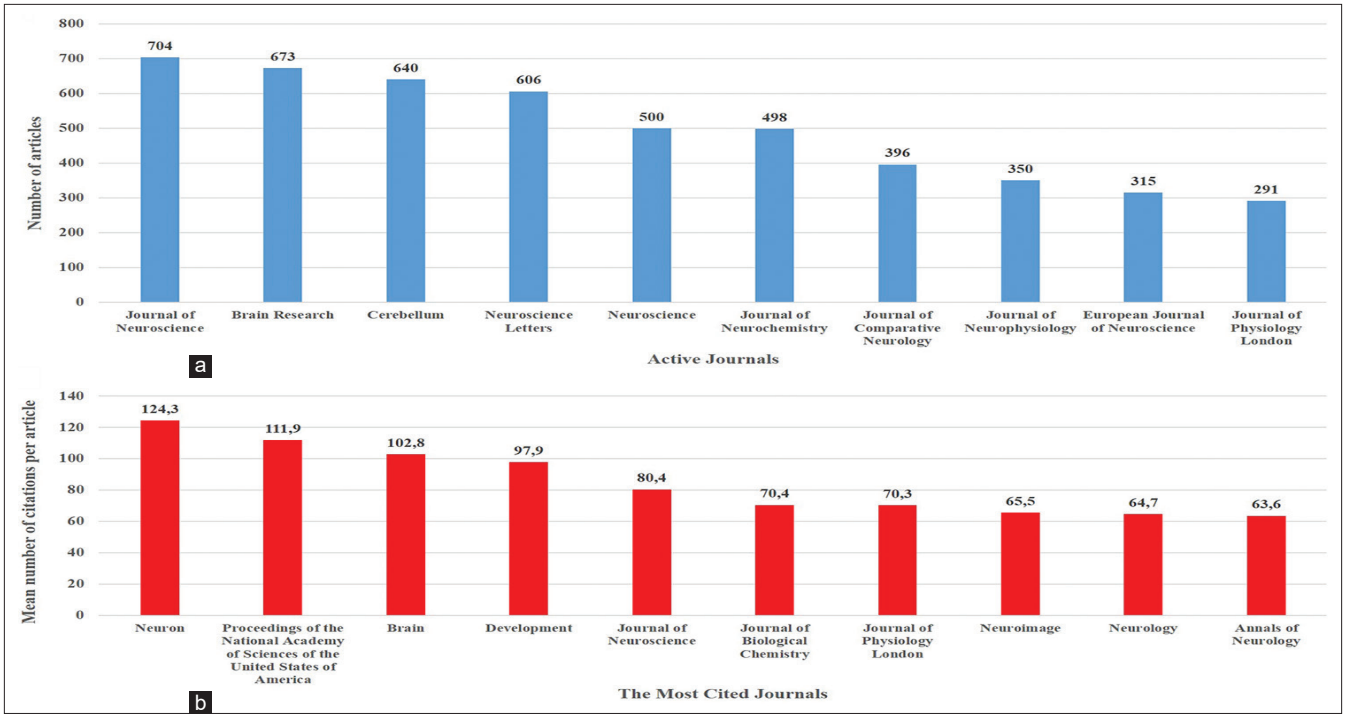


**Figure 4: (a) The top 10 most active journals that published articles on the cerebellum. (b) Top ten journals with the most citations per article**

Eccles *et al*., Palay and Chan-Palay, Marr, Schmahmann and Sherman, Albus(1972), Altman, Stoodley and Schmahmann, and Gallo *et al*., respectively.[14-23]

## Keyword analysis and trend topics

A total number of 25,267 different keywords were used in the 22,084 articles produced about the cerebellum. Table 4 shows at least 53 keywords used in at least 90 different articles. Figure 5 displays the cluster analysis performed with 124 keywords used in at least 50 different articles. Figure 6 demonstrates the network visualization map of the trend keyword analysis in the articles published between 1980 and 2019, the analysis aimed to identify the topic tendency according to the years and potential trends in future. The network visualization map regarding the keyword citation analysis in Figure 7 aimed to identify the effective topics that received more citations.

## Discussion

In the present study, we investigated global research output on cerebellum over the last 40 years. The results indicated

**Table 1: Active organizations and organizations-enhanced on the cerebellum**

| Organizations | RC | Organizations-Enhanced | RC |
|---|---|---|---|
| Harvard University | 314 | Centre National De La Recherche Scientifique CNRS | 656 |
| Johns Hopkins University | 308 | University of California System | 645 |
| CNRS | 268 | University of London | 645 |
| University Tokyo | 268 | Institut National De La Sante Et De La Recherche Medicale Inserm | 624 |
| UCL | 248 | University College London | 486 |
| CNR | 226 | Harvard University | 471 |
| University Pavia | 212 | National Institutes of Health (NIH) USA | 410 |
| University Tubingen | 205 | Sorbonne Universite | 390 |
| Inserm | 195 | Johns Hopkins University | 374 |
| Kyoto University | 191 | Assistance Publique Hopitaux Paris APHP | 354 |
| University Minnesota | 186 | Consiglio Nazionale Delle Ricerche CNR | 318 |
| University California Los Angeles | 183 | University of Texas System | 290 |
| University Paris 06 | 176 | University of Tokyo | 278 |
| Hokkaido University | 173 | Erasmus University Rotterdam | 259 |
| University Toronto | 172 | Riken | 243 |
| Riken | 170 | Eberhard Karls University of Tubingen | 235 |
| University Texas | 167 | Sapienza University Rome | 229 |
| University Colorado | 166 | Max Planck Society | 216 |
| Osaka University | 165 | University of Toronto | 216 |
| Northwestern University | 163 | University of Pavia | 215 |
| University California San Francisco | 162 | Hopital Universitaire Pitie Salpetriere APHP | 205 |
| University Munich | 162 | Erasmus MC | 204 |
| Washington University | 161 | University of Munich | 203 |
| Yale University | 150 | New York University | 199 |
| Erasmus MC | 148 | Kyoto University | 195 |

RC: Record count

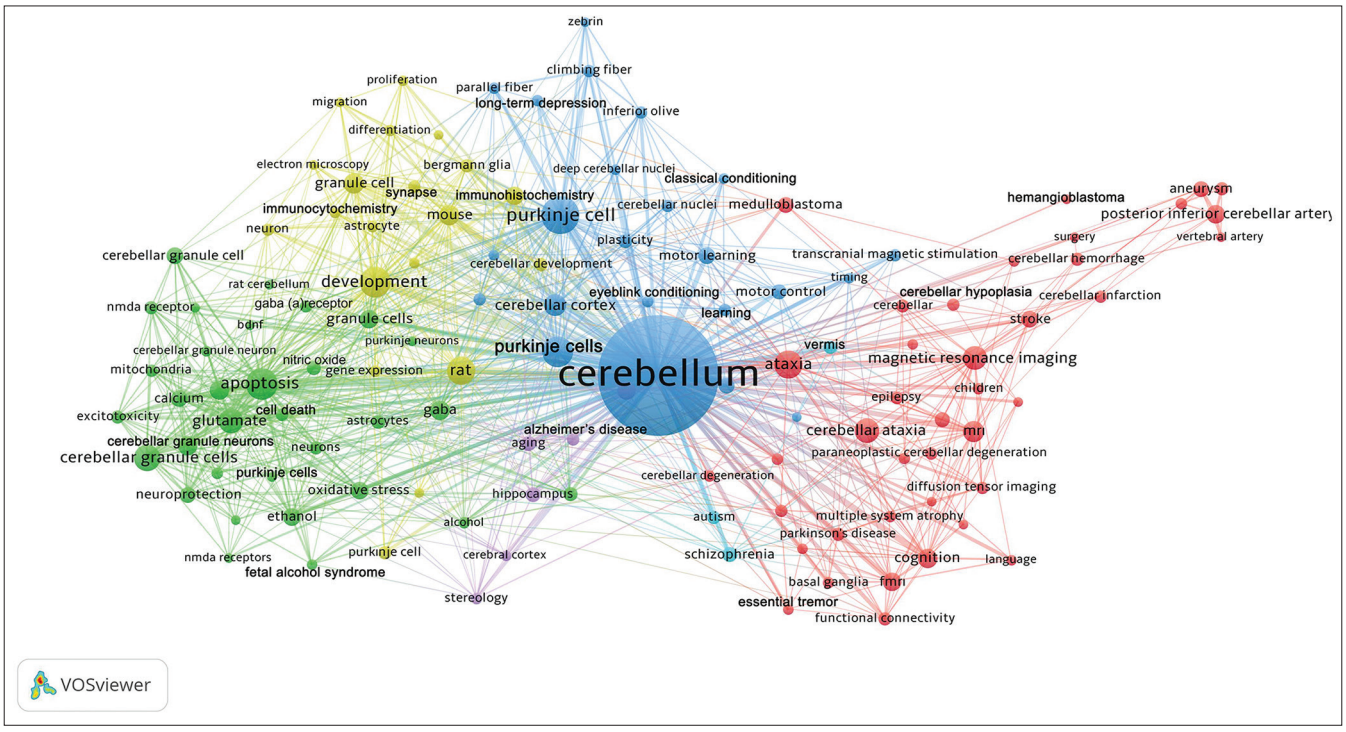


**Figure 5: Network visualization map for cluster analysis based on keyword analysis on the cerebellum. Footnote: Six different colors indicate the clustering between the keywords. The size of the circles indicates frequently used keywords. The thickness of the lines indicates that keywords are commonly used together in similar studies**

**Table 2: Active journals on the cerebellum**

| Journals | RC | C | AC |
|---|---|---|---|
| Journal of Neuroscience | 704 | 56,619 | 80.4 |
| Brain Research | 673 | 21,329 | 31.7 |
| Cerebellum | 640 | 11,551 | 18.1 |
| Neuroscience Letters | 606 | 14,139 | 23.3 |
| Neuroscience | 500 | 18,190 | 36.4 |
| Journal of Neurochemistry | 498 | 20,305 | 40.8 |
| Journal of Comparative Neurology | 396 | 19,273 | 48.7 |
| Journal of Neurophysiology | 350 | 20,095 | 57.4 |
| European Journal of Neuroscience | 315 | 12,866 | 40.8 |
| Journal of Physiology London | 291 | 20,452 | 70.3 |
| Experimental Brain Research | 265 | 10,236 | 38.6 |
| Developmental Brain Research | 257 | 8282 | 32.2 |
| Plos One | 237 | 3970 | 16.8 |
| Journal of Neuroscience Research | 233 | 7047 | 30.2 |
| Proceedings of the National Academy of Sciences of the United States of America | 226 | 25,281 | 111.9 |
| Neuroreport | 189 | 5304 | 28.1 |
| Journal of The Neurological Sciences | 174 | 3997 | 23 |
| Neurology | 174 | 11,255 | 64.7 |
| Neurochemical Research | 167 | 2786 | 16.7 |
| Neuron | 153 | 19,016 | 124.3 |
| Acta Neuropathologica | 152 | 4572 | 30.1 |
| Brain | 148 | 15,216 | 102.8 |
| Neurosurgery | 138 | 4111 | 29.8 |
| Neuropharmacology | 130 | 3660 | 28.2 |
| Journal of Neurosurgery | 129 | 4377 | 33.9 |
| Journal of Biological Chemistry | 126 | 8872 | 70.4 |
| American Journal of Neuroradiology | 122 | 4291 | 35.2 |
| International Journal of Developmental Neuroscience | 115 | 2017 | 17.5 |
| Neurochemistry International | 114 | 1902 | 16.7 |
| Neuroimage | 114 | 7464 | 65.5 |
| Journal of Neurology Neurosurgery and Psychiatry | 106 | 4305 | 40.6 |
| Neuroscience Research | 106 | 2011 | 19 |
| Journal of Neurology | 104 | 1851 | 17.8 |
| Surgical Neurology | 103 | 1775 | 17.2 |
| World Neurosurgery | 103 | 394 | 3.8 |
| Childs Nervous System | 102 | 1278 | 12.5 |
| Brain Research Bulletin | 100 | 1846 | 18.5 |
| Experimental Neurology | 97 | 2056 | 21.2 |
| Molecular Brain Research | 96 | 2865 | 29.8 |
| Annals of Neurology | 94 | 5975 | 63.6 |
| Acta Neurochirurgica | 93 | 1504 | 16.2 |
| Anatomy and Embryology | 93 | 2720 | 29.3 |
| Biochemical and Biophysical Research Communications | 90 | 2322 | 25.8 |
| Journal of Pharmacology and Experimental Therapeutics | 90 | 3688 | 41 |
| Neuroradiology | 90 | 1681 | 18.7 |
| Scientific Reports | 88 | 540 | 6.2 |
| Alcoholism Clinical and Experimental Research | 86 | 2546 | 29.6 |
| Development | 82 | 8024 | 97.9 |
| Journal of Child Neurology | 81 | 1680 | 20.7 |
| Journal of Clinical Neuroscience | 81 | 578 | 7.1 |
| Molecular and Cellular Neuroscience | 81 | 2421 | 29.9 |
| Neurologia Medico Chirurgica | 76 | 527 | 6.9 |

*Contd...*

**Table 2: Contd....**

RC: Record count, C: Number of citation, AC: Average citation per document

a general increase in the number of publications concerning the cerebellum in the last 40 years. A total number of 310 articles concerning the cerebellum were published in 1980. The number of articles published per year in the 10-year period was between 310 and 387. The number of articles between 1990 and 1995 was 425–498 per year, and the number of cerebellum-related articles notably increased up to 675 in 1996. The total number of articles, which was approximately 566–688 per year between 1996 and 2012 demonstrated a general increasing trend in recent years and has now reached approximately 800. An analysis of the publication trend of the cerebellum-related articles between 1980 and 2020 showed that although there was a slight decrease in the number of articles between 1998 and 2006, a general increasing trend was noted. Parallel to the growing awareness that the cerebellum is involved in many cognitive and emotional processes as well as a wide variety of neurological and psychiatric conditions, there has been a visible increase in the number of publications in the past decade.[24-26] In addition, the contribution of researchers from various scientific fields, ranging from cell biology to neurosciences led to increase in the number of publications in this field.[3,27] When considering similar publication trend from 1989 to 1993, publication trend predicted for the years from 2020 up to 2028 was expected to continue increasing and reach a total of 891 publications per year by the end of 2028. These results indicated that researchers' interest in the cerebellum topic will also continue to increase in the following years.

An analysis of the publication productivity of the countries with respect to the cerebellum showed that the top 10 most productive countries were primarily the USA and Japan, followed by the UK, Germany, Italy, France, Canada, Spain, China, and the Netherlands. Our results showed that the economic size of countries can be directly associated with publication productivity. This hypothesis is confirmed by the highly significant correlation determined between GDP and GDP PPP and the publication productivity of the countries. The significant correlation between HDI and publication productivity was lower than the correlation between GDP and GDP, PPP and publication productivity. This finding which demonstrates that the economic size of the countries was more effective than the development levels in publication productivity. Bibliometric studies conducted in recent years have also shown that

**Table 3: The 20 most cited articles concerning the cerebellum**

| No | Article | Author | Journal | PY | TC | AC |
|---|---|---|---|---|---|---|
| 1 | Function of the chemokine receptor cxcr4 in haematopoiesis and in cerebellar development | Zou YR *et al*. | Nature | 1998 | 1886 | 82 |
| 2 | Nitric-oxide mediates glutamate-linked enhancement of cgmp levels in the cerebellum | Bredt DS *et al*. | Proceedings of the National Academy of Sciences of the United States of America | 1989 | 1839 | 57.5 |
| 3 | The cerebellar cognitive affective syndrome | Schmahmann JD *et al*. | Brain | 1998 | 1660 | 72.2 |
| 4 | Bell-shaped calcium-response curves of ins (1,4,5) p3-gated and calcium-gated channels from endoplasmic-reticulum of cerebellum | Bezprozvanny I *et al*. | Nature | 1991 | 1454 | 48.5 |
| 5 | Impaired b-lymphopoiesis, myelopoiesis, and derailed cerebellar neuron migration in cxcr4- and sdf-1-deficient mice | Ma Q *et al*. | Proceedings of the National Academy of Sciences of the United States of America | 1998 | 1275 | 55.4 |
| 6 | Marrow stromal cells migrate throughout forebrain and cerebellum, and they differentiate into astrocytes after injection into neonatal mouse brains | Kopen GC *et al*. | Proceedings of the National Academy of Sciences of the United States of America | 1999 | 1272 | 57.8 |
| 7 | Autosomal dominant cerebellar ataxia (sca6) associated with small polyglutamine expansions in the alpha (1a)-voltage-dependent calcium channel | Zhuchenko O *et al*. | Nature Genetics | 1997 | 1194 | 49.8 |
| 8 | Basal ganglia and cerebellar loops: motor and cognitive circuits | Middleton FA *et al*. | Brain Research Reviews | 2000 | 1175 | 56 |
| 9 | Electro-physiological properties of *in vitro* purkinje-cell dendrites in mammalian cerebellar slices | Llinas R *et al*. | Journal of Physiology-London | 1980 | 967 | 23.6 |
| 10 | Electrophysiological properties of *in vitro* purkinje-cell somata in mammalian cerebellar slices | Llinas R *et al*. | Journal of Physiology-London | 1980 | 966 | 23.6 |
| 11 | Control of neuronal precursor proliferation in the cerebellum by sonic hedgehog | Wechsler-Reya RJ *et al*. | Neuron | 1999 | 914 | 41.5 |
| 12 | Anatomical evidence for cerebellar and basal ganglia involvement in higher cognitive function | Middleton FA *et al*. | Science | 1994 | 860 | 31.8 |
| 13 | Induction of apoptosis in cerebellar granule neurons by low potassium - inhibition of death by insulin-like growth factor-i and camp | D'mello SR *et al*. | Proceedings of the National Academy of Sciences of the United States of America | 1993 | 838 | 29.9 |
| 14 | Endogenous nitric-oxide release required for long-term synaptic depression in the cerebellum | Shibuki K *et al*. | Nature | 1991 | 826 | 27.5 |
| 15 | International cooperative ataxia rating scale for pharmacological assessment of the cerebellar syndrome | Trouillas P *et al*. | Journal of the Neurological Sciences | 1997 | 811 | 33.8 |

PY: Publication year, TC: Total citation, AC: Average citations per year

economic size is the most effective factor in publication productivity.[28,29]

An evaluation of the journals published articles about the cerebellum showed that the most active journals (i.e., more than 500 articles in total) were the Journal of Neuroscience, Brain Research, Cerebellum, Neuroscience Letters, and Neuroscience. When the total number of citations was considered, the most-cited articles (with more

**Table 4: The most used trend keywords on the cerebellum**

| Keyword | O |
|---|---|
| Cerebellum | 5262 |
| Purkinje cell | 620 |
| Apoptosis | 463 |
| Development | 429 |
| Purkinje cells | 424 |
| Ataxia | 360 |
| Rat | 358 |
| Cerebellar granule cells | 318 |
| Glutamate | 290 |
| Cerebellar ataxia | 279 |
| Magnetic resonance imaging | 270 |
| Cerebellar cortex | 235 |
| Mri | 215 |
| Mouse | 208 |
| Granule cell | 205 |
| Cerebellar granule neurons | 185 |
| Cognition | 182 |
| Neurotoxicity | 182 |
| Gaba | 179 |
| Brain | 177 |
| Granule cells | 176 |
| Posterior inferior cerebellar artery | 176 |
| Immunohistochemistry | 173 |
| Fmri | 165 |
| Oxidative stress | 157 |
| Ethanol | 153 |
| Calcium | 145 |
| Stroke | 143 |
| Cerebellar granule cell | 136 |
| Motor learning | 136 |
| Medulloblastoma | 134 |
| Neuroprotection | 128 |
| Aneurysm | 126 |
| Human | 124 |
| Schizophrenia | 117 |
| Motor control | 115 |
| Aging | 114 |
| Cerebellar atrophy | 114 |
| Hippocampus | 113 |
| Neurodegeneration | 107 |
| Nitric oxide | 105 |
| Astrocytes | 102 |
| Plasticity | 102 |
| Cerebellar | 98 |
| Cerebellar hemorrhage | 97 |
| Cerebellar development | 96 |
| Vermis | 96 |
| Autism | 95 |
| Excitotoxicity | 95 |
| Bergmann glia | 94 |
| Functional connectivity | 94 |
| Purkinje cell | 94 |
| Neurons | 91 |

O: Number of occurrences

than 15,000 total citations) were published in the Journal of Neuroscience, Proceedings of the National Academy of Sciences of the United States of America, Brain Research, Journal of Physiology London, Journal of Neurochemistry, Journal of Neurophysiology, Journal of Comparative Neurology, Neuron, Neuroscience and Brain, respectively. On the other hand, an evaluation of the journals published articles about the cerebellum according to the number of citations per article and the citation network map showed that the most active journals were the Neuron, Proceedings of the National Academy of Sciences of the United States of America, Brain, Development, Journal of Neuroscience, Journal of Biological Chemistry, Journal of Physiology London, Neuroimage, Neurology, and Annals of Neurology.

As the above-mentioned journals were the most effective and active journals in terms of the number and quality of the articles produced, these journals could be considered a potential source for the researchers specifically interested in the topic of the cerebellum. These journals could be a good guide for planning new studies or projects about the cerebellum, following current qualified studies, and identifying the most appropriate journal address for the completed studies.

Of the 22,084 articles analyzed, the most-cited study was the article entitled "Function of the chemokine receptor CXCR4 in hematopoiesis and in cerebellar development" written by Zou *et al*. and published in Nature.[30] The authors investigated the role of CXCR4, a chemokines receptor, in hematopoiesis and cerebellum development and reported that this receptor had a critical function in the cerebellar neuronal layer formation during the cerebellum development. The second most-cited article was entitled "Nitric-oxide mediates glutamate-linked enhancement of cGMP levels in the cerebellum" written by Bredt and Snyder and published in the Journal of Proceedings of the National Academy of Sciences of the United States of America.[31] The authors reported that nitric oxide as a messenger molecule mediated the stimulation of cGMP levels in the cerebellum with glutamate.

An analysis of the articles according to the number of citations per year showed that the most-cited study was conducted by Zou *et al*.[30] Second most-cited article was entitled "The cerebellar cognitive affective syndrome" written by Schmahmann and Sherman and published in the Brain Journal.[19] The third most-effective cerebellum article according to the average number of citations was the study entitled "Marrow stromal cells migrate throughout forebrain and cerebellum, and they differentiate into astrocytes after injection into neonatal mouse brains" written by Kopen *et al*. and published in the journal of Proceedings of the National Academy of Sciences of the United States of America.[32] The most-cited articles in the references sections of the 22,084 articles were the studies conducted by Ito, Lowry *et al*., Eccles *et al*., Palay and Chan-Palay,

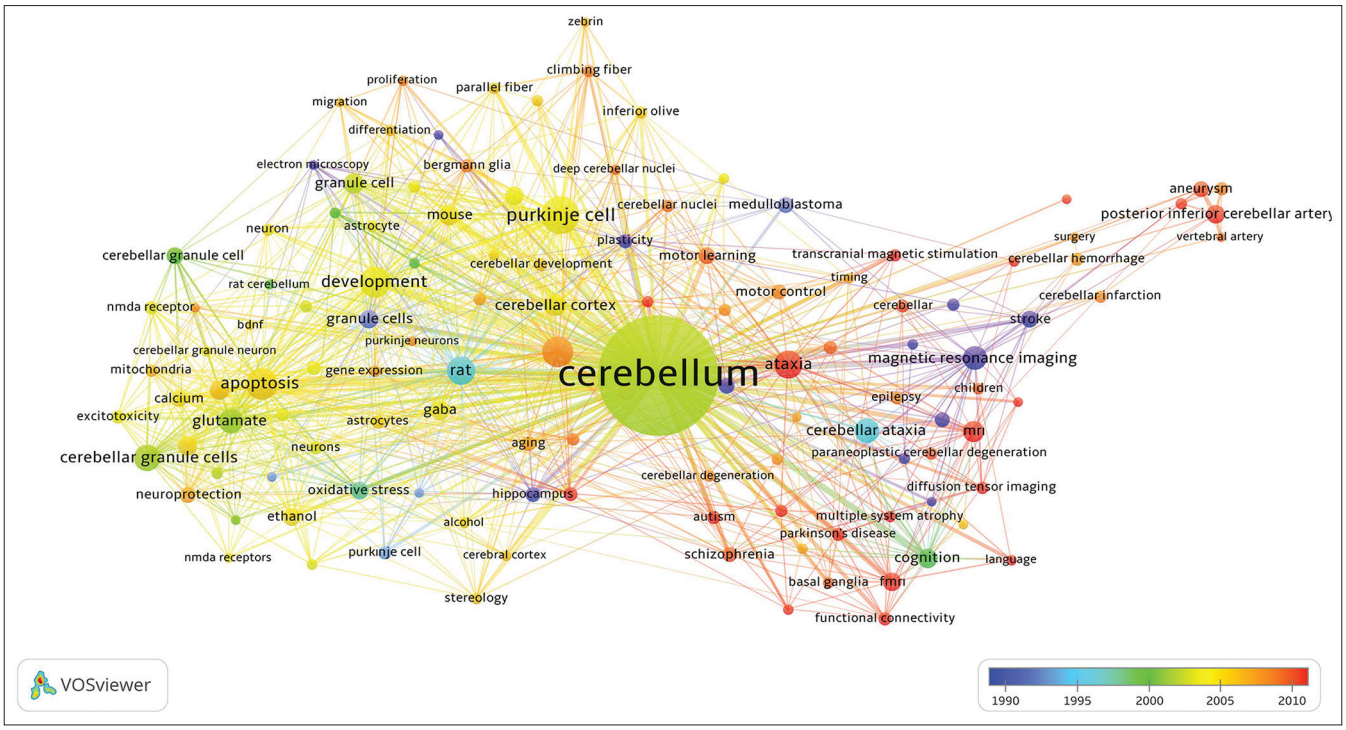


**Figure 6: Network visualization map for current trends based on keyword analysis on the cerebellum. Footnote: Indicator shows current publications from blue to red. Keywords in red indicate recently published articles**

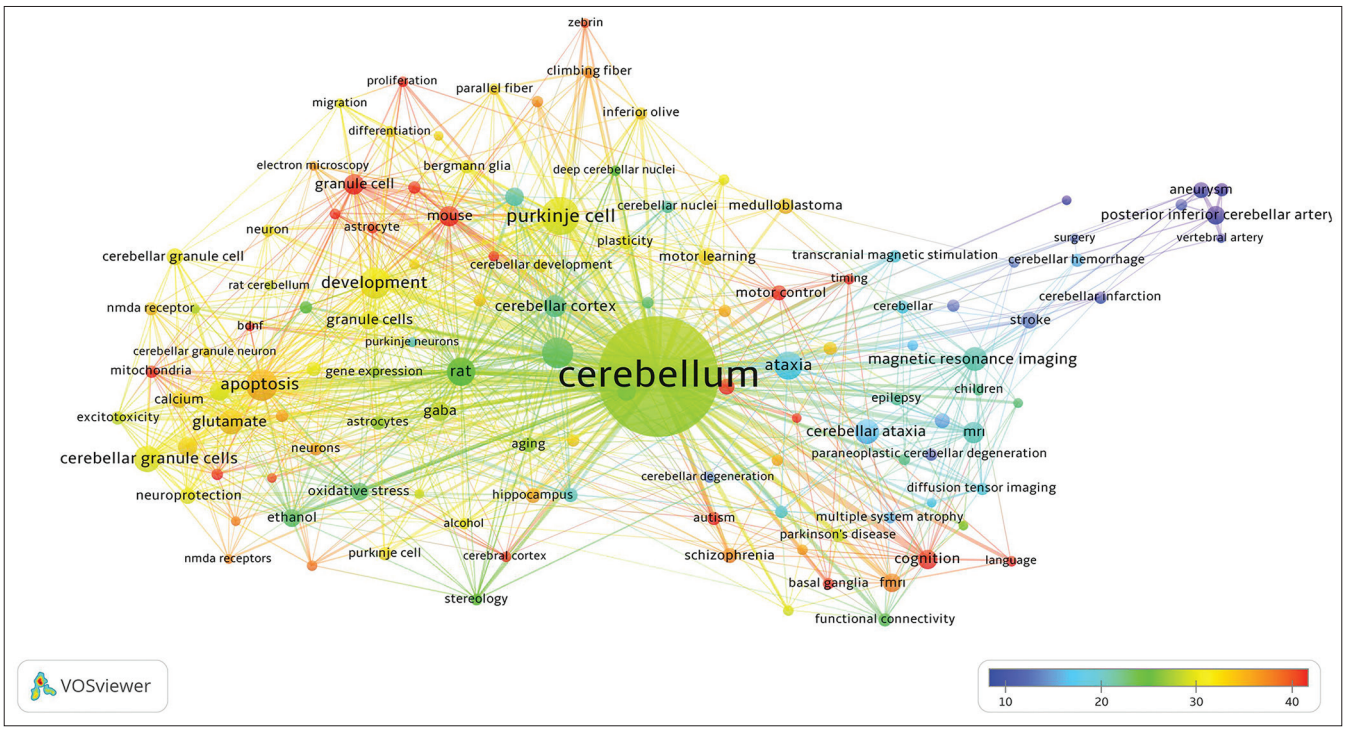


**Figure 7: Network visualization map for the most cited keyword on the cerebellum. Footnote: Keywords in red indicate the most cited keywords**

Marr, Schmahmann and Sherman, Albus(1972), Altman, Stoodley and Schmahmann, and Gallo *et al*., respectively. [14-23]

More qualified and effective studies could be produced if researchers interested in the topic of the cerebellum or planning new studies initially review the above-mentioned studies or the other most-cited papers in Table 3.

According to the keyword cluster analysis findings, cerebellum studies were performed in 6 different clusters which ataxia, Purkinje cell, schizophrenia, development,

aging, and apoptosis in cluster centers. The ataxia, Purkinje cell, and apoptosis centered clusters were predominant as the major research clusters.

An evaluation of the analysis results with a view to identifying the trend topics about the cerebellum articles from past to present showed that the most frequently used keywords around 1990 were magnetic resonance imaging (MRI), stroke, granule cell, hippocampus, plasticity medulloblastoma, neurogenesis, cerebellar atrophy, and electron microscopy. The most frequently used keywords around 1995 included rat, oxidative stress and cerebellar ataxia; and the keywords around 2000 were cerebellar granule cell (cells), glutamate, cognition, immunocytochemistry, and *in situ* hybridization, while the most frequently used keywords around 2005 included motor learning, motor control, apoptosis, aging, neurotoxicity, neuroprotection, GABI, development, mouse, cerebellar cortex, and calcium. The most frequently encountered keywords during the period from 2010 to 2019 included ataxia, posterior inferior cerebellar artery, aneurysm, MRI, functional MRI (fMRI), diffusion tensor imaging, transcranial magnetic stimulation, functional connectivity, cerebellar degeneration, schizophrenia, Parkinson's disease, autism, neurodegeneration, and multiple system atrophy. An analysis of the keywords used in cerebellum studies conducted after 2010 indicated that there was a trend in the cerebellar functional connectivity, cerebellar degeneration, and relationship of the cerebellum with various diseases and the use of the neuroimaging techniques.

When the citation analysis results of the cerebellum articles were evaluated, the most-cited keywords from past to present included motor control, timing, cognition, language, basal ganglia, autism, mouse, synapse, immunocytochemistry, mitochondria, brain-derived neurotrophic factor, N-methyl-D-aspartate, proliferation, cerebral cortex, granule cell, and astrocyte. Since these keywords were in the most-cited studies with a high impact level, it would be beneficial to consider these in planning research on the cerebellum. An analysis of the keywords used in the cerebellum articles to date showed that the cerebellum was included in several disciplines and studies that demonstrated different approaches in terms of topic and content.

As the WoS database indexes only the journals in the Science Citation Index Expanded and Emerging Science Citation Index, it is generally regarded as having more reliability than other databases such as PubMed and Scopus.[10,28] Therefore, this study did not use databases such as PubMed and Scopus, but only utilized the WoS database.

## Conclusion

The present study is the first attempt to provide a comprehensive analysis of scientific publications regarding the cerebellum since 1980. The study identified the most active countries, collaborations between countries, the journals with the highest number of and most qualified articles in the cerebellum-related publications, the most-cited cerebellum studies, and the most frequently used keywords by years. Recent studies concerning the cerebellum have mostly focused on the cerebellar degeneration, functional connections of the cerebellum and its relationship with various diseases, primarily ataxia, schizophrenia, Parkinson's disease, and autism, aneurysms and the use of fMRI, MRI, and diffusion tensor monitoring. The comprehensive analysis and the findings obtained in the present study, which covered a long period, can be considered to be of value as a good and useful guide for researchers interested in this topic.

### Financial support and sponsorship

Nil.

### Conflicts of interest

There are no conflicts of interest.

## References

1. Salman MS, Tsai P. The role of the pediatric cerebellum in motor functions, cognition, and behavior: A clinical perspective. Neuroimaging Clin N Am 2016;26:317-29.
2. Adamaszek M, D'Agata F, Ferrucci R, Habas C, Keulen S, Kirkby KC, *et al*. Consensus paper: Cerebellum and emotion. Cerebellum 2017;16:552-76.
3. Wagner MJ, Luo L. Neocortex-cerebellum circuits for cognitive processing. Trends Neurosci 2020;43:42-54.
4. Ito M. Cerebellar circuitry as a neuronal machine. Prog Neurobiol 2006;78:272-303.
5. Singh-Bains MK, Linke V, Austria MDR, Tan AYS, Scotter EL, Mehrabi NF, *et al*. Altered microglia and neurovasculature in the Alzheimer's disease cerebellum. Neurobiol Dis 2019;132:104589.
6. He H, Luo C, Luo Y, Duan M, Yi Q, Biswal BB, *et al*. Reduction in gray matter of cerebellum in schizophrenia and its influence on static and dynamic connectivity. Hum Brain Mapp 2019;40:517-28.
7. Rusholt EHL, Salvesen L, Brudek T, Tesfay B, Pakkenberg B, Olesen MV. Pathological changes in the cerebellum of patients with multiple system atrophy and Parkinson's disease-a stereological study. Brain Pathol 2020;30:576-88.
8. Howell OW, Schulz-Trieglaff EK, Carassiti D, Gentleman SM, Nicholas R, Roncaroli F, *et al*. Extensive grey matter pathology in the cerebellum in multiple sclerosis is linked to inflammation in the subarachnoid space. Neuropathol Appl Neurobiol 2015;41:798-813.
9. Pritchard A. Statistical bibliography or bibliometrics. J Doc 1969;25:348-9.
10. Demir E, Yaşar E, Özkoçak V, Yıldırım E. The evolution of the field of legal medicine: A holistic investigation of global outputs with bibliometric analysis. J Forensic Leg Med 2020;69:101885.
11. Durieux V, Gevenois PA. Bibliometric indicators: Quality measurements of scientific publication. Radiology 2010;255:342-51.
12. Kiraz M, Demir E. A bibliometric analysis of publications on spinal cord injury during 1980-2018. World Neurosurg 2020;136:e504-13.

13. van Eck NJ, Waltman L. Software survey: VOSviewer, a computer program for bibliometric mapping. Scientometrics 2010;84:523-38.
14. Ito M. The Cerebellum and Neural Control. New York: Raven Press; 1984.
15. Lowry OH, Rosebrough NJ, Farr AL, Randall RJ. Protein measurement with the Folin phenol reagent. J Biol Chem 1951;193:265-75.
16. Eccles JC, Ito M, Szentagothai J. The Cerebellum as a Neuronal Machine. Berlin, Heidelberg: Springer; 1967. p. 184-7.
17. Palay SL, Chan-Palay V. Cerebellar Cortex: Cytology and Organization. New York: Springer; 1974.
18. Marr D. A theory of cerebellar cortex. J Physiol 1969;202:437-70.
19. Schmahmann JD, Sherman JC. The cerebellar cognitive affective syndrome. Brain 1998;121 (Pt 4):561-79.
20. Albus JS. A theory of cerebellar cortex. Math Biosci 1972;10:25-61.
21. Altman J. Postnatal development of the cerebellar cortex in the rat. I. The external germinal layer and the transitional molecular layer. J Comp Neurol 1972;145:353-97.
22. Stoodley CJ, Schmahmann JD. Functional topography in the human cerebellum: A meta-analysis of neuroimaging studies. Neuroimage 2009;44:489-501.
23. Gallo V, Kingsbury A, Balázs R, Jørgensen OS. The role of depolarization in the survival and differentiation of cerebellar granule cells in culture. J Neurosci 1987;7:2203-13.
24. Guell X, Schmahmann J. Cerebellar functional anatomy: A didactic summary based on human fMRI evidence. Cerebellum 2020;19:1-5.
25. Schmahmann JD. The cerebellum and cognition. Neurosci Lett 2019;688:62-75.
26. Mitoma H, Manto M, Gandini J. Recent Advances in the Treatment of Cerebellar Disorders. Brain Sci 2020;10:11.
27. Martin KB, Williams IM, Cluzeau CV, Cougnoux A, Dale RK, Iben JR, *et al*. Identification of novel pathways associated with patterned cerebellar purkinje neuron degeneration in niemann-pick disease, Type C1. Int J Mol Sci 2020;21:292.
28. Doğan G, Kayır S. Global scientific outputs of brain death publications and evaluation according to the religions of countries. J Relig Health 2020;59:96-112.
29. Doğan G, İpek H. The development of necrotizing enterocolitis publications: A holistic evolution of global literature with bibliometric analysis. Eur J Pediatr Surg 2020;30:293-303.
30. Zou YR, Kottmann AH, Kuroda M, Taniuchi I, Littman DR. Function of the chemokine receptor CXCR4 in haematopoiesis and in cerebellar development. Nature 1998;393:595-9.
31. Bredt DS, Snyder SH. Nitric oxide mediates glutamate-linked enhancement of cGMP levels in the cerebellum. Proc Natl Acad Sci U S A 1989;86:9030-3.
32. Kopen GC, Prockop DJ, Phinney DG. Marrow stromal cells migrate throughout forebrain and cerebellum, and they differentiate into astrocytes after injection into neonatal mouse brains. Proc Natl Acad Sci U S A 1999;96:10711-6.

Original Article

# A Study of Microscopic Changes in the Placenta in Gestational Diabetes Mellitus

**Vishram Singh, Kumud Ranjan, S. L. Tewarson[1]**

*Department of Anatomy Santosh Deemed to be University, Ghaziabad NCR, Delhi, [1]Department of Pathology, GMC, Azamgarh, Uttar Pradesh, India*

## Abstract

**Introduction:** Gestational diabetes mellitus is a complication connected with pregnancy defined as any degree of glucose intolerance that appears during pregnancy with normal values before and usually after the pregnancy. We investigated histological changes of the gestational diabetic placenta and non-diabetic placenta. Research work accomplished in the department of Anatomy, government medical college and superfacility hospital Azamgarh. Placenta collected from the labour room/operation theatre of the department of Obstetrics and Gynecology, government medical college and superficiality hospital, Azamgarh. **Material and Methods:** Sixty-two freshly delivered placentas were collected – 31 placentas from diabetic mother and 31 placentas from non-diabetic mother (control group). All parturient were aged between 20 to 44 years. This placenta measured on a weighing machine graduated in grams. An approximately 5mm piece of the diabetic placenta was taken and processed for histological examination. **Results:** Microscopic examination explained dilated blood vessels, subtrophoblastic basement membrane thickness and chorangiosis present in all gestational diabetic placenta. Vessels thrombosis present in 83.87 per cent of the gestational diabetic placenta. Nucleated RBCs. were present in 93.54 per cent of the gestational diabetic placenta. **Discussion and Conclusion:** Gestational diabetes mellitus induces significant changes in the placenta, both gross and histologic. Effective glycemic regulation is better options for reducing anomalies that cause gestational diabetes. We find dilated blood vessels and necrosis in 100 percent of gestational diabetic placenta and 9.60 percent of nondiabetic placenta. The thickness of the subtrophoblastic basement membrane was present in 100% of the gestational diabetic placenta and 16.12% of the non-diabetic placenta. Vessel thrombosis occurs in 83.87% of gestational diabetic placenta, and 12.90% of non-diabetic placenta. In 93.54 percent of gestational diabetic placenta and 32.25 percent of non-diabetic placenta, nucleated RBC occurs.

**Keywords:** *Chorangiosis, gestational diabetes mellitus, microscopic, placenta*

## Introduction

The placenta is a fetomaternal organ. It consists of two components: (a) fetal component and (b) maternal component. Fetal component develops from chorion frondosum and maternal component develops from decidua basalis. This is a complex organ of short life span. This is responsible for the transfer of nutrients and waste products between fetal and maternal circulations. The placenta must integrate signals from fetus and mother in an effort to match fetal demand with maternal nutrient.[1,2] It actually plays an important role in fetal growth and development. Maternal disease that results in abnormal growth and development of the placenta during early pregnancy and mid-pregnancy is directly associated with decreased fetal growth and development in the late pregnancy.[3] Gestational diabetes mellitus (GDM) is a complication connected with pregnancy defined as any degree of glucose intolerance that appears during pregnancy with normal values before and usually after the pregnancy. Diabetes mellitus in pregnancy is known as GDM because woman is nondiabetic before pregnancy. Any degree of glucose intolerance commencement during pregnancy is known as GDM.[4,5] GDM represents nearly 90% of all pregnancies complicated by diabetes mellitus.[6] It affects 2%–5% of all pregnancies.[7] GDM during pregnancy produces varieties of placental abnormalities such as distension of basal membrane of trophoblast proliferation of cells of the endothelium and decreased vascular surfaces of terminal villi. These changes depend



**How to cite this article:** Singh V, Ranjan K, Tewarson SL. A study of microscopic changes in the placenta in gestational diabetes mellitus. J Anat Soc India 2020;69:XX-XX.

**Article Info**

**Received:** 13 July 2020
**Accepted:** 02 September 2020
**Available online:** ***

***Address for correspondence:***
*Mr. Kumud Ranjan, PhD Scholar, Department of Anatomy, Santosh Deemed to be University, Ghaziabad, NCR, Delhi, India.*
*E-mail: drkumudranjan@gmail.com*

**Access this article online**

**Website:** www.jasi.org.in
**DOI:** 10.4103/JASI.JASI_133_20
**Quick Response Code:**

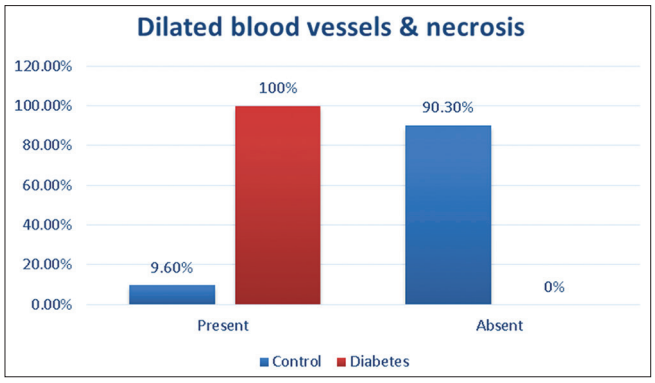


**Figure 1: Dilated blood vessel and necrosis present in 100% of the gestational diabetic placenta and 9.60% of the nondiabetic placenta**

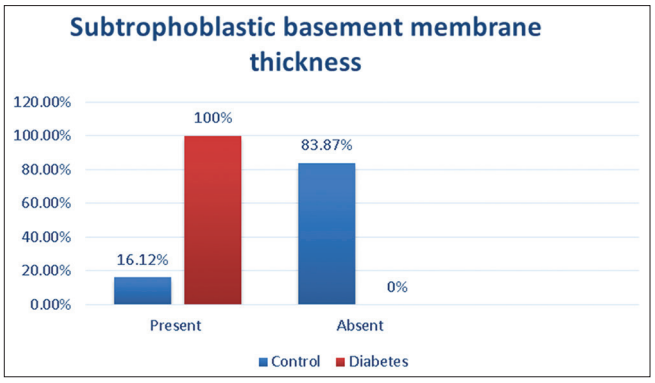


**Figure 2: Subtrophoblastic basement membrane thickness present in 100%of the gestational diabetic placenta & 16.12% of the nondiabetic placenta**

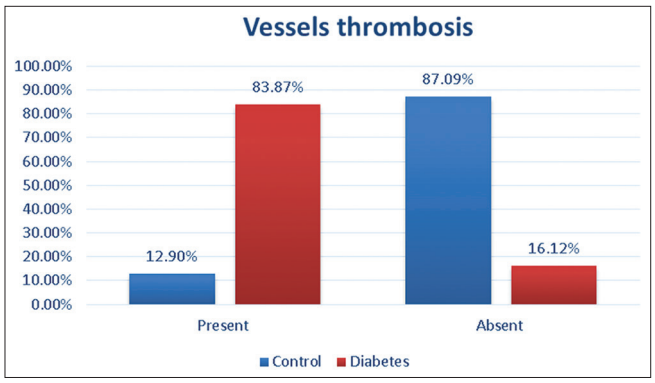


**Figure 3: Vessels thrombosis present in 83.87% of the gestational diabetic placenta and 12.90% of the non-diabetic placenta**

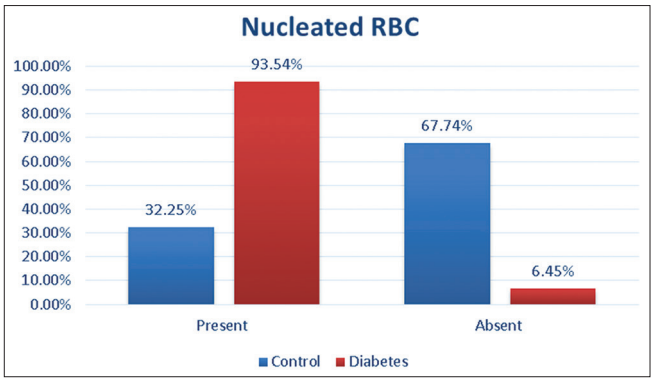


**Figure 4: Nucleated RBCs present in 93.54% of the gestational diabetic placenta and 32.25% of the non-diabetic placenta.**

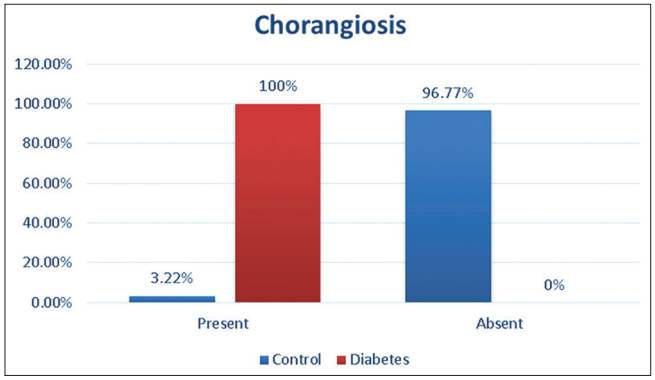


**Figure 5: Chorangiosis present in 100% of the gestational diabetic placenta and 3.22% of the non- diabetic placenta**

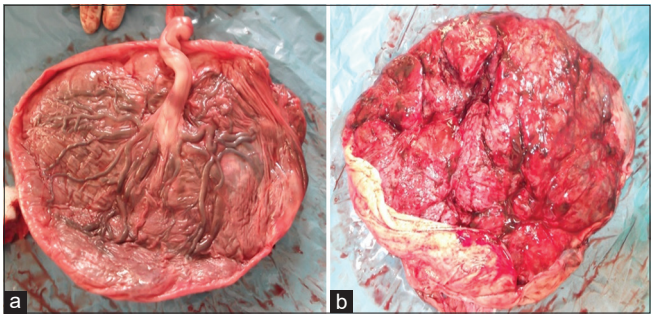


**Figure 6: (a) Fetal surface of the gestational diabetic placenta. (b) Maternal surface of the gestational diabetic placenta**

upon the quality of glycemic control achieved during the critical period of the placental development.[1] An alteration of the placental function due to uncontrolled GDM results in disturbances of the growth and development of fetus macrosomia, congenital malformations, and intrauterine growth retardation.[8,9]

## Material and Methods

Sixty-two freshly delivered placentas were collected – 31 placentas from the diabetic mother and 31 placentas from the nondiabetic mother (control group). All parturient were aged between 20 and 44 years. Research work was accomplished in the Department of Anatomy, Government Medical College and Superfacility Hospital, Azamgarh. Placenta was collected from the labor room/operation theater of the Department of Obstetrics and Gynaecology, Government Medical College and Superfaciality Hospital, Azamgarh. There were no differences according to race culture or environment. The placenta was obtained either from the vaginal route or cesarean section. After washed with the running tap water and dried with the blotting paper, the collected placenta was weighed from the weighing machine graduated in the grams. We took morphometric and macroscopic examination; after that, the placenta was kept

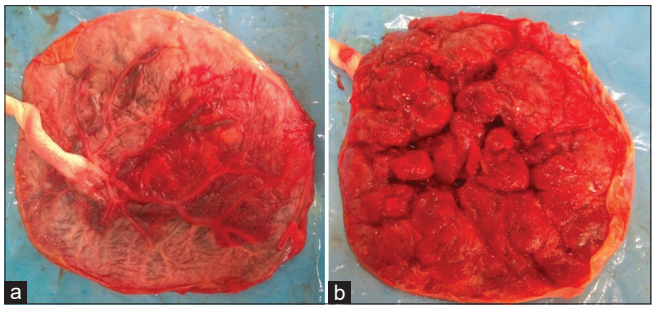

**Figure 7: (a) Fetal surface of the nondiabetic placenta. (b) Maternal surface of the nondiabetic placenta**

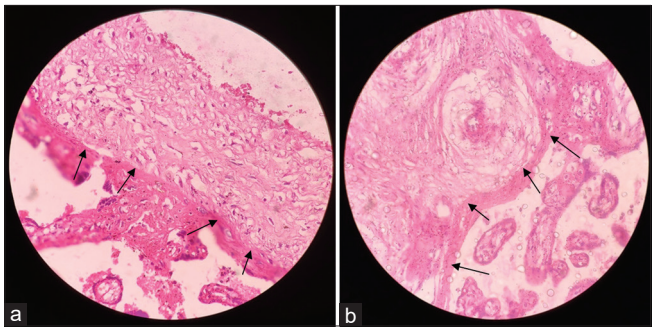

**Figure 9: (a) The histological slide of the gestational diabetic placenta - Arrow showing subtrophoblastic basement membrane thickness, ×40. (b) The histological slide of the nondiabetic placenta - Arrow showing basement membrane of the trophoblast, ×40**

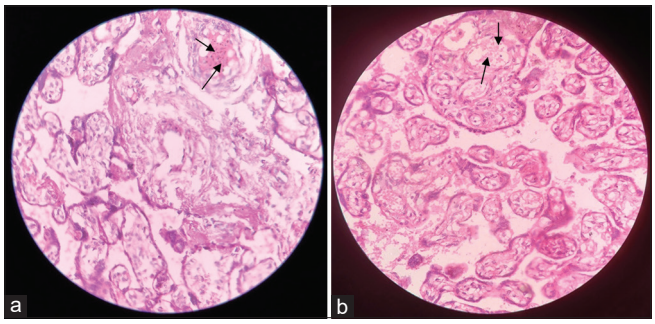

**Figure 11: (a) The histological slide of the gestational diabetic placenta - Arrow showing nucleated red blood cell, ×40. (b) The histological slide of the nondiabetic placenta - Arrow showing nonnucleated red blood cell, ×40**

in 10% formalin for 24 h for fixation. After 24 h, this fixed tissue of the placenta passes through a series of procedure from dehydration and clearing to wax impregnation before being sectioned from the microtome. Time took for processing was 24 h, and using microtome instrument, tissues were sectioned at 5 µm. APES-coated glass slide was used for sectioned tissues. The slide was placed on the hot metallic plate at 60° for 30 min before staining. After that, hematoxylin and eosin staining was done. Slides were prepared and they are passed through xylene-1 for 10 min and xylene-2 for the next 10 min. After that, slides were placed into 100%, 95%, 80%, and 70% alcohol for 5 min each to dehydrate the slides. Slides were placed into the Harris hematoxylin solution for 5–10 min and rehydrate with water thereafter. Again, tissues were washed

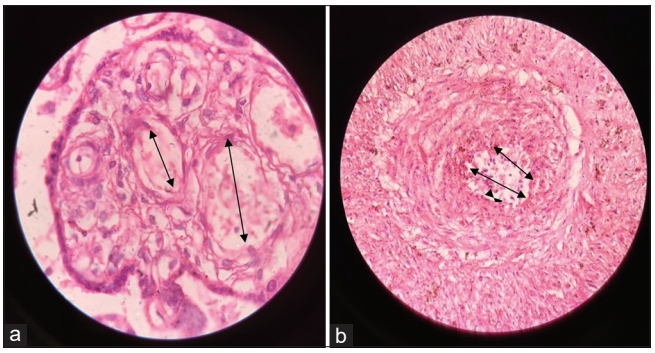

**Figure 8: (a) The histological slide of the gestational diabetic placenta - Arrow showing dilated blood vessel and necrosis, ×100. (b) The histological slide of the nondiabetic placenta - Arrow showing blood vessels, ×40**

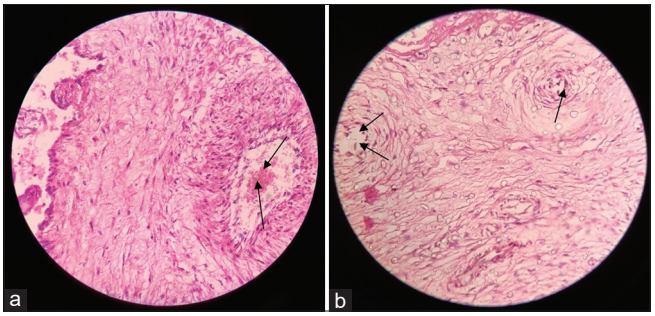

**Figure 10: (a) The histological slide of the gestational diabetic placenta - Arrow showing vessel thrombosis, ×40. (b) The histological slide of the nondiabetic placenta - Arrow showing blood vessel without thrombosis, ×40**

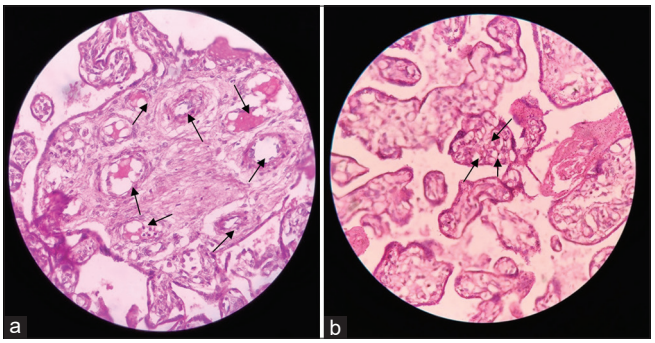

**Figure 12: (a) The histological slide of the gestational diabetic placenta - Arrow showing chorangiosis in the chorionic villi, ×40. (b) The histological slide of the nondiabetic placenta - Arrow showing fetal blood vessels in chorionic villi, ×40**

with tap water and then placed into 1% eosin for approximately 1–2 min. Finally, tissues were dehydrated by passing through increasing concentration of alcohol and cleared in the solution of xylene for 5 min. Prepared slides were mounted in DPX and covered with the cover slip. Through binocular light microscope, slides were examined at ×10, ×40, and ×100.

## Results

Dilated blood vessel and necrosis present in 100% of the gestational diabetic placenta and 9.60% of the nondiabetic placenta shows in Table 1.

**Table 1: Presents a comparison of the diabetic (gestational diabetes) and non-diabetic placenta histological changes**

| | Nondiabetic (control) (%) | Diabetic (gestational diabetes mellitus) (%) |
|---|---|---|
| Dilated blood vessels and necrosis | | |
| Present | 9.60 | 100 |
| Absent | 90.30 | 0 |
| Subtrophoblastic basement membrane thickness | | |
| Present | 16.12 | 100 |
| Absent | 83.87 | 0 |
| Vessels thrombosis | | |
| Present | 12.90 | 83.87 |
| Absent | 87.09 | 16.12 |
| Nucleated red blood cell | | |
| Present | 32.25 | 93.54 |
| Absent | 67.74 | 6.45 |
| Chorangiosis | | |
| Present | 3.22 | 100 |
| Absent | 96.77 | 0 |

Subtrophoblastic basement membrane thickness presents in 100% of the gestational diabetic placenta and 16.12% of the nondiabetic placenta.

Vessels thrombosis presents in 83.87% of the gestational diabetic placenta and 12.90% of the nondiabetic placenta shows in Table 1.

Nucleated red blood cell (RBCs) present in 93.54% of the gestational diabetic placenta and 32.25% of the nondiabetic placenta shows in Table 1.

Chorangiosis presents in 100% of the gestational diabetic placenta and 3.22% of the nondiabetic placenta shows in Table 1.

Hence, in our study, chorangiosis subtrophoblastic basement membrane thickness and dilated blood vessels and necrosis present in 100% of the gestational diabetic placenta [Table 1].

## Discussion

GDM is a complication connected with pregnancy defined as any degree of glucose intolerance that appears during pregnancy with normal values before and usually after the pregnancy. Diabetes mellitus in pregnancy is known as GDM because woman is nondiabetic before pregnancy. Any degree of glucose intolerance commencement during pregnancy is known as GDM.[4,5] The disturbance in the adaptation in the metabolism of carbohydrate during the pregnancy causes GDM. The poorly controlled gestational diabetic placenta shows villous edema and marked fibrin thrombi in the syncytiotrophoblast. Brudenell and Doddridge[10] suggested that villous edema is common in the diabetic placenta. Shen-Schwarz *et al*.[11] observed similar findings. The diabetes mellitus influences organ system such as cardiovascular excretory and central nervous system.[12] Diabetes mellitus during pregnancy affects both mother and fetuses.[13] When metabolic control is good, the mortality rate reduces in the normal population.[14] The macrosomia and large babies are common in GDM.[15] The villous immaturity are most common in the GDM.[16] We observed that the gestational diabetic placenta shows dilated blood vessel and necrosis in 100% of cases. However, the nondiabetic placenta shows dilated blood vessel and necrosis only in 9.60% of the placenta. According to the study of Jauniaux and Burton (2006),[17] GDM causes dilatation of blood vessels and necrosis of the blood vessels. Subtrophoblastic basement membrane thickness increases in the placenta due to GDM. We observed that 100% of the gestational diabetic placenta has subtrophoblastic basement membrane thickness and 16.12% of the nondiabetic placenta has subtrophoblastic basement membrane thickness [Table 1]. According to Hirota[18] and Okudaira *et al*.,[19] the poorly controlled GDM thickness of the basement membrane of syncytiotrophoblast increases. The basement membrane thickness in the gestational diabetic placenta is due to the deposition of mucopolysaccharide. We observed that thrombosis presents 83.87% of the gestational diabetic placenta and 12.90% of the nondiabetic placenta shows in Table 1. We observed that 93.54% of the gestational diabetic placenta has nucleated RBC and 32.25% of the nondiabetic placenta has nucleated RBC [Table 1]. According to Daskalakis *et al*.,[20] nucleated RBC presents more in the gestational diabetic placenta. We observed that chorangiosis presents in 100% of the gestational diabetic placenta and 3.22% of the nondiabetic placenta [Table 1]. Verma *et al*.[21] observed chorangiosis seen more in the gestational diabetic placenta as compared to the control. The GDM causes reduced flow of blood through the intervillous space. This reduced supply of the blood is due to vascular compromise.[2] The angiogenesis occurs due to uncontrolled GDM. 25% surfaces of the villi were taken up by the capillary bed in the gestational diabetic placenta and 50% surfaces of the villi were taken up by the capillary bed in the nondiabetic placenta. Maternal hyperglycemia may impact on the vascular permeability of the placenta. Hyperglycemia has shown to have a direct effect, acting as a proconstrictor,[22] procoagulator,[23] proinflammatory,[24] proangiogenic[25] and propermeability agent.[26] According to Lal *et al*.,[27] the gestational diabetic placenta showed degenerative changes (dilated blood vessels and necrosis), vessel thrombosis, subtrophoblastic basement membrane thickness, and presence of nucleated RBC. This observation supports our findings. According to Verma *et al*.,[28] finding of the histological examination such as fibrinoid necrosis, villous edema, villous fibrosis, and chorangiosis more often present in the gestational diabetic placenta compared with the control. This finding supports our findings. Hence, in our study, chorangiosis, subtrophoblastic basement membrane

thickness, and dilated blood vessels and necrosis present in 100% of the gestational diabetic placenta [Table 1].

## Conclusion

Diabetes mellitus causes profound gross as well as histological changes in the placenta. The good glycemic control is better options for reducing diabetes-induced abnormalities. In our research work, we found dilated blood vessel and necrosis in 100% of the gestational diabetic placenta and 9.60% of the nondiabetic placenta [Table 1]. Subtrophoblastic basement membrane thickness present in 100% of the gestational diabetic placenta and 16.12% of the nondiabetic placenta [Table 1]. Vessels thrombosis presents in 83.87% of the gestational diabetic placenta and 12.90% of the nondiabetic placenta [Table 1]. Nucleated RBC presents in 93.54% of the gestational diabetic placenta and 32.25% of the nondiabetic placenta. Hence, in our study, chorangiosis, subtrophoblastic basement membrane thickness, and dilated blood vessels and necrosis present in 100% of the gestational diabetic placenta.

### Ethical approval

The study was approved by the institutional ethics committee.

### Financial support and sponsorship

Nil.

### Conflicts of interest

There are no conflicts of interest.

## References

1. Desoye G, Shafrir E. The human placenta in diabetic pregnancy. Diabetes Rev 1996;4:70-89.
2. Calderon IM, Damasceno DC, Amorin RL, Costa RA, Brasil MA, Rudge MV. Morphometric study of placental villi and vessels in women with mild hyperglycemia or gestational or overt diabetes. Diabetes Res Clin Pract 2007;78:65-71.
3. Hay WW Jr., Catz CS, Grave GD, Yaffe SJ. Workshop summary: Fetal growth: Its regulation and disorders. Pediatrics 1997;99:585-91.
4. Forsbach-Sánchez G, Tamez-Peréz HE, Vazquez-Lara J. Diabetes and pregnancy. Arch Med Res 2005;36:291-9.
5. American Diabetes Association. Diagnosis and classification of diabetes mellitus. Diabetes Care 2009;32 Suppl 1:S62-7.
6. American Diabetes Association. Diagnosis and classification of diabetes mellitus. Diabetes Care 2006;29 Suppl 1:S43-8.
7. Crowther CA, Hiller JE, Moss JR, McPhee AJ, Jeffries WS, Robinson JS, *et al*. Effect of treatment of gestational diabetes mellitus on pregnancy outcomes. N Engl J Med 2005;352:2477-86.
8. Evers IM, Nikkels PG, Sikkema JM, Visser GH. Placental pathology in women with type 1 diabetes and in a control group with normal and large-for-gestational-age infants. Placenta 2003;24:819-25.
9. Langer O, Yogev Y, Most O, Xenakis EM. Gestational diabetes: The consequences of not treating. Am J Obstet Gynecol 2005;192:989-97.
10. Brudenell M, Doddridge MC. Diabetic pregnancy. New Delhi: Churchill Livingstone, London; 1989. p. 99-134.
11. Shen-Schwarz S, Ruchelli E, Brown D. Villous oedema of the placenta: A clinical pathological study. Placenta 1989;10:297-307.
12. Saydah SH, Miret M, Sung J, Varas C, Gause D, Brancati FL. Postchallenge hyperglycemia and mortality in a national sample of U.S. adults. Diabetes Care 2001;24:1397-402.
13. Kjos SL, Buchanan TA. Gestational diabetes mellitus. N Engl J Med 1999;341:1749-56.
14. Platt MJ, Stanisstreet M, Casson IF, Howard CV, Walkinshaw S, Pennycook S, *et al*. St Vincent's Declaration 10 years on: Outcomes of diabetic pregnancies. Diabet Med 2002;19:216-20.
15. Ashfaque MA, Janjua ZJ, Channa A. Effects of gestational diabetes and maternal hypertention on gross morphology of placenta. J Ayub Med Coll Abotabad 2005;17:44-7.
16. Al-Okail MS, and O. Al-Attas S. Histological changes in placental syncytiotrophoblasts of poorly controlled gestational diabetic patients. Endocrine Journal 1994;41;355-61.
17. Jauniaux E, Burton GJ. Villous histomorphometry and placental bed biopsy investigation in Type I diabetic pregnancies. Placenta 2006;27:468-74.
18. Hirota K. Electromicroscopic observations on the human placenta in maternal diabetes. Abstr in Federation Processing 1964;23:575.
19. Okudaira Y, Hirota K, Cohen S, Strauss L. Ultrastructure of the human placenta in maternal diabetes mellitus. Lab Invest 1966;15:910-26.
20. Daskalakis G, Marinopoulos S, Krielesi V, Papapanagiotou A, Papantoniou N, Mesogitis S, *et al*. Placental pathology in women with gestational diabetes. Acta Obstet Gynecol Scand 2008;87:403-7.
21. Verma R, Mishra S, Kaul MJ. Cellular changes in the placenta in pregnancies complicated with diabetes. Int J Morphol 2010;28:259-64.
22. Boden G, Vaidyula VR, Homko C, Cheung P, Rao AK. Circulating tissue factor procoagulant activity and thrombin generation in patients with type 2 diabetes: Effects of insulin and glucose. J Clin Endocrinol Metab 2007;92:4352-8.
23. Kario K, Matsuo T, Kobayashi H, Matsuo M, Sakata T, Miyata T. Activation of tissue factor-induced coagulation and endothelial cell dysfunction in non-insulin-dependent diabetic patients with microalbuminuria. Arterioscler Thromb Vasc Biol 1995;15:1114-20.
24. Sweet IR, Gilbert M, Maloney E, Hockenbery DM, Schwartz MW, Kim F. Endothelial inflammation induced by excess glucose is associated with cytosolic glucose 6-phosphate but not increased mitochondrial respiration. Diabetologia 2009;52:921-31.
25. Ettelaie C, Su S, Li C, Collier ME. Tissue factor-containing microparticles released from mesangial cells in response to high glucose and AGE induce tube formation in microvascular cells. Microvasc Res 2008;76:152-60.
26. Chiarelli F, Cipollone F, Romano F, Tumini S, Costantini F, di Ricco L, *et al*. Increased circulating nitric oxide in young patients with type 1 diabetes and persistent microalbuminuria: Relation to glomerular hyperfiltration. Diabetes 2000;49:1258-63.
27. Lal BK, Samreen M, Pushpa G, Shamshad B. Change in normal morphology of placenta and its possible effects on fetal outcome in diabetic mothers as compared to non diabetic mothers. JLUMHS 2013;12:49-54.
28. Saddler TW. Placenta and fetal membranes. In: Langman's Medical Embryology. New Delhi: Lippincott Williams & Wilkins; 2004. p. 91-111.

Original Article

# Evaluation of Vascular and Neural Anatomy of the Hand in Adult Cadavers

**Yadigar Kastamoni, Afitap Anil[1], Tuncay Peker[1], Feza Anil[2]**

*Department of Anatomy, Faculty of Medicine, Suleyman Demirel University, Isparta, [1]Department of Anatomy, Faculty of Medicine, Gazi University, Ankara, [2]Department of Nursing, Aksehir Kadir Yallagoz School of Health, Selcuk University, Konya, Turkey*

## Abstract

**Introduction:** We aimed to investigate the vascular and neural anatomy of the hand in adult cadavers and to determine the normal anatomical structure and variations of these structures. **Material and Methods:** Twenty hands of adult cadavers were examined by the dissection method. After the superficial palmar arch (SPA), the ulnar nerve (UN), median nerve (MN), and deep palmar arch (DPA) were identified, their anatomical structures and variations were evaluated. Then, they were classified according to the number of branches they give off and the course of these branches. **Results:** When the number of the common palmar digital arteries emerging from the SPA was examined, four branches were observed to emerge from the arch in 80%, and five branches in 20%. When the innervation of the MN and UN was evaluated, 3.5 + 1.5 fingers innervation was observed in 90%, 3 + 1.5 fingers innervation and 3 + 2 fingers innervation were observed in 5% of the samples. When the DPA samples were examined, four metacarpal palmar arteries were observed to emerge from the arch in all of the samples. According to the number of branches they gave off and the course of these branches, the SPA was gathered under seven groups, the nerves were gathered under four groups, and the DPA was gathered under three groups. **Discussion and Conclusion:** We believe that the data obtained in our study will be used, especially in anatomy education and will guide neurologists, surgeons, orthopedists, radiologists, and anatomists in their studies, diagnosis, and treatments.

**Keywords:** *Classification, deep palmar arch, median nerve, superficial palmar arch, ulnar nerve*

## Introduction

The hand plays an important role in the daily life of humans. The hand enables us to position, orient, and grasp objects by touching them and provides our communication with the outside world.[1] In addition to the innervation of the hand and hand-related structures, which take such an essential place in our lives, its nutrition is also vital.

The superficial palmar arch (SPA) and deep palmar arch (DPA), which are formed by the ulnar artery (UA) and radial artery (RA), are the structures feeding the hand.[2] Most of the studies on the SPA have been performed by the anatomical dissection method.[3-5] Furthermore, there are also studies conducted with angiography[6,7] and Doppler-ultrasonography[8] methods. In our literature review, few studies on the DPA were encountered.[3,4,9] In the Turkish population, there are few studies using the anatomical dissection method concerning the SPA[10,11] and DPA.[12]

The extrinsic and intrinsic muscles of the hand provide hand movements. The extrinsic muscles of the hand are innervated by the radial nerve (RN), ulnar nerve (UN), and median nerve (MN). The intrinsic muscles of the hand are innervated by the UN and MN.[2] There are many studies on the innervation of the extrinsic muscles[13-15] and intrinsic muscles[16-19] of the hand. When the studies on the intrinsic muscles of the hand were examined, it was seen that their dates back to very old times and these studies about the motor innervation of muscles. In our literature review, it was seen that there a few studies about the cutaneous distribution of nerves in the palm.[20-22] However, no studies about typing these nerves according to the distribution of fingers were found.

This study's goal was to investigate the normal anatomy and variations of the vascular and neural structures of the hand by examining the hands of adult cadavers by the anatomical dissection method.

**How to cite this article:** Kastamoni Y, Anil A, Peker T, Anil F. Evaluation of vascular and neural anatomy of the hand in adult cadavers. J Anat Soc India 2020;69:XX-XX.



**Article Info**

**Received:** 07 November 2019
**Revised:** 13 August 2020
**Accepted:** 19 August 2020
**Available online:** ***

***Address for correspondence:***
*Dr. Yadigar Kastamoni, Department of Anatomy, Faculty of Medicine, Suleyman Demirel University, 32260, Isparta, Turkey.*
*E-mail: yadigarkastamoni@hotmail.com*

**Access this article online**

**Website:** www.jasi.org.in
**DOI:** 10.4103/JASI.JASI_216_19
**Quick Response Code:**

## Material and Methods

Twenty adult cadaver hands, which had been previously fixed in a 10% formaldehyde solution, were examined by the anatomical dissection method. Approval was obtained from the Clinical Research Ethics Committee for this study (Date: October 26, 2015, Decision No: 40).

Dissections were performed under a surgical microscope (Carl Zeiss Opmi Pico, Germany) at × 5 magnification. To remove the skin of each hand, two transverse incisions passing through the wrist fold and finger roots and a vertical incision joining the midpoint of these two incisions were made. After the skin was removed, subcutaneous adipose tissue was cleaned, and the palmar aponeurosis was removed.

Firstly, the presence of the SPA and whether it was a complete arch (complete/incomplete) in case of its presence were evaluated. If the SPA was formed by the UA and superficial palmar branch of the RA, it was evaluated as the "complete" SPA. If it was formed only by the UA, it was evaluated as the "incomplete" SPA. However, according to the definitions in the literature,[3,4] the SPA formed only by the UA was included in the "complete" SPA category if it reached the first interosseous space. Furthermore, in our study, the number of the common palmar digital arteries emerging from the SPA and the interosseal space of each of these branches were determined. After the measurements of the SPA were completed, the number of branches from the MN and UN, and the interosseal space of each of these branches were recorded. According to the data obtained, the SPA, UN, and MN were classified.

After these procedures, the SPA, UN, and MN were cut from the wrist fold and lifted toward the fingers. The lumbrical muscles and flexor muscle tendons were removed. The DPA was defined, and the number of the metacarpal palmar arteries emerging from the DPA and the interosseal space of these branches were determined. Then, the DPA was classified according to the data obtained.

## Results

All of our samples had the SPA. Of the samples, 90% ($n$ = 18) had the "complete" SPA and 10% ($n$ = 2) had the "incomplete" SPA. When the "complete" SPAs were examined, it was revealed that the arch was formed by the UA and superficial palmar branch of the RA (radio-ulnar type) in 83.33% ($n$ = 15) of the samples and only by the UA (ulnar type) in 16.67% ($n$ = 3) of the samples.

When the number of the common palmar digital arteries emerging from the SPA was examined, four branches were observed to emerge from the arch in 80% ($n$ = 16), and five branches emerged from the arch in 20% ($n$ = 4) of the samples. It was detected that 65% ($n$ = 13) of the first branch emerging from the arch ran medially in hand, and 35% ($n$ = 7) ran in the fourth interosseous space. Of the second branch emerging from the arch, 55% ($n$ = 11) was observed to run in the fourth interosseous space and 45% ($n$ = 9) in the third interosseous space. Of the third branch emerging from the arch, 55% ($n$ = 11) was determined to run in the third interosseous space and 45% ($n$ = 9) in the second interosseous space. Of the fourth branch emerging from the arch, 55% ($n$ = 11) was observed to run in the second interosseous space and 45% ($n$ = 9) in the first interosseous space. In the four samples in which the fifth branch emerged, the whole branch was found to run in the first interosseous space.

While classifying the SPA, whether the arch is "complete" or "incomplete," the type of arteries that formed the arch (radio-ulnar type, ulnar type), the number of the common palmar digital arteries given off by the arch, and the course of these branches were taken into consideration, and the arch was gathered under seven main groups [Figures 1-5].

When the innervation of the MN and UN was evaluated, 3.5 + 1.5 fingers innervation was observed in 90% ($n$ = 18), 3 + 1.5 fingers innervation was observed in 5% ($n$ = 1), and 3 + 2 fingers innervation was observed in 5% ($n$ = 1) of the samples.

When 18 samples with 3.5 + 1.5 fingers innervation were examined, the MN was determined to be separated into four branches at the terminal in 94.44% ($n$ = 17) and into five branches in 5.56% ($n$ = 1) of the samples. In the samples in which the MN was separated into four branches, the first branch was observed to course laterally in the hand, the second branch coursed in the first interosseous space, the third branch coursed in the second interosseous space, and the fourth branch coursed in the third interosseous space. In the sample in which the MN was separated into five branches at the terminal, the first branch was observed to run laterally in the hand. The second branch was determined to run in the first interosseous space and innervate the thumb medial. The third branch was determined to run in the first interosseous space, but innervate the lateral of the second finger. The fourth branch emerging from the MN was observed to run in the second interosseous space, and the fifth branch ran in the third interosseous space. In all of the 18 samples with 3.5 + 1.5 fingers innervation, the UN was separated into two branches at the terminal. The first branch emerging from the nerve was observed to course in the fourth interosseous space, and the second branch coursed medially in the hand [Figures 6 and 7].

When the sample with 3 + 1.5 fingers innervation was examined, the MN was determined to be separated into three branches at the terminal. The first one of these branches was observed to course in the first interosseous space, the second branch coursed in the second interosseous space, and the third branch coursed in the third interosseous space. In this sample on the right side, it was noted that there were no branches on the lateral side of the thumb. In the same sample, the UN was observed to be separated into two branches at

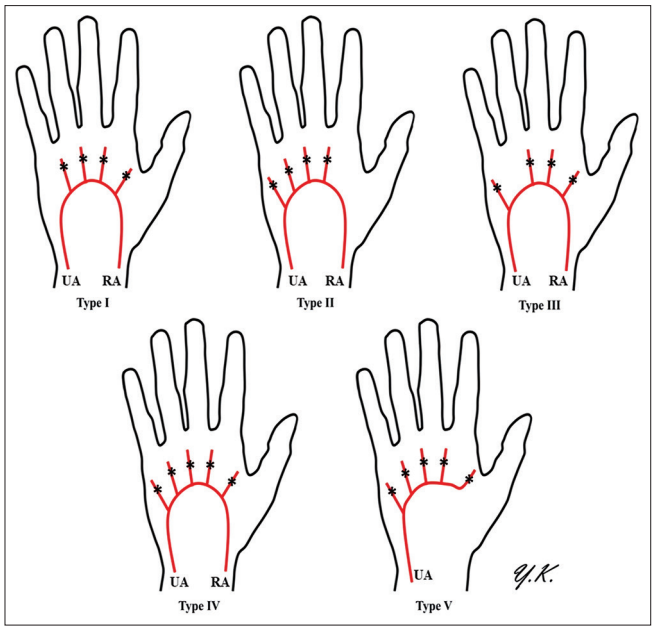


**Figure 1: Schematic classification of the "complete" superficial palmar arch. UA: Ulnar artery, RA: Radial artery, *common palmar digital artery**

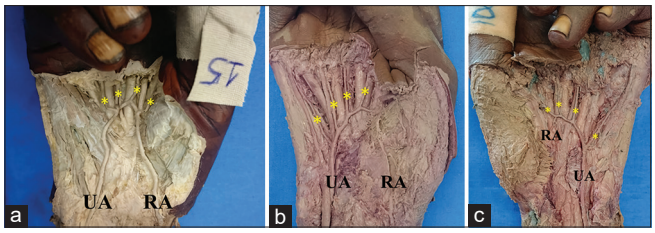


**Figure 3: Types of the "complete" superficial palmar arch that gives off four branches. (a) Type I, (b) Type II, (c) Type III. UA: Ulnar artery, RA: Radial artery, *common palmar digital artery**

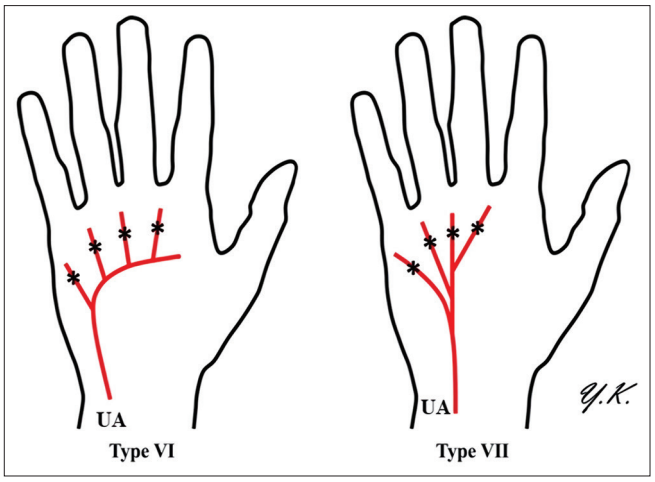


**Figure 2: Schematic classification of the "incomplete" superficial palmar arch. UA: Ulnar artery, RA: Radial artery, *common palmar digital artery**

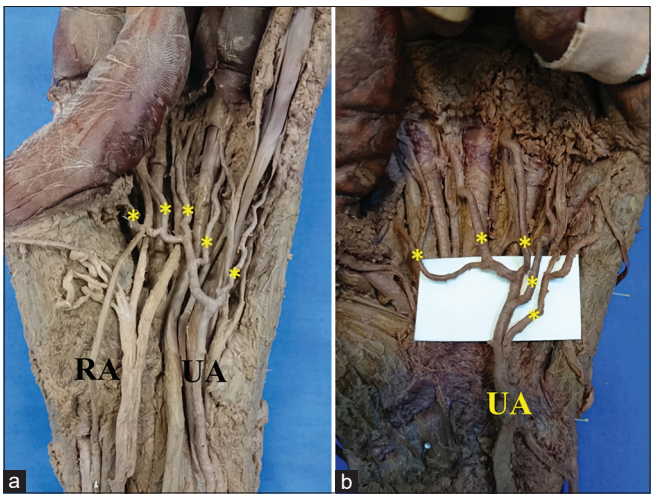


**Figure 4: Types of the "complete" superficial palmar arch that gives off five branches. (a) Type IV, (b) Type V. UA: Ulnar artery, RA: Radial artery, *common palmar digital artery**

the terminal. The first branch emerging from the UN was observed to course in the fourth interosseous space, and the second branch coursed medially in hand [Figures 6 and 8].

When the sample with 3 + 2 fingers innervation was examined, the MN was observed to be separated again into four branches. However, when their courses were examined, the branch, which coursed in the third interosseous space, was observed to innervate only the medial of the third finger, i.e., not to innervate the lateral of the 4th finger. The other branches of the MN coursed normally. In this sample, two branches were determined to emerge from the UN. The first one of these branches was observed to run in the fourth interosseous space, and the second branch ran medially in hand. The branch in the fourth interosseous space was determined to be separated into two at the terminal. It was determined that one of these branches innervated the lateral of the fourth finger, the other one continued to run in the fourth interosseous space and innervated the medial of the fourth finger and the lateral of the fifth finger [Figures 6 and 8].

The MN and UN were classified by considering the distribution of the nerves, the number of branches into which these nerves were separated at the terminal, and the course of these branches. Accordingly, the nerves were gathered under four main groups [Figures 6 and 8].

When the DPA samples were examined, four metacarpal palmar arteries were observed to emerge from the arch in all of the samples. It was found that 100% ($n$ = 20) of the first branch ran in the first interosseous space, 95% ($n$ = 9) of the second branch ran in the second interosseous space, and 5% ($n$ = 1) ran in the third interosseous space. Of the third branch emerging from the arch, 95% ($n$ = 19) was observed to run in the third interosseous space and 5% ($n$ = 1) ran in the fourth interosseous space. Of the fourth branch, 90% ($n$ = 18) was observed to run in the fourth interosseous space, and 10% ($n$ = 2) ran medially in hand.

The DPA was classified according to the number of the metacarpal palmar arteries given off by the arch and the course of these branches. Accordingly, the DPA was gathered under three main groups [Figures 9 and 10].

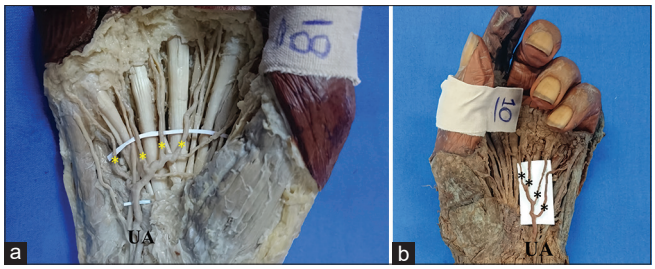


**Figure 5: Types of the "incomplete" superficial palmar arch. (a) Type VI, (b) Type VII. UA: Ulnar artery, RA: Radial artery, *common palmar digital artery**

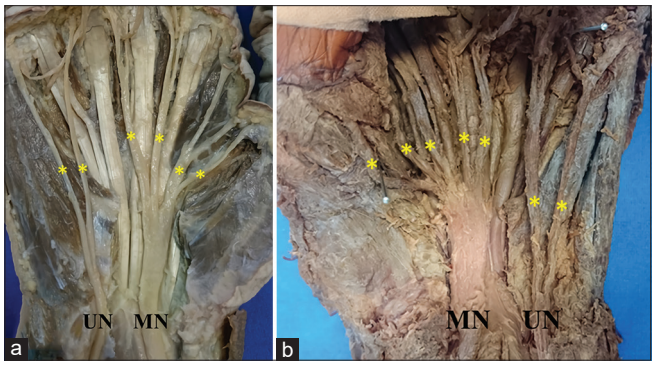


**Figure 7: Types of the nerves on the hand with 3.5 + 1.5 finger innervation. (a) Type I, (b) Type II. MN: Median nerve, UN: Ulnar nerve, *terminal branches of the nerves**

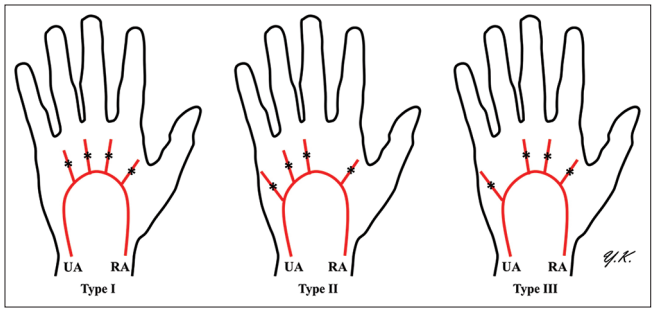


**Figure 9: Schematic classification of the deep palmar arch. UA: Ulnar artery, RA: Radial artery, *metacarpal palmar artery**

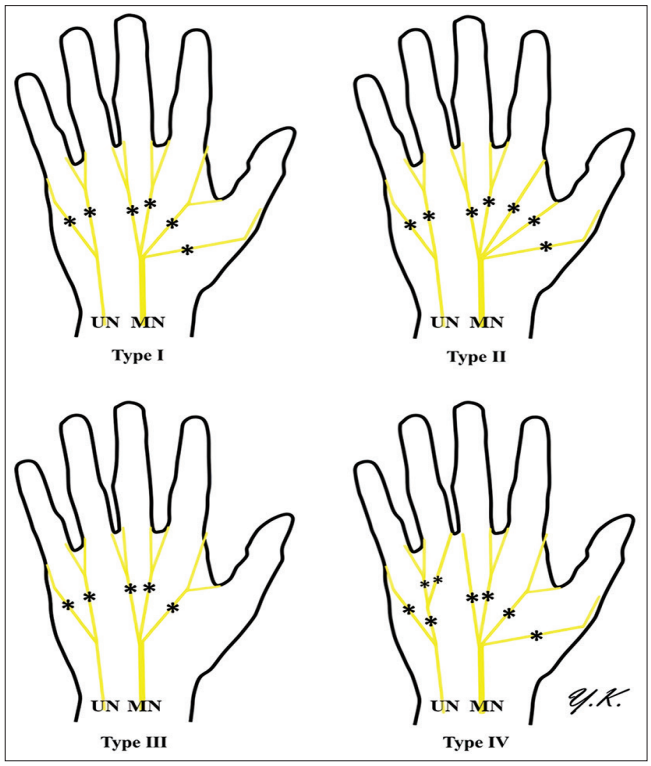


**Figure 6: Schematic classification of the median nerve and ulnar nerve. MN: Median nerve, UN: Ulnar nerve, *terminal branches of the nerves**

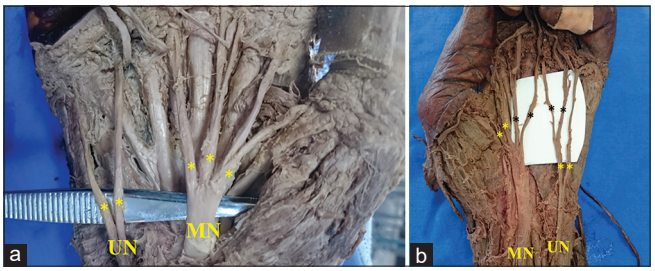


**Figure 8: (a) Type of the nerves on the hand with 3 + 1.5 finger innervation, Type III. (b) Type of the nerves on the hand with 3 + 2 finger innervation, Type IV. MN: Median nerve, UN: Ulnar nerve, *terminal branches of the nerves**

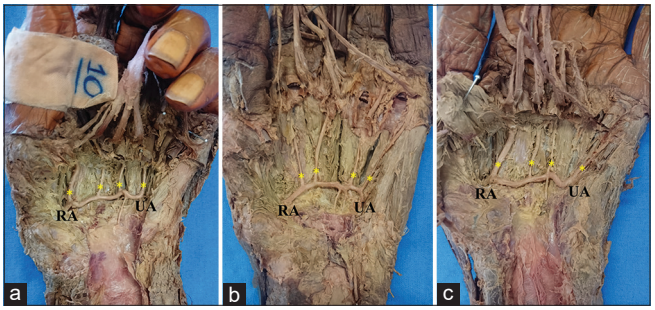


**Figure 10: Types of the deep palmar arch. (a) Type I, (b) Type II, (c) Type III. UA: Ulnar artery, RA: Radial artery, *metacarpal palmar artery**

The frequency and distribution of the SPA types in the right and left hands are presented in Table 1, the frequency and distribution of the MN and UN types in the right and left hands are presented in Table 2, and the frequency and distribution of the DPA types in the right and left hands are presented in Table 3.

## Discussion

The vascular structure of the hand, which is a highly complex area, has been investigated in many studies to date. Especially with advances in microsurgery, the vascular structure of the hand has become even more important in reconstructive hand surgery.[10]

The incidence and variations of the SPA were first defined in the 19th century. In 1897, Jaschtschinski described the "complete" and "incomplete" arch together with its different subtypes. Jaschtschinski separated the "complete" SPA into subtypes as the radio-ulnar arch, median-ulnar arch, radio-median-ulnar arch, and ulnar arch.[23]

The SPA and the frequency of its being complete/incomplete are presented in Table 4.

Upon examining Table 4, the results obtained from our study were observed to be consistent with the general average. Moreover, according to the table, the results varied in a wide range. For example, the presence of the "complete" SPA ranged between 45.23% and 95%. We think that this variability may be due to differences, such as ethnicity, gender, the number of samples, study method, and classification.

**Table 1: Frequency of the superficial palmar arch types and their distribution in the right and left hands, *n* (%)**

| Types | Right hand | Left hand | Total |
|---|---|---|---|
| Type I | 4 (20) | 3 (15) | 7 (35) |
| Type II | 4 (20) | 1 (5) | 5 (25) |
| Type III | 1 (5) | 1 (5) | 2 (10) |
| Type IV | - | 1 (5) | 1 (5) |
| Type V | - | 3 (15) | 3 (15) |
| Type VI | 1 (5) | - | 1 (5) |
| Type VII | - | 1 (5) | 1 (5) |

*n*: Number of extremities

**Table 2: Frequency of the median nerve and ulnar nerve types and their distribution in the right and left hands, *n* (%)**

| Types | Right hand | Left hand | Total |
|---|---|---|---|
| Type I | 9 (45) | 8 (40) | 17 (85) |
| Type II | - | 1 (5) | 1 (5) |
| Type III | 1 (5) | - | 1 (5) |
| Type IV | - | 1 (5) | 1 (5) |

*n*: Number of extremities

**Table 3: Frequency of the deep palmar arch types and their distribution in the right and left hands, *n* (%)**

| Types | Right hand | Left hand | Total |
|---|---|---|---|
| Type I | 10 (50) | 8 (40) | 18 (90) |
| Type II | - | 1 (5) | 1 (5) |
| Type III | - | 1 (5) | 1 (5) |

*n*: Number of extremities

The studies conducted on the classification of the arch according to the arteries that form the "complete" SPA and their results are presented in Table 5.

When Table 5 was examined, the "complete" SPA was detected to be usually formed by the UA and superficial palmar branch of the RA (radio-ulnar type). This was followed by the ulnar type (the formation of the SPA only by the UA). Only in the studies conducted by Singh *et al*. and Joshi *et al*.,[4,24] the ulnar type was found to be more common than the radio-ulnar type. In the studies carried out, the radio-ulnar-median type (the SPA is formed by the UA, the superficial palmar branch of the RA and persistent median artery) was encountered at the lowest rate. When these results were evaluated in terms of types, our study was observed to bear similarities with other studies.

In the studies in Table 5, it was determined that the SPA was classified according to whether it was complete/incomplete and the type of the arteries forming the arch. However, in our study, in addition to these data, the classification was made by also considering the number of the common palmar digital arteries leaving the arch and the course of these branches [Figures 1 and 2].

The SPA plays an essential role in microsurgery after hand injuries. The collateral circulation of the hand continues even if any artery in the hand is occluded. Plastic surgeons and hand surgeons should know the normal anatomy and variations of these arteries well before performing surgical procedures such as vascular repair and grafting. Since our study was carried out by considering more data on classification, we believe that our study will constitute a basis for future studies and will shed light on surgical procedures.

Although there are various studies on the sensory innervation of the hand in the literature,[21,29,30] there are no studies involving the classification of nerve distribution

**Table 4: The superficial palmar arch and frequency of its being complete/incomplete in the literature**

| Researchers, year | Population | Total number of samples (*n*, number of hands) | Complete superficial palmar arch, *n* (%) | Incomplete superficial palmar arch, *n* (%) |
|---|---|---|---|---|
| Our study | Turkish | 20 | 18 (90) | 2 (10) |
| Loukas *et al*.[3] | American | 200 | 180 (90) | 20 (10) |
| Singh *et al*.[4] | South African | 100 | 92 (92) | 8 (8) |
| Suma *et al*.[5] | Indian | 20 | 19 (95) | 1 (5) |
| Gokhroo *et al*.[6] | Indian | 200 | 149 (74.5) | 51 (25.5) |
| Al-Turk and Metcalf[8] | Caucasian | 50 | 42 (84) | 8 (16) |
| Bilge *et al*.[10] | Turkish | 50 | 43 (86) | 7 (14) |
| Tagıl *et al*.[11] | Turkish | 20 | 15 (75) | 5 (25) |
| Joshi *et al*.[24] | Indian | 100 | 82 (82) | 18 (18) |
| Sarkar *et al*.[25] | Indian | 42 | 19 (45.23) | 23 (54.76) |
| Ottone *et al*.[26] | Argentinian | 86 | 50 (58) | 36 (42) |
| de Moraes *et al*.[27] | Brazilian | 30 | 18 (60) | 12 (40) |

**Table 5: Classification of the arch according to the arteries forming the "complete" superficial palmar arch in the literature**

| Researchers, year | Population | Radio-ulnar type (%) | Ulnar type (%) | Radio-ulnar-median type (%) | Ulnar-median type (%) | Ulnar-arcus palmaris profundus type (%) |
|---|---|---|---|---|---|---|
| Our study | Turkish | 75 | 15 | - | - | - |
| Loukas *et al*.[3] | American | 40 | 35 | 6.1 | 15 | 3.9 |
| Singh *et al*.[4] | South African | 44 | 46 | 2 | - | - |
| Al-Turk and Metcalf[8] | Caucasian | 78 | - | 2 | 4 | - |
| Bilge *et al*.[10] | Turkish | 62 | 14 | - | 4 | 6 |
| Joshi *et al*.[24] | Indian | 30 | 66 | - | 4 | - |
| Sarkar *et al*.[25] | Indian | 89.47 | - | - | - | 10.52 |
| Ottone *et al*.[26] | Argentinian | 37.1 | 20.9 | - | - | - |
| de Moraes *et al*.[27] | Brazilian | 36.67 | 23.34 | - | - | - |
| Madhyastha *et al*.[28] | Indian | 93.75 | 2.08 | - | - | - |

according to fingers. In our study, the samples were evaluated for innervation by considering the distribution of the MN and UN in hand. Accordingly, 3.5 + 1.5 fingers innervation was observed in 90%, 3 + 1.5 fingers innervation was observed in 5% of the samples, and 3 + 2 fingers innervation was observed in the remaining 5%.

In this study, which we performed by the anatomical dissection method, the MN and UN were classified by considering the distribution of the nerves, the number of branches into which the nerves were separated at the terminal, and the course of these branches [Figure 6]. Our study may be a basic study on this subject. The anatomical dissection method is also known to provide more reliable and accurate results than imaging methods. Therefore, we believe that our study will help to identify and distinguish structures in neurology clinics, neurosurgery, orthopedics, plastic, reconstructive and aesthetic surgery and will provide a basis for studies on the subject.

While there are many studies related to DPA in the literature review,[3,4,9] this number is very low when the Turkish population is examined.[12]

In the study conducted by Loukas *et al*.,[3] the DPA was separated into three types according to the arteries forming the arch. According to this study, if the DPA was formed by the RA and inferior deep palmar branch of the UA, it was defined as "type D-I." If it was formed by the RA and superior deep palmar branch of the UA, it was defined as "type D-II." If it was formed by the RA and both deep palmar branches of the UA, it was defined as "type D-III." In the study, type D-I was found at a rate of 60% ($n$ = 120), type D-II was found at a rate of 30% ($n$ = 60), and type D-III was found at a rate of 10% ($n$ = 20).

In the study performed by Singh *et al*.,[4] the DPA was separated into five types according to the arteries forming the arch. According to this study, if the DPA was formed by the RA and deep palmar branch of the UA, it was defined as "type G." If it was formed by the RA, deep palmar branch of the UA and interosseous artery, it was defined as "type H." If the deep palmar branch of the UA was separated into superior and inferior branches and formed an arch with the RA, it was defined as "type I." If the deep palmar branch of the UA was separated into superior and inferior branches, and one of these branches formed an arch with the RA, it was defined as "type J." If the interosseous artery also joined the combination in type "J" and formed an anastomosis with either the arch or the branch of the additional UA, it was defined as "type K." In the study, type G was found at a rate of 72% ($n$ = 72), type H at a rate of 12% ($n$ = 12), type I at a rate of 8% ($n$ = 8), type J at a rate of 4% ($n$ = 4) and type K was found at a rate of 4% ($n$ = 4).

In both studies, the DPA was observed to be classified according to whether the arch was complete/incomplete and the type of the arteries forming the arch.[3,4] In our study, during classification, as in the SPA, in addition to the data mentioned above, the number of the metacarpal palmar arteries given off by the arch and the course of these branches were also taken into consideration [Figure 9].

There are some limitations of this study since a smaller number of samples. However, in our study, unlike previous studies, more information was given, especially in terms of the course of the branches given by the arches and nerves and typing was made according to the course of these branches.

## Conclusions

Understanding the anatomical structure and variations of the arteries and nerves of the hand is particularly important during the surgical reconstruction of the hand in hand injuries. It is known that the lack of knowledge about the anatomy of the palmar region increases the risk of complications during surgical procedures applied to this region. We think that the data obtained on the vascular and neural anatomy of the hand in our study will be included, especially in anatomy education. At the same time, while determining pathologies and variations related to the structures, these data will contribute to the diagnosis and

treatment in orthopedics, surgery, radiology and neurology clinics, and other science branches. Thus, it will guide anatomists and other scientists in studies on the subject.

### Financial support and sponsorship

Nil.

### Conflicts of interest

There are no conflicts of interest.

## References

1. Pena-Pitarch E, Falguera NT, Yang JJ. Virtual human hand: Model and kinematics. Comput Methods Biomech Biomed Engin 2014;17:568-79.
2. Standring S. Gray's Anatomy. 40th ed. London: Elsevier Churchill Livingstone; 2008. p. 894-8.
3. Loukas M, Holdman D, Holdman S. Anatomical variations of the superficial and deep palmar arches. Folia Morphol (Warsz) 2005;64:78-83.
4. Singh S, Lazarus L, De Gama BZ, Satyapal KS. An anatomical investigation of the superficial and deep palmar arches. Folia Morphol 2016;76:219-25.
5. Suma MP, Vijay Kumar S, Priya R. An anatomical study of superficial palmar arch. Int J Anat Res 2014;2:735-9.
6. Gokhroo R, Bisht D, Gupta S, Kishor K, Ranwa B. Palmar arch anatomy: Ajmer Working Group classification. Vascular 2016;24:31-6.
7. Kaplanoglu H, Beton O. Evaluation of anatomy and variations of superficial palmar arch and upper extremity arteries with CT angiography. Surg Radiol Anat 2017;39:419-26.
8. Al-Turk M, Metcalf WK. A study of the superficial palmar arteries using the Doppler ultrasonic flowmeter. J Anat 1984;138:27-32.
9. Olave E, Prates JC. Deep palmar arch patterns in Brazilian individuals. Surg Radiol Anat 1999;21:267-71.
10. Bilge O, Pinar Y, Ozer MA, Gövsa F. A morphometric study on the superficial palmar arch of the hand. Surg Radiol Anat 2006;28:343-50.
11. Tagıl SM, Cicekcibası AE, Ogun TC, Buyukmumcu M, Salbacak A. Variations and clinical ımportance of the superficial palmar arch. SDU Med Facult J 2007;14:11-6.
12. Bilge O, Özer MA, Pınar Y, Gövsa F. Deep palmar arch in man. Turk Klinikleri J Med Sci 2009;29:816-820.
13. Dogan NU, Uysal II, Karabulut AK, Fazliogullari Z. The motor branches of median and ulnar nerves that innervate superficial flexor muscles: A study in human fetuses. Surg Radiol Anat 2010;32:225-33.
14. Albay S, Kastamoni Y, Sakalli B. Motor branching patterns of the ulnar nerve in the forearms of fetal cadavers. Surg Radiol Anat 2013;35:951-6.
15. Paulos R, Leclercq C. Motor branches of the ulnar nerve to the forearm: An anatomical study and guidelines for selective neurectomy. Surg Radiol Anat 2015;37:1043-8.
16. Brooks HS. Variations in the nerve supply of the lumbrical muscles in the hand and foot, with some observations on the ınnervation of the perforating flexors. J Anat Physiol 1887;21:575-85.
17. Amoiridis G. Median--ulnar nerve communications and anomalous innervation of the intrinsic hand muscles: An electrophysiological study. Muscle Nerve 1992;15:576-9.
18. Murata K, Tamai M, Gupta A. Anatomic study of variations of hypothenar muscles and arborization patterns of the ulnar nerve in the hand. J Hand Surg Am 2004;29:500-9.
19. Homma T, Sakai T. Anatomy of intrinsic hand muscles. Kaibogaku Zasshi 1994;69:123-42.
20. Born T, Mahoney J. Cutaneous distribution of the ulnar nerve in the palm: Does it cross the incision used in carpal tunnel release? Ann Plast Surg 1995;35:23-25.
21. Sulaiman S, Soames R, Lamb C. Ulnar nerve cutaneous distribution in the palm: Application to surgery of the hand. Clin Anat 2015;28:1022-8.
22. Smith JL, Ebraheim NA. Anatomy of the palmar cutaneous branch of the median nerve: A review. J Orthop 2019;16:576-9.
23. Feigl GC, Petrac M, Pixner T, Ulz H, Mörth C, Dreu M. The superficial palmar arch and median artery as an example of misleading results due to a small number of investigated specimens or the use of different classifications. Ann Anat 2012;194:389-95.
24. Joshi SB, Vatsalaswamy P, Bahetee BH. Variation in formation of superficial palmar arches with clinical implications. J Clin Diagn Res 2014;8:6-9.
25. Sarkar A, Dutta S, Bal K, Biswas J. Handedness may be related to variations in palmar arterial arches in humans. Singapore Med J 2012;53:409-12.
26. Ottone NE, Prum N, Dominguez M, Blasi E, Medan C, Shinzato S, *et al.* Analysis and clinical importance of superficial arterial palmar irrigation and its variants over 86 cases. Int J Morphol 2010;28:157-64.
27. de Moraes SR, de Araújo TN, da Silva AR, de Paula AR, Salgado JL. Morphologic variations of the superficial palmar arc. Acta Cir Bras 2003;18:183-8.
28. Madhyastha S, Murlimanju BV, Jiji PJ, Saralaya VV, Rai A, Vadgaonkar R. Morphological variants of the human superficial palmar arch and their clinical implications. J Morphol Sci 2011;28:261-4.
29. Martin CH, Seiler JG, Lesesne JS. The cutaneous innervation of the palm: An anatomic study of the ulnar and median nerves. J Hand Surg Am 1996;21:634-8.
30. Filfilan R, Kinsella A, Yong L, Davidson DM. A cadaveric study of the distribution pattern of the cutaneous sensory fibres of the distal palm of the hand. J Hand Surg Eur 2016;41:848-51.

Case Report

# Multiple Renal Vasculature

**Abstract**

Variations in the renal vasculature are often encountered in routine cadaveric dissection. In this case, variations were found in the right renal vein (RRV), right renal artery (RRA) and left renal artery (LRA) of a formalin-fixed cadaver. The RRV had two tributaries and the RRA had three branches. The LRA had two branches and was anterior to the left renal vein. Such vascular anomalies are significant clinically.

**Keywords:** *Left renal artery, left renal vein, right renal artery, right renal vein*

**V. Vijaynath, Vishnu Ravi, Maya Mukundan[1], T. S. Tintu[2]**

*Department of Rachana Shareera (Anatomy), Government Ayurveda Medical College, Tripunithura, [2]Department of Anatomy, Amrita School of Medicine, Amrita Vishwa Vidyapeetham, Kochi, [1]Department of Rachana Shareera (Anatomy), Government Ayurveda Medical College, Kannur, Kerala, India*

## Introduction

The large renal veins lie anterior to the renal arteries and open into the inferior venacava almost at the right angles. The left renal vein (LRV) three times longer than the right (7.5 cm and 2.5 cm, respectively). For this reason, the left kidney is the preferred side for live donor nephrectomy. The right renal vein (RRV) can be extremely short (<1 cm) such that safe nephrectomy may require excision of a cuff of the inferior venacava. The RRV has no significant collateral drainage like that of the left and cannot be ligated with impunity.

Renal arteries branch laterally from the abdominal aorta just below the origin of the superior mesenteric artery. Both the arteries cross the corresponding crus of the diaphragm at right angles to the aorta. The right renal artery (RRA) is longer and often higher, passing posterior to the inferior venacava, RRV, head of the pancreas and splenic vein.

A single renal artery to each kidney is present in approximately 70% of individuals. The arteries vary in their level of origin and in their caliber, obliquity, and precise relations. In its extra renal course, each renal artery gives off one or more inferior suprarenal arteries, a branch to the ureter, and branches which supply perinephric tissue, the renal capsule and the pelvis. Near the renal hilum each artery divides into an anterior and a posterior division, and these divide into segmental arteries supplying the renal vascular segments. Accessory renal arteries are common (30% of the individuals) and usually arise from the aorta above or below (most commonly below) the main renal artery and follow it to the renal hilum. They are regarded as persistent embryonic lateral splanchnic arteries. Accessory vessels to the inferior pole cross anterior to the ureter and may, by obstructing the ureter, cause hydronephrosis. Rarely, accessory renal arteries arise from the coeliac or from the superior mesenteric arteries near the aortic bifurcation or from the common iliac arteries.[1]

Supernumerary renal arteries are relatively common. They represent persistent fetal renal arteries which grow in sequence from the aorta to supply the kidney as it ascends from the pelvis. Their occurrence is clinically important because a supernumerary artery may cross the pelviureteral junction and obstruct the outflow of urine, producing dilatation of the calyces and pelvis, a condition known as hydronephrosis.[2]

Aberrant real vessels from the development of kidney it is clear that there may be an aberrant renal artery supplying the kidney. Such artery is usually small and insignificant, but occasionally it may be large and become significant due to the fact that it supplies a segment of the kidney. Such artery is more often seen supplying the lower pole of the kidney. This artery may be associated with hydronephrosis



**How to cite this article:** Vijaynath V, Ravi V, Mukundan M, Tintu TS. Multiple renal vasculature. J Anat Soc India 2020;69:XX-XX.

**Article Info**

**Received:** 25 December 2019
**Accepted:** 22 May 2020
**Available online:** ***

***Address for correspondence:***
*Dr. V. Vijaynath, Department of Rachana Shareera (Anatomy), Government Ayurveda Medical College, Tripunithura, Kochi, Kerala, India.*
*E-mail: drvijaynathv@gmail.com*

**Access this article online**

**Website:** www.jasi.org.in
**DOI:** 10.4103/JASI.JASI_232_19
**Quick Response Code:**

by compressing the pelvi-ureteric junction or it simply accompanies it, is a point of debate. One must be careful in dividing such aberrant artery as it may cause infarction of the corresponding segment of the renal tissue if it be the only arterial supply to that region.

Aberrant renal artery is more often seen on the left side, and it is more common in females. There may be aberrant renal vein but its significance is much less than aberrant renal artery and it is also less common. Moreover, due to venous collateral circulation, its importance is insignificant.[3]

## Case Report

During routine dissection of a 55-year old male cadaver in the department of anatomy, variations were found in the RRV, RRA, and left renal artery (LRA) simultaneously. There were two tributaries for the RRV, the upper tributary emerged slightly below the middle of the hilum, ran upwards and to the left with an inclination of 45° with the horizontal plane. The upper tributary was about 1.5 cm long and joined the lower tributary at an acute angle. The lower tributary was slender than the upper one and emerged from lower part of the hilum, 1 cm below the exit of the upper tributary. It also ran upwards and to the left, parallel to the upper tributary and joined the upper one at an acute angle after a course of 1.5 cm. The combined wider single RRV, about 1.5 cm wide, continued upward and left for a length of 3 cm and joined the inferior vena cava on its right margin. The tributaries and the single RRV were anterior to the RRA and its branches [Figure 1].

The single RRA emerged from the abdominal aorta under cover of the inferior vena cava and after a course of 1 cm toward the right and in upward direction, divided into three before entering the hilum. The upper branch, 2 cm long, continued upward and to the right, above the upper margin of RRV and entered the hilum at its upper angle. The middle branch ran almost horizontal above the RRV for a distance of 3 cm and entered the hilum just above its center. The lower branch curved downward and entered the hilum near the lower pole. The division of the artery into upper and middle branches was visible just above the middle of the upper border of the RRV [Figure 2].

The LRV was single throughout its length. The vein 1.5 cm wide and 7 cm long, emerged from the middle of the hilum posterior to the entrance of the branches of LRA, ran almost horizontal, dorsal to the branches of LRA. The origin of the superior mesenteric artery lies immediately above the terminal part of the LRV. The terminal part of the LRV curved upward and to the right and entered the inferior vena cava at its left margin, opposite to the entrance of the RRV.

The LRA originated as two branches, upper and lower, from the abdominal aorta, immediately below and slightly to the left of the origin of superior mesenteric artery. The upper branch originated from the left margin and after a very short course of 2 cm divided into two twigs, dorsal and ventral. The origin of branches lay posterior to the LRV. The two branches after a course to the left appeared on the left side of the opening of the lumbar vein to the LRV. The upper branch of LRA then subdivided into ventral and dorsal twigs. The dorsal twig of upper branch ran horizontally to the left and entered the upper angle of the hilum. The ventral twig separated from the common trunk ran slightly downward to the right above the upper margin of the LRV and divided into two. The upper subdivision of the ventral twig of LRA ran horizontally to enter the upper part of the hilum just below the entrance of the upper branch. The lower subdivision of the ventral twig ran almost vertically downward and to the left, crossed the LRV and entered the lower part of the hilum, below the exit of the LRV.

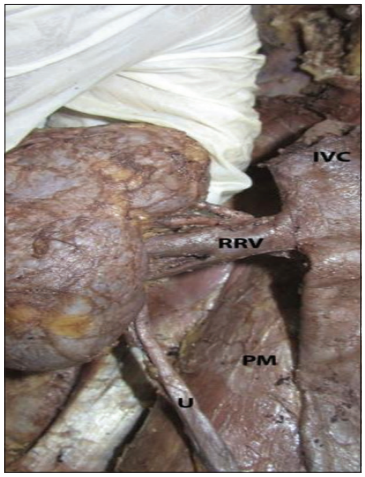


**Figure 1: Single right renal vein and its tributaries located in the front of the right renal artery and its branches. (IVC: Inferior vena cava, RRV: Right renal vein with its upper and lower tributaries, PM: Psoas major muscle, U: Ureter)**

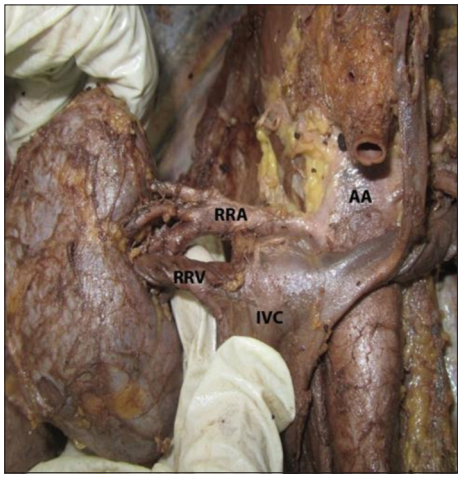


**Figure 2: Divisions of the right renal artery into upper and middle branches visible just above the middle of the upper border of the right renal vein. Inferior vena cava reflected downward. (RRA: Right renal artery with upper, middle and lower branches, RRV: Right renal vein, AA: Abdominal aorta, IVC: Inferior vena cava)**

The separate lower branch emerged from the aorta slightly anterior to and below the origin of the common trunk of upper and lower branches and ran upward and anteriorly, wound around the upper margin of LRV and continued downward and to the left crossing anterior to the LRV. The branch opened into the lower pole of the kidney anterior to the renal pelvis [Figure 3].

## Discussion

The large renal veins lie anterior to the renal arteries and open into the inferior vena cava almost at right angles. The LRVs are three times longer than the right (7.5 cm and 2.5 cm, respectively). For this reason, the left kidney is the preferred side for live donor nephrectomy. The RRV can be extremely short (<1 cm) such that safe nephrectomy may require excision of a cuff of the inferior vena cava. The RRV has no significant collateral drainage like that of the left and cannot be ligated with impunity.

Renal arteries branch laterally from the abdominal aorta just below the origin of the superior mesenteric artery. Both the arteries cross the corresponding crus of the diaphragm at right angles to the aorta. The RRA is longer and often higher, passing posterior to the inferior vena cava, RRV, head of the pancreas and splenic vein.

A single renal artery to each kidney is present in approximately 70% of individuals. The arteries vary in their level of origin and in their caliber, obliquity, and precise relations. In its extra renal course, each renal artery gives off one or more inferior suprarenal arteries, a branch to the ureter, and branches which supply perinephric tissue, the renal capsule and the pelvis. Near the renal hilum each artery divides into an anterior and a posterior division, and these divide into segmental arteries supplying the renal vascular segments. Accessory renal arteries are common (30% of the individuals) and usually arise from the aorta above or below (most commonly below) the main renal artery and follow it to the renal hilum. They are regarded as persistent embryonic lateral splanchnic arteries. Accessory vessels to the inferior pole cross anterior to the ureter and may, by obstructing the ureter, cause hydronephrosis. Rarely, accessory renal arteries arise from the coeliac or superior mesenteric arteries near the aortic bifurcation or from the common iliac arteries.[1]

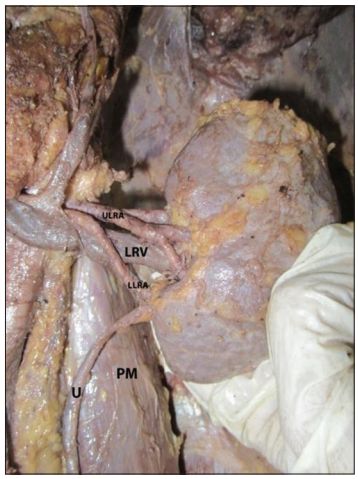


**Figure 3: Left renal artery with its upper and lower branches and their distribution. (ULRA: Upper branch of the left renal artery with its dorsal and ventral twigs, LLRA: Lower branch of the left renal artery, U: Ureter, PM: Psoas major muscle, LRV: Left renal vein)**

Supernumerary renal arteries are relatively common. They represent persistent fetal renal arteries which grow in sequence from the aorta to supply the kidney as it ascends from the pelvis. Their occurrence is clinically important because a supernumerary artery may cross the pelvi-ureteral junction and obstruct the outflow of urine, producing dilatation of the calyces and pelvis, a condition known as hydronephrosis.[2]

Aberrant real vessels from the development of the kidney it is clear that there may be an aberrant renal artery supplying the kidney. Such artery is usually small and insignificant, but occasionally, it may be large and become significant due to the fact that it supplies a segment of the kidney. Such artery is more often seen supplying the lower pole of the kidney. This artery may be associated with hydronephrosis by compressing the pelviureteric junction or it simply accompanies it, is a point of debate. One must be careful in dividing such aberrant artery as it may cause infarction of the corresponding segment of the renal tissue if it be the only arterial supply to that region.

Aberrant renal artery is more often seen on the left side, and it is more common in females. There may be aberrant renal vein, but its significance is much less than aberrant renal artery and it is also less common. Moreover, due to venous collateral circulation, its importance is insignificant.[3]

The variations in renal vasculature, though very usual in occurrence, are very significant from the surgical point of view. Renal artery variations are of two types: early division and extra renal artery. Branching of the main renal arteries into segmental branches more proximally than the renal hilum level is called early division. Extra renal arteries are of two types: hilum (accessory) and polar (aberrant) arteries. Hilum arteries enter the kidneys from the hilum with the main artery, whereas polar arteries enter the kidney directly from the capsule outside the hilus.[4]

The LRA in the current case thus showed both the two varieties of the variations. The upper branch showed early division and the lower branch can be considered as an extra renal artery and comes under the polar variety of the extra renal artery. The lower branch can be considered as the aberrant renal artery, and its presence is important from the clinical point of view as this artery may be associated with hydronephrosis by compressing the pelviureteric junction or infarction of the corresponding segment of the renal tissue

if it be the only arterial supply to that region.[3] The RRA showed early division variety of renal artery variation.

In the study conducted by Ozkan *et al*., including 855 patients, one renal artery was observed feeding both the kidneys in 76% of the patients. More than one renal artery was observed in 24% patients, of which 16% were on the right side and 13% on the left side. In 5% patients, more than one renal artery was present on both sides.[4] In this case, the extra real artery and early divisions of the renal artery were present in the left side and early division alone in the right side.

Gulas *et al*. has reported that with regard to ethnicity, the incidence of accessory renal arteries fluctuates from 4% in a Malaysian population to 61.5% in a Brazilian population. The frequency is the lowest in the Eastern and Southern Asia (from 4% to 18.4%). In some, not ethnically homogenous populations, wide span of occurrence of accessory renal arteries is described (e.g., American – averaging from 18% to 28.8%). A higher frequency of accessory renal arteries was observed in fetuses compared to adults.[5]

Dhar and Lal has reported in a study of 40 cadavers that revealed a single main renal artery on either side in 80% of the specimens. Multiple (accessory) renal arteries were observed in 20% of the specimens with unilateral anomaly (15%) being more commonly encountered than bilateral anomaly (5%).[6]

The right kidney in the present case showed the presence of supernumerary renal vein which is an additional renal vein arising from the renal hilum and draining into the inferior vena cava.

Glodny *et al*., in a study on hypertension associated with multiple renal arteries on 62 individuals, has concluded that patients with multiple renal arteries constitute a group who have high plasma renin activity and may therefore be prone to develop arterial hypertension.[7]

Kumar *et al*. has reported a case of an accessory RRV draining into the posterior aspect of the inferior vena cava.[8] Kumar *et al*. has reported a case of bilateral variations at the hilum involving both renal veins and arteries.[9] Mukundan *et al*. has reported a case of bilateral double renal vein.[10]

Satyapal, states that statistically significant changes have been noted in the drainage pattern of right and LRVs. Three hundred and six kidneys were studied and three major types (I, II, and III) of kidney drainage were observed. Type IA consisted of 2 primary tributaries only-an upper and a lower which occurred in 118 (38.6%). It was commonly present on the left side. In addition to upper and lower primary tributaries, a posterior primary tributary was also present in Type IB. This type was observed in 77 (25.2%) cases. In Type IIA, the existence of more than two tributaries, i.e., upper, middle, and lower, were observed. A maximum of five primary tributaries was identified and was noted in 36 (11.8%) cases. In Type IIB, in addition to the primary tributaries present in Type IIA, a posterior primary tributary was also present. Type II B was present in 31 (10.1%) out of the 306 kidneys. Type III consisted of either Types IA, IB, IIA, or IIB along with an additional renal vein or veins. Such variety occurred in 44 (14.4%) cases.[11]

## Conclusion

Variations in the renal vasculature are important from an urologist's perspective. A correct knowledge of this vasculature will help a surgeon while performing renal transplantation and other vascular surgeries. The clinicians dealing with the renal vessels ought to know these variations to keep away from the harm's way.

### Financial support and sponsorship

Nil.

### Conflicts of interest

There are no conflicts of interest.

## References

1. Standring S, editor. Gray's Anatomy: The Anatomical Basis of Clinical Practice. 40th ed. London: Elsevier, Churchill Livingstone; 2005. p. 1231-3.
2. Snell RS. Clinical Anatomy by Regions. 9th ed. New Delhi: Wolters Kluwer (India) Pvt Ltd; 2012. p. 213.
3. Das S. A Concise Textbook of Surgery. 4th ed. Kolkata: Old Mayors' Court (India); 2006. p. 1150-1.
4. Ozkan U, Oğuzkurt L, Tercan F, Kizilkiliç O, Koç Z, Koca N. Renal artery origins and variations: Angiographic evaluation of 855 consecutive patients. Diagn Interv Radiol 2006;12:183-6.
5. Gulas E, Wysiadecki G, Cecot T, Majos A, Stefanczyk L, Topol M, *et al*. Accessory (multiple) renal arteries – Difference in frequency according to population, visualizing techniques and stage of morphological development. Vascular 2016;24:531-7.
6. Dhar P, Lal K. Main and accessory renal arteries – A morphological study. Ital J Anat Embryol 2005;110:101-10.
7. Glodny B, Cromme S, Reimer P, Lennarz M, Winde G, Vetter H. Hypertension associated with multiple renal arteries may be rennin – Dependent. J Hypertens 2000;18:1437-44.
8. Kumar N, Swamy RS, Patil J, Nayak SB, Shetty SD, Aithal A. Accessory right renal vein draining into inferior vena cava. OA Case Rep 2014;3:48.
9. Kumar N, Aithal AP, Guru A, Nayak SB. Bilateral vascular variations at the renal hilum: A case report. Case Rep Vasc Med 2012;2012:968506.
10. Mukundan M, Vijaynath V, Ravi V. Bilateral variation of renal vein: A case report. Int J Anat Res 2016;4:3153-5.
11. Satyapal KS. Classification of the drainage patterns of the renal veins. J Anat 1995;186 (Pt 2):329-33.

Case Report

# Moyamoya Disease in a 29-Year-Old Female of Indian Origin

**Abstract**

The case presented here is a 29-year-old female patient with complaints of weakness over the left upper and lower limbs for 2 weeks. Digital subtraction angiography of the brain was suggestive of cerebral arteries, showing proliferation of cortical as well as collateral arteries arising from the internal carotid arteries (ICAs). Moyamoya is a progressive steno-occlusive disease at the terminal portions of the bilateral ICAs, with the development of "moyamoya vessels" giving a "Puff of Smoke" appearance on catheter angiography. Cerebral angiography is gold standard for diagnosis and helpful for detecting aneurysm and for surgical planning. There is no standardized surgical strategy for the treatment of this disease. Innumerable revascularization procedures have been employed with the aim of decelerating the progression of disease. Recognition of various symptoms of moyamoya would enable early diagnosis so that it could be treated surgically, as soon as possible, leading to a better neurological outcome.

**Keywords:** *Digital subtraction angiography, moyamoya disease, moyamoya syndrome, neurosurgical interventions, revascularization, stroke*

**Suyashi Sharma, Shilpi Gupta Dixit, Pushpinder S. Khera[1], Pawan K. Garg[1], Ashish K. Nayyar, Surajit Ghatak**

*Departments of Anatomy and [1]Diagnostic and Interventional Radiology, All India Institute of Medical Sciences, Jodhpur, Rajasthan, India*

## Introduction

Moyamoya disease was first narrated in 1957 by Takeuchi and Shimizu in Japan. Cases have been reported worldwide, but this disease is most common in Japan.[1] Many cases have been reported in India too.[2] It is a rare cerebrovascular disease with an incidence of 0.086/100,000 population.[3] Exact etiology of this disease is not known. It is a progressive steno-occlusive disease. The site of its occurrence is at the terminal portions of the bilateral internal carotid arteries (ICAs). Collateral channels of circulation develop. These small, multiple vessels at the base of the brain are known as "moyamoya vessels." This appearance was observed on catheter angiography and was given the name moyamoya, which in Japanese means "puff of smoke."[4,5] Cerebral revascularization surgery leads to favorable outcome of disease progression. Patients are likely to suffer stroke–ischemic or hemorrhagic.[6] Moyamoya disease generally occurs either in the pediatric age group between 5 and 10 years or in the fourth decade of life.[7] Generally, ischemic stroke is there in the pediatric group while hemorrhagic stroke in the adults.[8] Demographically, the ratio of females to males is 2:1.[9] Although moyamoya syndrome is linked with other medical conditions such as arteriosclerosis, Down syndrome, head trauma, autoimmune disease neurofibromatosis type 1, meningitis, or previous radiation therapy, it has the same angiographic appearance as moyamoya disease.[6]

## Case Report

This study was conducted at AIIMS, Jodhpur. Clearance of the institutional ethics committee was taken before commencement of the study. Institutional ethics committee stated "after through consideration accorded its approval on the above project."

A 29-year-old female was admitted to our hospital with complaints of weakness of the left upper and lower limbs for 2 weeks. There was a history of occasional headache and sudden fall thrice in the past 5 months. These sudden falls indicate transient ischemic attacks. There was no history of fever, vomiting, convulsion, and ear discharge. There was no past history of head injury, central nervous system infections, and facial palsy. There was no history of consumption of drugs or noxious substances. She was a full-term vaginal delivery with no complications. There was no history of delayed mile stones. On

**How to cite this article:** Sharma S, Dixit SG, Khera PS, Garg PK, Nayyar AK, Ghatak S. Moyamoya disease in a 29-year-old female of Indian origin. J Anat Soc India 2020;69:XX-XX.



**Article Info**

**Received:** 23 August 2020
**Accepted:** 22 May 2020
**Available online:** ***

***Address for correspondence:***
*Dr. Shilpi Gupta Dixit, Department of Anatomy, All India Institute of Medical Sciences, Jodhpur - 342 005, Rajasthan, India.*
*E-mail: shilpidr@gmail.com*

**Access this article online**

**Website:** www.jasi.org.in
**DOI:** 10.4103/JASI.JASI_111_19
**Quick Response Code:**

neurological examination, gait was hemiplegic, and tone as well as power was decreased over the left side. Blood, urine, and cerebrospinal fluid investigations were normal. Family history was negative for this disease or any other central nervous system disorder. Hence, after magnetic resonance imaging (MRI) brain, digital subtraction angiography (DSA) of the brain was done. In MRI, many small round and twisted portions of the artery were observed at the base of the brain. DSA was suggestive of significant stenosis of the bilateral ICAs, with the presence of multiple collateral arteries at the base of the brain supplied by vertebral and external carotid arteries, forming "puff of smoke" appearance [Figures 1 and 2].

## Discussion

Moyamoya disease is a progressive occlusion of Circle of Willis arteries. This leads to the development of collateral arteries around blocked vessels. This helps in compensating for the blockage. However, the collateral arteries are small and weak. Hence, they are vulnerable to bleeding, thrombosis, and aneurysm. These collateral arteries appear as "puff of smoke" on angiography.[4] Histopathology of these vessels suggested of thickened intima due to smooth muscle proliferation, as well as tortuous duplicated internal elastic lamina. Abnormalities of the vascular growth factors and inflammatory mediators also have role in the etiology of moyamoya disease.[10]

Clinical features of moyamoya disease are different in children and adults. In adults, there is history of subarachnoid or intra-parenchymal hemorrhage. However, in children, there is a history of recurrent transient ischemic attacks or infarction of the cerebral artery. Classical symptoms of moyamoya disease are monoparesis, hemiparesis, dysarthria, aphasia, headache, convulsions, and involuntary movements. If diagnosis is done late, then there can be mental impairment too. Two factors on which prognosis of moyamoya disease patients depend are age and type of presentation of disease. Patients with a history of transient ischemic attacks or epilepsy have better prognosis compared to infarctions.[11]

DSA shows the arteries and collaterals supplying the brain. It is used to visualize the anatomy of the vessels and the presence of aneurysm and hence helps in the confirmation of diagnosis.[11] In the present case also, DSA showed immense collateral flow through the perforating vessels. Attenuation of the bilateral supraclinoid ICAs with multiple collaterals forming puff of smoke appearance was visualized [Figures 1 and 2].

Antiplatelet agents (including aspirin) and calcium channel blockers are given. Antiplatelet agents are given to prevent clots. Calcium channel blockers provide supportive management of moyamoya disease. Surgery is the best management of moyamoya disease.[12,13] Moyamoya usually affects the ICA and adjacent anterior and middle cerebral arteries. Therefore, surgeons can use external carotid artery or superficial temporal artery to replace its circulation. The arteries are either sewn directly into brain circulation or placed on the surface of the brain to re-establish new circulation within a few weeks. Revascularization procedures are done at present to increase the perfusion of the hypoxic brain cells. This will ultimately prevent ischemic injury by increasing collateral blood flow.[14,15] Revascularization procedures can be divided into three main groups: indirect (nonanastomotic) bypass techniques, direct (anastomotic) bypass techniques, and combined techniques. Results of direct techniques have been better than indirect and combined techniques.[16] Angiographic follow-ups have resulted in favorable consequence.

This case emphasizes the significance of considering moyamoya disease as one of the differential diagnoses in patients with a history of recurrent headaches, which cannot be relieved by routine medical treatment.

## Conclusion

Early diagnosis and management will lead to favorable results in moyamoya disease patients.

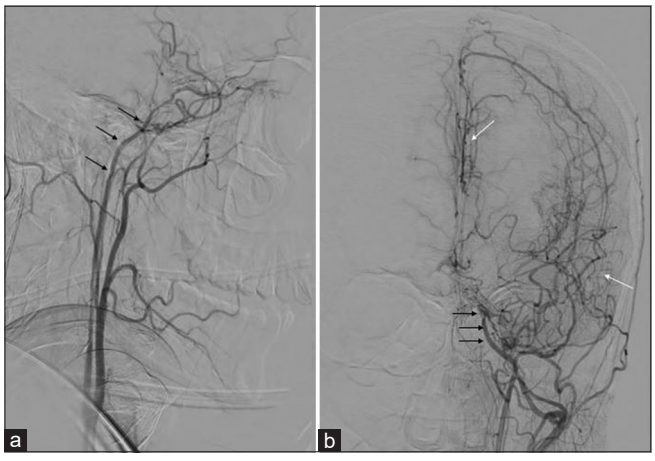


**Figure 1: Digital subtraction angiography of the left common carotid artery lateral (a) and anteroposterior (b) view showing significant attenuation of the supraclinoid internal carotid artery (black arrows) and terminating as ophthalmic artery. Extensive collaterals seen arising from the branches of the external carotid artery (white arrows)**

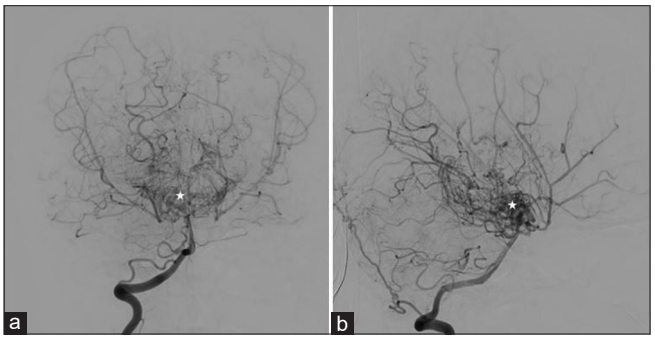


**Figure 2: Digital subtraction angiography of the right vertebral artery anteroposterior (a) and lateral (b) view showing extensive collaterals at base of the skull forming puff of smoke appearance (asterisk). Majority of anterior circulation flow is maintained by vertebral artery**

DSA helps a lot in diagnosis and henceforth in the management of this disease. This knowledge will be crucial in planning neurosurgical interventions and hence will influence prognosis of moyamoya disease.

### Declaration of patient consent

The authors certify that they have obtained all appropriate patient consent forms. In the form the patient(s) has/have given his/her/their consent for his/her/their images and other clinical information to be reported in the journal. The patients understand that their names and initials will not be published and due efforts will be made to conceal their identity, but anonymity cannot be guaranteed.

### Financial support and sponsorship

Nil.

### Conflicts of interest

There are no conflicts of interest.

## References

1. Takeuchi K, Shimizu K. Hypoplasia of the bilateral internal carotid arteries. Brain Nerve 1957;9:37-43.
2. Menon G, Hegde A. Moyamoya disease. Arch Med Health Sci 2019;7:224-32.
3. Uchino K, Johnston SC, Becker KJ, Tirschwell DL. Moyamoya disease in Washington State and California. Neurology 2005;65:956-8.
4. Suzuki J, Kodama N. Moyamoya disease-a review. Stroke 1983;14:104-9.
5. Atlas SW. MR angiography: Techniques and Clinical Applications MRI of the Brain and Spine. 3rd ed. Philadelphia, PA, USA: Lippincott Williams and Wilkins; 2002.
6. Lutterman J, Scott M, Nass R, Geva T. Moyamoya syndrome associated with congenital heart disease. Pediatrics 1998;101:57-60.
7. Baba T, Houkin K, Kuroda S. Novel epidemiological features of moyamoya disease. J Neurol Neurosurg Psychiatry 2008;79:900-4.
8. Soriani S, Scarpa P, Voghenzi A, De Carlo L, Cilio R. Moyamoya disease in childhood: A familial case report. Childs Nerv Syst 1993;9:215-9.
9. Scott RM, Smith JL, Robertson RL, Madsen JR, Soriano SG, Rockoff MA. Long-term outcome in children with moyamoya syndrome after cranial revascularization by pial synangiosis. J Neurosurg 2004;100:142-9.
10. Fukui M, Kono S, Sueishi K, Ikezaki K. Moyamoya disease. Neuropathology 2000;20 Suppl: S61-4.
11. Joarder MA, Chandy M. Moyamoya disease in a child: A case report. Pulse 2013;6:62-5.
12. Ibrahimi DM, Tamargo RJ, Ahn ES. Moyamoya disease in children. Childs Nerv Syst 2010;26:1297-308.
13. Scott RM. Moyamoya syndrome: A surgically treatable cause of stroke in the pediatric patient. Clin Neurosurg 2000;47:378-84.
14. Oya S, Tsutsumi K, Ueki K. Adult-onset moyamoya disease with repetitive ischemic attacks successfully treated by superficial temporal-middle cerebral artery bypass-case report. Neurol Med Chir (Tokyo) 2003;43:138-41.
15. Golby AJ, Marks MP, Thompson RC, Steinberg GK. Direct and combined revascularization in pediatric moyamoya disease. Neurosurgery 1999;45:50-8.
16. Fung LW, Thompson D, Ganesan V. Revascularisation surgery for paediatric moyamoya: A review of the literature. Childs Nerv Syst 2005;21:358-64.